Electronic Supplemental information

for

Isomeric effect of naphthyl spacers on structure and property of isostructural porous crystalline frameworks

Yuto Suzuki, Mao Yamaguchi, Ryusei Oketani and Ichiro Hisaki

Division of Chemistry, Graduate School of Engineering Science, Osaka University,

1-3 Machikaneyama, Toyonaka, Osaka 560-8531, Japan.

Table of Contents

1. General

All reagents and solvents were used as received from commercial suppliers. Gel permeation chromatography (GPC) was performed on JAIGEL-1H and -2H with $CHCl_3$ as a solvent. ^1H and ^{13}C NMR spectra were measured on a JEOL 400 YH (400 MHz) spectrometer or Bruker AV400M (400 MHz) spectrometer. Residual proton and carbon of deuterated solvents were used as internal standards for the measurements: δ = 7.26 ppm ($CDCl_3$) and δ = 2.49 ppm (DMSO-d_6) for ^1H NMR, δ = 77.00 ppm ($CDCl_3$) and δ = 39.50 ppm (DMSO-d_6) for ^{13}C NMR. HR-MS analyses were conducted on a JEOL JMS-700 instrument or autoflex III Bruker. Thermo gravimetric (TG) analyses were performed on Rigaku Thermo plus EVO2 (TG-DTA8122) under an N_2 purge (300 mL/min) at a heating rate of 5 °C min^{-1}. Crystal structures were drawn using mercury[S1] or VESTA[S2] software.

1-1. Single crystal X-ray or electron diffraction measurement and analysis.

Diffraction data of **C2N6DBC-1**, **C2N6DBC-2** and **C1N5DBC-1** were collected with synchrotron radiation (λ = 0.81981, 0.81063 and 0.81059 Å, respectively) at BL40XU in SPring-8.[S8] A Data of **C1N4DBC-1x** was collected with electron radiation (λ = 0.0251 Å) using a Rigaku Synergy-ED equipped with a Rigaku HyPix3000 fast detector. Diffraction Data collection, cell refinement, and data reduction were carried out with CrysAlis PRO.[S3] SHELXT[S4] was used for the structure solution of the crystals. These calculations were performed with the observed reflections [$I > 2\sigma(I)$] with the program OLEX-2 crystallographic software.[S5] Structural refinement was performed by SHELXL.[S6] All non-hydrogen atoms were refined with anisotropic displacement parameters, and hydrogen atoms were placed in idealized positions and refined as rigid atoms with the relative isotropic displacement parameters. SQUEEZE function equipped in the PLATON program was used to treat severely disordered solvent molecules in voids.[S7]

1-2. Powder X-ray diffraction measurement.

Powder X-ray diffraction (PXRD) data were collected on a Rigaku Ultima-IV (40 kV, 44 mA) or PANalytical XPert PRO X'Celerator (45 kV, 40 mA) using Cu-Kα radiation at room temperature and with a scan rate of 2.0° min^{-1}, or 1.2° min^{-1}, respectively. For structural analysis and *in situ* experiment, the powder samples were loaded in a Lindemann glass capillary with 0.5 mm outer diameter (for a measurement with gas or vaper introduction) or a borosilicate glass capillary with 0.5 mm outer diameter (for a measurement under ambient condition or heat). The diffraction data were recorded using a MYTHEN detector with the synchrotron radiation (λ = 1.0000 or 1.0800 Å) at BL02B2 in SPring-8[S8] with the approval of JASRI (proposal No. 2021A1567). The Pawley PXRD refinement is performed using the Reflex module in the Material Studio ver 6.0,[S9] in which a Pseudo-Voigt profile function was used for the profile fitting (background subtracting, peak smoothing, and broadening were taken into account). Then the powder pattern was indexed by the X-cell[S10] software, following the Pawley refinement[S11] of the cell was performed ($2° < 2\theta < 45°$) and assigned to each space group. [**C1N4DBC-1**: *Pnnn*, **C1N4DBC-1a**: *Pn*, **C1N4DBC-1(benzene)**: *Pn*]

1-3. Variable temperature PXRD (VT-PXRD) data

VT-PXRD of **C1N5DBC-1** and **C2N6DBC-1** were collected in a Rigaku Ultima-IV (40 kV, 44 mA) with a temperature control unit. For this VT-PXRD, the HOF powders were placed on an aluminum substrate, and the measurements were conducted in atmospheric conditions. The sample temperature increased from room temperature to 360 °C with a rate of 1.0 °C min^{-1}. PXRD scan of each measurement was collected with a difference in the temperature of ca. 6 °C. A VT-PXRD of **C1N4DBC-1** were conducted at BL02B2 in SPring-8[S8]. The powder samples were loaded in a borosilicate glass capillary with 0.5 mm outer diameter. The diffraction data were recorded using a MYTHEN detector with the synchrotron radiation (λ = 1.0800 Å) with 10-°C steps.

1-4. *In situ* sorption-PXRD measurements.

In situ sorption-PXRD measurements of **C1N4DBC-1a** were performed for N_2, CO_2, and benzene vapour. The crystalline powder of **C1N4DBC-1a** was placed into a borosilicate glass capillary with a diameter of 0.5 mm. The diffraction patterns were recorded using a MYTHEN detector with synchrotron radiation (λ = 1.0000 Å) at beamline BL02B2 of SPring-8[S8]. The patterns of gas were recorded at 198 K by increasing the pressure to 0 atm, 0.5 atm, and 1 atm, then decreasing the pressure to 0.5 atm and 0 atm in that order. The patterns of benzene vapour were recorded at 298 K as the vapour was gradually loaded at 0 kPa to 10 kPa with 1-kPa steps and removed to 0 kPa, following activated at 333 K under vacuum to thoroughly remove benzene in the channel.

1-5. Powder X-ray diffraction analysis of **C1N4DBC-1a**.

The calculation was performed using the Reflex Plus software implemented in Material Studio ver 6.0.[S9] The powder pattern was indexed by the X-cell[S10] software using 28 reflections, resulting in 5 solutions. A top-ranked solution with relative figures of merit of 0.626, the zero-point shift of −0.00667°, and two impurity peaks were refined by the Pawley method ($2° < 2\theta < 45°$) and assigned to space group *Pn* (#7). The Pawley refinement[S11] of the cell was again performed ($2° < 2\theta < 45°$). The subsequent crystal structure solution was carried out by using the Monte Carlo/parallel tempering method using the Powder Solve software.[S12] Atomic coordinates in the initial structures were adopted by optimizing the single crystal structure of electron diffraction measurement without bonding between the DBC core and naphthyl group by DFT method at B3LYP-D3/6-31G** level. In the Monte Carlo calculation, lengths and angles of covalent bonds between the DBC core and naphthyl groups were refined. A Rietveld refinement[S13] ($2° < 2\theta < 50°$) was performed under the following conditions: (1) The pseudo-Voigt function was used for the simulation of the peak shape. (2) The Bragg-Brentano method was used for line shift refinement. (3) The Berar-Baldinozzi method[S14] was used for asymmetric refinement. (4) The background was determined by linear interpolation using 20 terms. (5) The March-Dollas method[S15] was applied to correct the effects of preferred orientation. (6) For the refinement of temperature factors, global isotropic temperature factors were used. The molecular conformation was refined by varying the torsion angles around all single bonds. Crystal data for **C1N4DBC-1a**: $C_{70}H_{40}O_8$, *Fw* 1009.082, monoclinic, space group *Pn* (#7), a = 17.8138(43) Å, b = 43.313(11) Å, c = 3.9778(10) Å, β = 90.798(49)°, V = 3068.85 $Å^3$, Z = 2, $d = 1.092\ g\ cm^{-3}$, T = 298(2) K, R_p = 0.0501, R_{wp} = 0.0759.

1-6. Adsorption/desorption experiment

Gas sorption. The activated bulk samples of **C1N4DBC-1a**, **C1N5DBC-1a**, and **C2N6DBC-1a** were used for gas sorption measurements, which were performed on BELSORP-max (BEL, Japan). The adsorption isotherms of N_2, CO_2 were corrected at 77K and 195 K, respectively. Brunauer–Emmett–Teller (BET) specific surface area: $S_{A(BET)}$ was based on N_2 absorption isotherms.

2. Synthesis of building block molecules

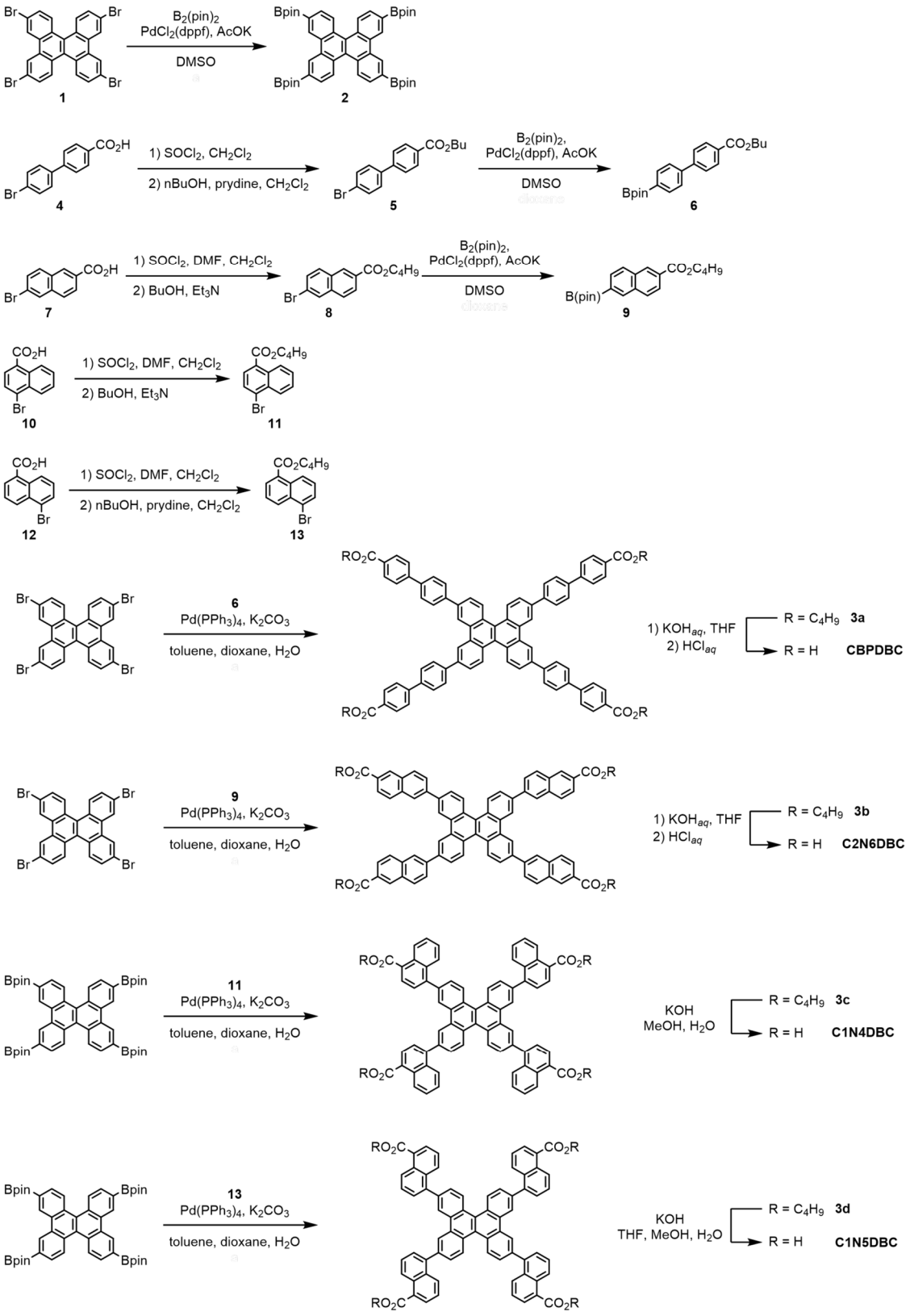

Scheme S1. Synthesis of DBC derivatives. Compound **1**, **5**, and **6** was synthesized by a reported procedure.[S17,19]

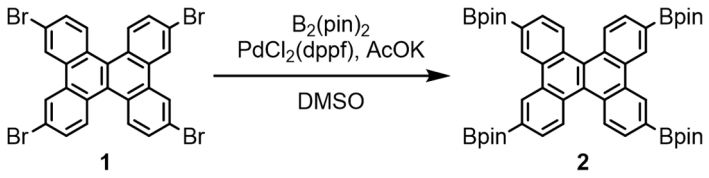

Synthesis of 2. A 100 mL three-necked flask was charged with compound **1** (1.10 g, 1.71 mmol), B_2pin_2 (2.16 g, 8.50 mmol), AcOK (1.47 g, 15.0 mmol), and $PdCl_2$(dppf) (0.279 g, 0.341 mmol) under nitrogen. Then degassed DMSO (35 mL) were added and at vacuumed at rt for 15 min. The reaction mixture was stirred at 90 °C for 24 h. After cooled to room temperature, the reaction mixture was poured into water (300 mL). was collected by filtration and washed well with water. The dried crude product was purified with short column chromatography (silica gel, $CHCl_3$), following wash with hexane to give compound **2** as a pale-yellow solid (0.959 g, 68%).

M.p. 289 °C. ^{1}H NMR (400 MHz, $CDCl_3$): δ 9.27 (s, 4H), 8.65 (d, 4H, J = 8.0 Hz), 8.03 (d, 4H, J = 8.4 Hz), 1.46 (s, 48H) ppm. ^{13}C NMR (100 MHz, $CDCl_3$): δ 132.23, 131.25, 130.78, 130.45, 129.04, 128.04, 84.08, 24.97 ppm.

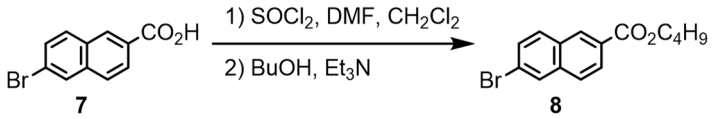

Synthesis of 8.

A 300 mL three-necked flask was charged with 6-bromo-2-naphthoic acid (1.55 g, 6.17 mmol) in dehydrated CH_2Cl_2 (20 mL) under nitrogen. Then $SOCl_2$ (0.45 mL, 6.05 mmol) and DMF (1 drop) were added dropwise at rt. The mixture was refluxed at 45 °C for 6 h. After cooling to room temperature, solvent was removed under vacuum and dissolved dehydrated CH_2Cl_2. Then dehydrated n-butanol (1.5 mL) and triethylamine (5.0 mL) were added and stirred at rt for 18 h. The organic phase was diluted with CH_2Cl_2 (40 mL) and washed with HCl_{aq}, water and brine, dried with anhydrous $MgSO_4$, and filtered. The crude product was purified with short column chromatography (silica gel, AcOEt/hexane = 1/2) to give compound **8** (1.41 g, 92%) as a colourless oil.

^{1}H NMR (400 MHz, $CDCl_3$): δ 8.56 (s, 1H), 8.14–8.04 (m, 2H), 7.86–7.76 (m, 2H), 7.60–7.50 (m, 1H), 4.39 (t, 2H, J = 6.8 Hz) , 1.85–1.75 (m, 2H) , 1.51–1.30 (m, 6H) , 1.01 (t, 3H, J = 7.4 Hz) ppm. ^{13}C NMR (100 MHz, $CDCl_3$): δ 166.44, 136.37, 130.94, 130.83, 130.75, 130.11, 129.90, 128.26, 127.16, 126.40, 122.51, 65.12, 30.83, 19.30, 13.76 ppm. HR-MS (EI^+): calcd. For $C_{15}H_{15}O_2Br$ $[M]^+$ 306.0255; found: 306.0255.

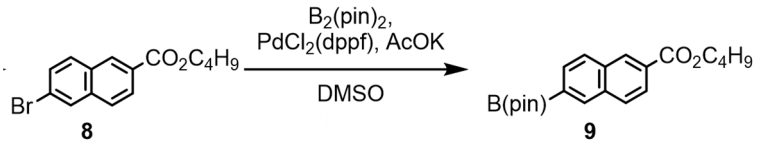

Synthesis of 9. A 100 mL three-necked flask was charged with compound **8** (4.00 g, 13.0 mmol), B_2pin_2 (3.34 g, 13.2 mmol), AcOK (3.14 g, 32.0 mmol), and $PdCl_2$(dppf) (0.503 g, 0.783 mmol) under nitrogen. Then degassed dioxane (25 mL) were added and the mixture was stirred at 100 °C for 18 h. After removing solvent under vacuum, the product was extracted with $CHCl_3$. The organic phase was combined and washed with water, dried with anhydrous $MgSO_4$,

and filtered. The crude product was purified with column chromatography (silica gel, AcOEt / hexane = 1 / 2) to give compound **9** (3.73 g, 81%) as a white solid.

M.p. 57 °C. ^{1}H NMR (400 MHz, $CDCl_3$): δ 8.58 (d, 1H, *J* = 1.2 Hz), 8.39 (s, 1H), 4.32 (dd, 1H, *J* = 8.8, 1.6 Hz), 8.00–7.90 (m, 3H), 4.39 (t, 2H, *J* = 6.6 Hz), 1.84–1.77 (m, 2H), 1.55–1.48 (m, 2H), 1.40 (s, 12H), 1.01 (t, 3H, *J* = 7.4 Hz) ppm. ^{13}C NMR (100 MHz, $CDCl_3$): δ 166.7, 135.8, 134.7, 134.0, 131.1, 128.8, 128.7, 128.3, 125.2, 84.09, 83.44, 63.97, 30.82, 24.99, 19.29, 13.74 ppm.

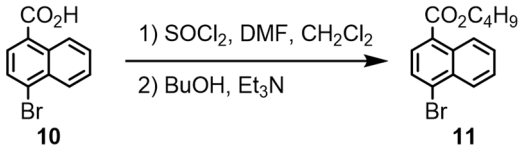

10 **11**

Synthesis of 11. A 300 mL three-necked flask was charged with 4-bromo-1-naphthoic acid (2.00 g, 7.97 mmol) in dehydrated CH_2Cl_2 (20 mL) under nitrogen. Then $SOCl_2$ (0.65 mL, 9.00 mmol) and DMF (1 drop) were added dropwise at rt. The mixture was refluxed at 50 °C for 2 h. After cooling to room temperature, solvent was removed under vacuum and dissolved dehydrated CH_2Cl_2. Then dehydrated n-butanol (2.0 mL) and pyridine (4.0 mL) were added and stirred at rt for 18 h. The organic phase was diluted with CH_2Cl_2 (40 mL) and washed with 3M-HCl_{aq}, water and brine, dried with anhydrous $MgSO_4$, and filtered. The crude product was purified with short column chromatography (silica gel, CH_2Cl_2) to give compound **11** (2.00 g, 82%) as a colourless oil.

^{1}H NMR (400 MHz, $CDCl_3$): δ 9.00–8.90 (m, 1H), 8.40–8.30 (m, 1H), 7.98 (d, 1H, *J* = 7.6 Hz), 7.83 (d, 1H, *J* = 7.6 Hz), 7.70–7.60 (m, 2H), 4.42 (t, 2H, *J* = 6.8 Hz), 1.87–1.75 (m, 2H), 1.57–1.45 (m, 2H), 1.01 (t, 3H, *J* = 7.4 Hz) ppm. ^{13}C NMR (100 MHz, $CDCl_3$): δ 166.78, 132.27, 131.99, 129.75, 128.70, 128.18, 127.45, 127.35, 127.22, 126.15, 64.97, 30.66, 19.23, 13.65 ppm. HR-MS (EI^+): calcd. For $C_{15}H_{15}O_2Br$ $[M]^+$ 306.0255; found: 306.0240.

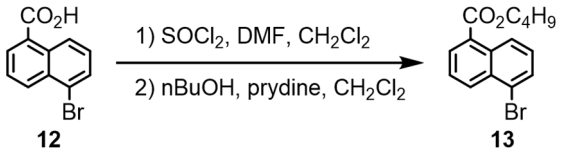

12 **13**

Synthesis of 13. In a 100 mL three necked flask was stirred a mixture of 5-bromo-1-naphthoic acid (1.00 g, 3.98 mmol), H_2SO_4 (0.050 mL) in ^{n}BuOH (15 mL). The mixture was stirred at reflux (100 °C) for 18 h, and then cooled to ambient temperature. The solution was poured into sat. $NaHCO_{3aq}$ and extracted with CH_2Cl_2. The organic phase was combined and washed with water, sat. $NaHCO_{3aq}$, and brine, dried with anhydrous $MgSO_4$, and filtered. The crude product was purified with column chromatography (silica gel, CH_2Cl_2) to give compound **13** (2.09 g, 70%) as a pale-yellow oil.

^{1}H NMR (400 MHz, $CDCl_3$): δ 8.89 (dt, 1H, *J* = 8.8, 1.0 Hz), 8.45 (dt, 1H, *J* = 8.8, 1.0 Hz), 8.20 (dd, 1H, *J* = 7.2, 1.2 Hz), 7.85 (dt, 1H, *J* = 8.0, 0.8 Hz), 7.61 (dd, 1H, *J* = 8.6, 7.4 Hz), 7.44 (dt, 1H, *J* = 8.8, 7.2 Hz), 4.43 (t, 2H, *J* = 6.8 Hz) , 1.87–1.77 (m, 2H), 1.58–1.48 (m, 2H), 1.01 (t, 3H, *J* = 7.8 Hz) ppm. ^{13}C NMR (100 MHz, $CDCl_3$): δ 16629, 132.67, 132.26, 132.07, 130.54, 130.48, 128.24, 127.77, 125.90, 125.77, 123.27, 65.22, 30.81, 19.35, 13.75 ppm. HR-MS (EI^+): calcd. For $C_{15}H_{15}O_2Br$ $[M]^+$ 306.0255; found: 306.0254.

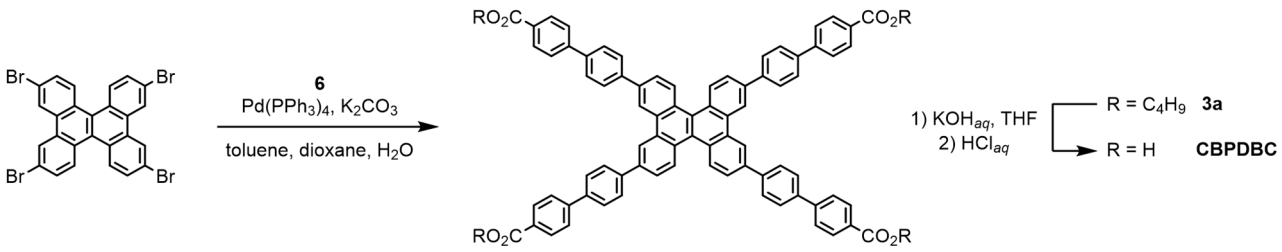

Synthesis of 3a. A 300 mL three-neck flask was charged with compound **1** (0.501 g, 0.778 mmol), compound **6** (1.42 g, 3.72 mmol), K_2CO_3 (1.10 g, 7.96 mmol), and $Pd(PPh_3)_4$ (0.201 g, 0.174 mmol) in degassed toluene (10 mL), dioxane (25 mL), and H_2O (3 mL) under nitrogen. Then the reaction mixture was stirred at 110 °C for 48 h. The solution was blue on the surface due to fluorescence and yellow inside. After removing solvent under vacuum, the product was extracted with $CHCl_3$, washed with water, dried with anhydrous $MgSO_4$, and filtered to give a yellow-brown solid. The crude product was purified by preparative HPLC to give compound **3a** (0.509 g, 49%) as a yellow solid.

M.p. 272 °C. ^{1}H NMR (400 MHz, $CDCl_3$): δ 8.97 (s, 4H), 8.79 (d, 4H), 8.16 (d, 4H), 7,94 (d, 8H), 7.79 (m, 14H), 4.38 (t, 8H), 1.80 (m, 8H), 1.01 (t, 12H) ppm. ^{13}C NMR (100 MHz, $CDCl_3$): δ 166.45, 144.68, 140.43, 139.06, 138.03, 130.96, 130.19, 129.51, 129.20, 128.40, 127.20, 126.87, 126.19, 125.37, 121.61, 64.92, 30.85, 19.32, 13.79 ppm. HR-MS (MALDI): calcd. For $C_{94}H_{80}O_8$ $[M]^+$ 1336.5848; found: 1336.5866.

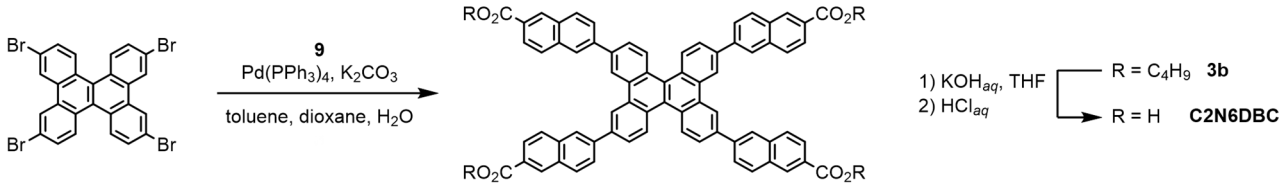

Synthesis of 3b. A 100 mL three-necked flask was charged with compound **9** (705 mg, 3.10 mmol), compound **1** (250 mg, 0.388 mmol), $Pd(PPh_3)_4$ (98.7 mg, 0.0852 mmol), and K_2CO_3 (414 mg, 3.01 mmol) in degassed toluene (10 mL), dioxane (15 mL) and degassed water (5 mL) under nitrogen. Then the reaction mixture was refluxed at 110 °C for 48h. After removing solvent under vacuum, the product was extracted with $CHCl_3$. The organic phase was combined and washed with water, dried with anhydrous $MgSO_4$, and filtered. The crude product was purified with column chromatography (silica gel, $CHCl_3$/hexane = 1/2→1/1) and preparative HPLC to give compound **3b** (68.6 mg, 41%) as a yellow solid.

M.p. 246 °C. ^{1}H NMR (400 MHz, $CDCl_3$): δ 8.45 (s, 4H), 8.24 (s, 4H), 7.94 (d, 4H, J = 8.4 Hz), 7.77 (s, 4H), 7.74 (d, 4H, J = 8.4 Hz), 7.61 (d, 4H, J = 8.8 Hz), 7.55 (d, 4H, J = 8.0 Hz), 7.33 (d, 4H, J = 8.4 Hz), 4.44 (t, 8H, J = 6.6 Hz), 1.93–1.77 (m, 8H), 1.67–1.50 (m, 8H), 1.08 (d, 12H, J = 7.4 Hz) ppm. ^{13}C NMR (100 MHz, $CDCl_3$): δ 166.63, 140.09, 138.18, 135.67, 131.71, 130.60, 130.00, 129.16, 128.37, 128.33, 127.98, 126.12, 125.88, 125.68, 125.62, 121.95, 65.09, 30.91, 19.38, 13.85 ppm. HR-MS (MALDI): calcd. For $C_{86}H_{72}O_8$ $[M]^+$ 1232.5222; found: 1232.5221.

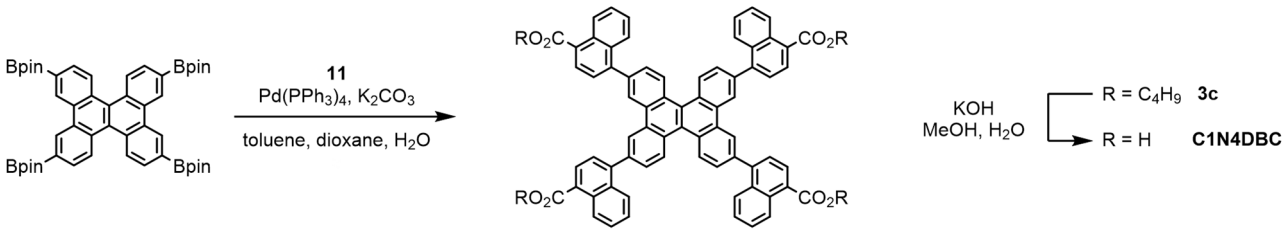

Synthesis of 3c. A 100 mL schulenk tube was charged with compound **2** (0.740 g, 0.889 mmol), compound **11** (1.23 g, 4.00 mmol), $Pd(PPh_3)_4$ (0.231 mg, 0.200 mmol), and K_2CO_3 (1.42 mg, 10.3 mmol) in degassed toluene (15 mL), dioxane (5.0 mL) and degassed water (3.0 mL) under nitrogen. Then the reaction mixture was refluxed at 110 °C for 24 h. After removing solvent under vacuum, the product was extracted with $CHCl_3$. The organic phase was combined and washed with water, dried with anhydrous $MgSO_4$, and filtered. The crude product was purified with column chromatography (silica gel, $CHCl_3$/hexane = 1/1→1/0) and preparative HPLC to give compound **3c** (314 mg, 29%) as a yellow green solid.

M.p. 172 °C. ^{1}H NMR (400 MHz, $CDCl_3$): δ 9.02 (d, 8H, J = 8.4 Hz), 9.85 (d, 4H, J = 1.6 Hz), 8.26 (d, 4H, J = 7.6 Hz), 8.09 (d, 4H, J = 8.4 Hz), 7.88 (d, 4H, J = 1.6 Hz), 7.70–7.58 (m, 4H), 4.46 (t, 8H, J = 6.6 Hz), 1.80–1.70 (m, 8H), 1.60–1.50 (m, 8H), 1.46 (t, 12H, J = 6.6 Hz) ppm. ^{13}C NMR (100 MHz, $CDCl_3$): δ 167.64, 144.74, 138.94, 132.25, 131.87, 130.95, 129.39, 128.97, 128.92, 128.86, 127.87, 127.41, 126.59, 126.51, 126.23, 126.10, 125.12, 65.04, 30.88, 19.40, 13.79 ppm. HR-MS (FAB^+): calcd. For $C_{86}H_{72}O_8$ $[M]^+$ 1232.5222; found: 1232.5230.

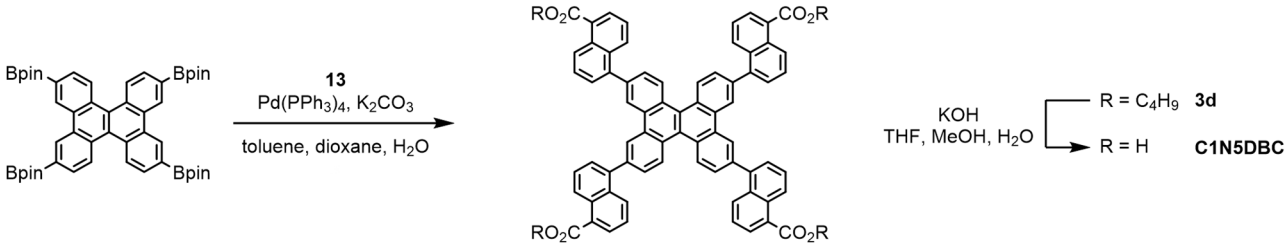

Synthesis of 3d. A 100 mL schulenk tube was charged with compound **2** (740 mg, 0.889 mmol), compound **13** (882 mg, 2.87 mmol), $Pd(PPh_3)_4$ (161 mg, 0.140 mmol), and K_2CO_3 (830 mg, 6.00 mmol) in degassed dioxane (25 mL) and degassed water (3.0 mL) under nitrogen. Then the reaction mixture was refluxed at 100 °C for 24h. After removing solvent under vacuum, the product was extracted with $CHCl_3$. The organic phase was combined and washed with water, dried with anhydrous $MgSO_4$, and filtered. The crude product was purified by flash purification (Isorera one®, Sfär HC Duo 10g, $CHCl_3$/hexane = 1/2→1/1) and preparative HPLC to give compound **3d** (250 mg, 34%) as a yellow green solid.

M.p. 227 °C (decomp.). ^{1}H NMR (400 MHz, $CDCl_3$): δ 9.01 (d, 4H, J = 8.4 Hz), 8.96 (d, 4H, J = 7.6 Hz), 8.84 (d, 4H, J = 0.8 Hz), 8.24 (d, 4H, J = 8.4 Hz), 8.17 (d, 4H, J = 6.4 Hz), 7.85 (d, 4H, J = 8.8 Hz), 7.77–7.60 (m, 8H), 4.46 (t, 8H, J = 8.2 Hz), 1.90–1.75 (m, 8H), 1.65–1.50 (m, 8H), 1.02 (d, 12H, J = 7.8 Hz) ppm. ^{13}C NMR (100 MHz, $CDCl_3$): δ 167.86, 140.39, 139.32, 132.28, 131.72, 131.01, 130.97, 129.81, 128.91, 128.72, 127.23, 127.68, 127.04, 125.73, 125.27, 124.83, 65.07, 30.87, 19.39, 13.78 ppm. HR-MS (MALDI): calcd. For $C_{86}H_{72}O_8$ $[M]^+$ 1232.5222;

found: 1232.5230.

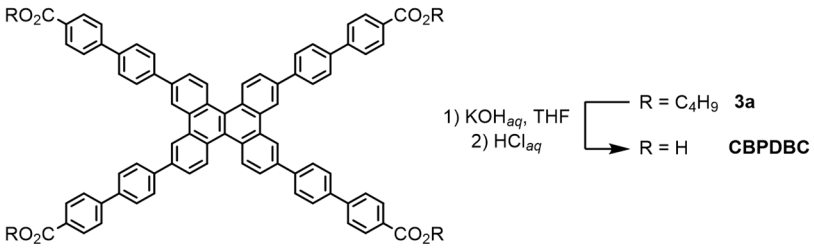

Synthesis of CBPDBC. A 100 mL round-bottomed flask was charged with compound **3a** (143 mg, 106 μmol) and 5%KOH_{aq} (10 mL), and THF (10 mL). Then the suspension was refluxed at 80 °C for 48 h. After removing THF in vacuo, the resultant water suspension was neutralized by 3M-HCl_{aq}. The precipitate was separated by centrifuge, and washed with water three times, methanol once, and acetone once to give **CBPDBC** (119 mg, 99%) as a yellow solid. M.p. >300 °C. ^{1}H NMR (400 MHz, DMSO-d_6): δ 8.74 (d, 16H, J = 2.0 Hz), 8.43 (d, 16H, J = 8.8 Hz), 7.76 (q, 12H, J = 6.8 Hz) ppm. HR-MS (FAB^+): calcd. For $C_{78}H_{48}O_8$ $[M]^+$ 1112.3343; found: 1112.3349.

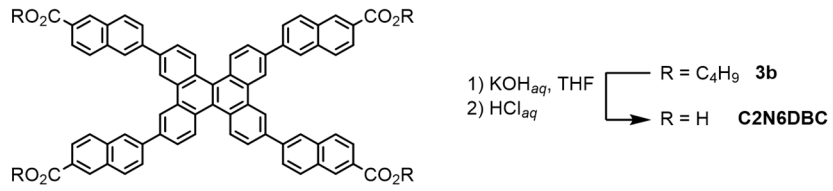

Synthesis of C2N6DBC. A reaction mixture of compound **3b** (134 mg, 0.109 mmol) in THF (40 mL), MeOH (10 mL), and 5%-KOH aqueous solution (40 mL) was stirred for 2 days at 90 °C. After cooled to room temperature, organic phase was removed in vacuo, following addition of 5M-H_2SO_{4aq} into the reaction mixture until precipitate was not formed anymore. The precipitate was collected by filtration, washed well with water, MeOH, $CHCl_3$, and acetone. The filtrate was dried in vacuo to yield **C2N6DBC** (78.7 mg, 71%) as yellow green solid.
M.p. >300 °C. ^{1}H NMR (400 MHz, DMSO-d_6): δ 9.53 (s, 4H), 8.85 (d, 4H, J = 8.8 Hz), 8.70 (s, 8H), 8.45–8.25 (m, 12H), 8.17 (d, 4H, J = 6.0 Hz), 8.05 (d, 4H, J = 9.6 Hz) ppm. ^{13}C NMR (100 MHz, DMSO-d_6, ca. 10 mg/mL): δ 167.37, 139.23, 137.34, 135.15, 133.38, 131.32, 130.46, 130.14, 129.71, 128.47, 128.01, 127.49, 126.33, 126.27, 125.49, 125.26, 121.96 ppm. HR-MS (MALDI): calcd. For $C_{70}H_{40}O_8$ $[M]^+$ 1008.2718; found: 1008.2724.

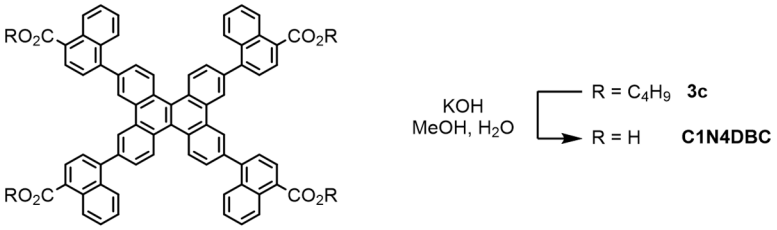

Synthesis of C1N4DBC. A 50 mL round-bottomed flask was charged with compound **3c** (120 mg, 0.0975 μmol) and KOH (800 mg, 14.3 mmol) in MeOH (35 mL) and water (2.0 mL). Then the suspension was refluxed at 90 °C for 3 days. After cooled to room temperature, H_2SO_{4aq} was added into the reaction mixture following stirring over 1h. The precipitate was collected by filtration, washed well with water, MeOH, $CHCl_3$, and acetone. The filtrate was dried in vacuo to yield **C1N4DBC** (75.8 mg, 77%) as yellow green solid.

M.p. >300 °C. ^{1}H NMR (400 MHz, DMSO-d_6): δ 9.13 (s, 4H), 9.02 (d, 4H, J = 9.6 Hz), 8.98 (d, 4H, J = 9.6 Hz), 8.21 (d, 4H, J = 8.0 Hz), 8.06 (d, 4H, J = 8.8 Hz), 7.96 (d, 4H, J = 8.8 Hz), 7.75 (d, 4H, J = 7.6 Hz), 7.66 (t, 4H, J = 7.2 Hz), 7.58 (t, 4H, J = 7.2 Hz) ppm. ^{13}C NMR (100 MHz, DMSO-d_6, ca.10 mg mL^{-1}): δ 167.64, 144.74, 138.94, 132.25, 131.87, 130.95, 129.39, 128.97 128.92, 127.87, 127.56, 127.41, 126.59, 126.51, 126.23, 126.10, 125.12 ppm. HR-MS (MALDI): calcd. For $C_{70}H_{40}O_8$ $[M]^+$ 1008.2718; found: 1008.2719.

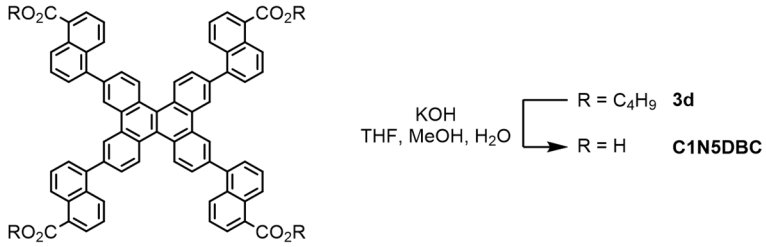

Synthesis of C1N5DBC. A 100 mL shulenck tube was charged with compound **3d** (190 mg, 0.154 mmol) and KOH (505 mg, 9.00 mmol) in THF (12 mL), MeOH (5.0 mL), and water (6.0 mL). Then the suspension was refluxed at 70 °C for 3days. After cooled to room temperature, 4M-HCl_{aq} was added into the reaction mixture until precipitate was not formed anymore. The precipitate was collected by centrifugation, washed well with water, and corrected by filtration. The filtrate was washed well with H_2O, MeOH, and $CHCl_3$, and dried in vacuo. Then this crude solid was dissolved in DMF to remove white insoluble and purified with recrystallization to yield **C1N5DBC** (106 mg, 68%) as light green solid.

M.p. >300 °C. ^{1}H NMR (400 MHz, DMSO-d_6): δ 9.09 (s, 4H), 9.02 (d, 4H, J = 8.8 Hz), 8.96–8.87 (m, 4H), 8.25–8.05 (m, 8H), 7.93 (d, 4H, J = 8.8 Hz), 7.78–7.70 (m, 8H), 7.58 (t, 4H, J = 7.8 Hz) ppm. ^{13}C NMR (100 MHz, DMSO-d_6, ca. 7 mg mL^{-1}): δ 168.84, 139.75, 138.83, 131.51, 130.96, 130.49, 130.11, 129.37, 129.23, 128.71, 128.47, 127.81, 127.75, 126.91, 126.88, 125.40, 125.28 ppm. HR-MS (MALDI): calcd. For $C_{70}H_{40}O_8$ $[M]^+$ 1008.2718; found: 1008.2712.

3. Crystallography

DBC carboxylic acids were dissolved in a mixed solvent of a polar solvent (DMF or 1,4-dioxane) and an aromatic guest solvent (*o*-xylene: Xy, mesitylene: Mes, methyl benzoate: MeBz, 1,2,4-trichlorobenzene: TCB, or 5-*tert*-butyl-*m*-xylene: tBuXy). Recrystallizations were conducted using a vapour diffusion method for **C1N4DBC** in DMF and Xy, and a solvent volatilization method for the others. (Table S1 and Fig. S1)

CBPDBC was recrystallized with DMF and TCB at 100 °C, affording low crystalline participation of HOF: **CBPDBC-1** due to the poor solubility. **C1N4DBC** yielded micro crystals of HOF: **C1N4DBC-1** under any conditions (All crystals showed the same diffraction patterns shown in Fig. S7). Unless otherwise noted, crystal included Mes is denoted a **C1N4DBC-1(Mes)** and the one included Xy is denoted as **C1N4DBC-1(Xy)**. **C1N5DBC** and **C2N6DBC** were recrystallized with tBuXy at 70 °C and yielded needle single crystals **C1N5DBC-1** and **C2N6DBC-1**. **C2N6DBC** was also yielded a single crystal from the mixture of DMF and MeBz: **C2N6DBC-2**, which is isostructural as **C2N6DBC-1** (Figs. S5 and S6). **C1N4DBC-1(Mes)** include approximately three mesitylene molecules in the pore as determined by TGA and NMR (Figs. S12 and S15).

Table S1. Crystallization conditions and resultant frameworks

Compound name	Polar solvent [a]	Guest solvent [a]	Method	Framework
CBPDBC	DMF	TCB	volatilization	**CBPDBC-1**
C1N4DBC	DMF	Xy	vapour diffusion	**C1N4DBC-1**
	dioxane	Xy	volatilization	**C1N4DBC-1**
	DMF	Mes	volatilization	**C1N4DBC-1**
	dioxane	Mes	volatilization	**C1N4DBC-1**
C1N5DBC	DMF	tBuXy	volatilization	**C1N5DBC-1**
C2N6DBC	DMF	tBuXy	Volatilization	**C2N6DBC-1**
	DMF	MeBz	Volatilization	**C2N6DBC-2**

[a] Abbreviations in polar solvent and guest solvent defined in the above description.

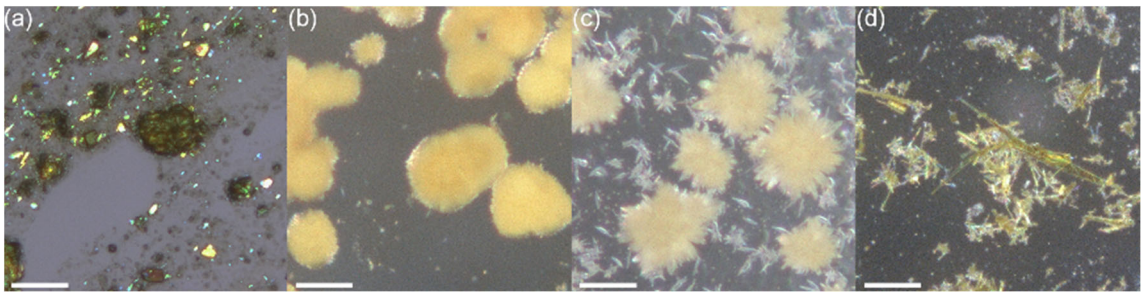

Fig. S1 Polarized optical microscopy (POM) images of (a) **CBPDBC-1**, (b) **C1N4DBC-1**, (c) **C1N5DBC-1** and (d) **C2N6DBC-1** under daylight. Scale bar: 200 mm.

3-1. Crystallography of **C1N5DBC-1**

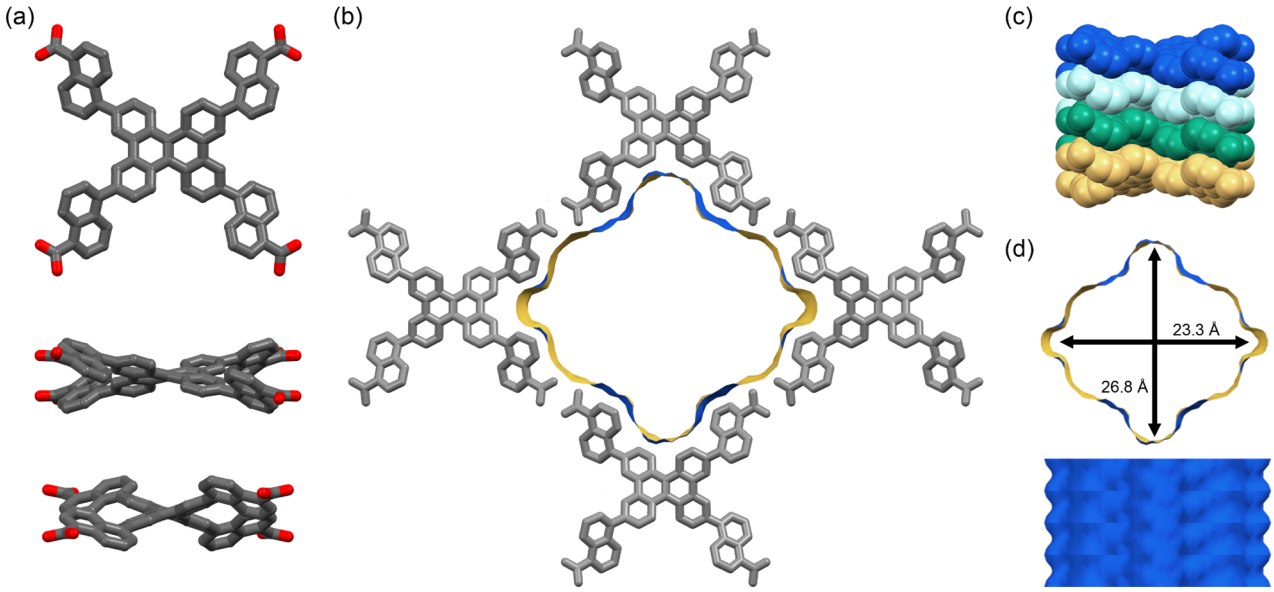

Fig. S2 Crystal structure of **C1N5DBC-1** with the major site. (a) molecular conformations viewed down the *c* axis (top), *b* axis (middle), and *a* axis (bottom). (b) packing diagrams and visualized void surface with blue (outside) and yellow (inside). (c) 1D π-stacked columnar structure. (d) visualized void surface viewed down along the c axis (top) and the ab planes (bottom). The structure of the minor site is not shown for clarity.

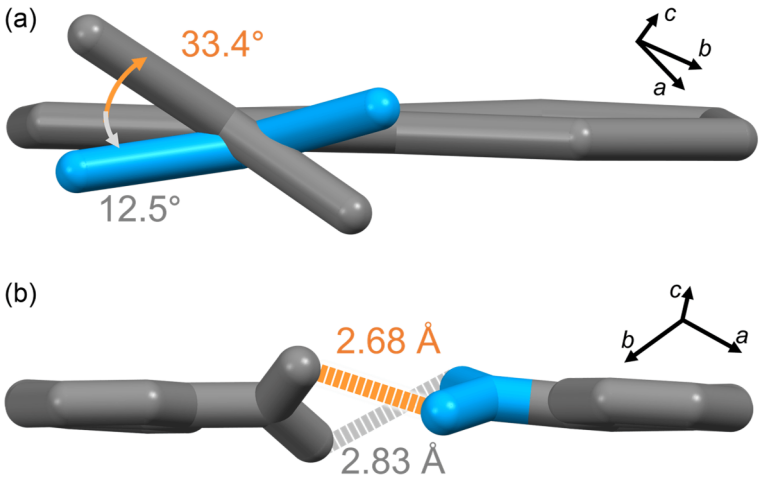

Fig. S3 Disordered carboxylic acid of **C1N5DBC-1**. Colour code: Gray (major site), cyan (minor site). (a) Dihedral angles of carboxylic acids viewed parallel toward the plane of naphthyl moiety. (b) Distorted complimentary dimer of H-bond between the major and minor sites, which is twisted by 45°.

3-2. Crystallography of **C2N6DBC-1**

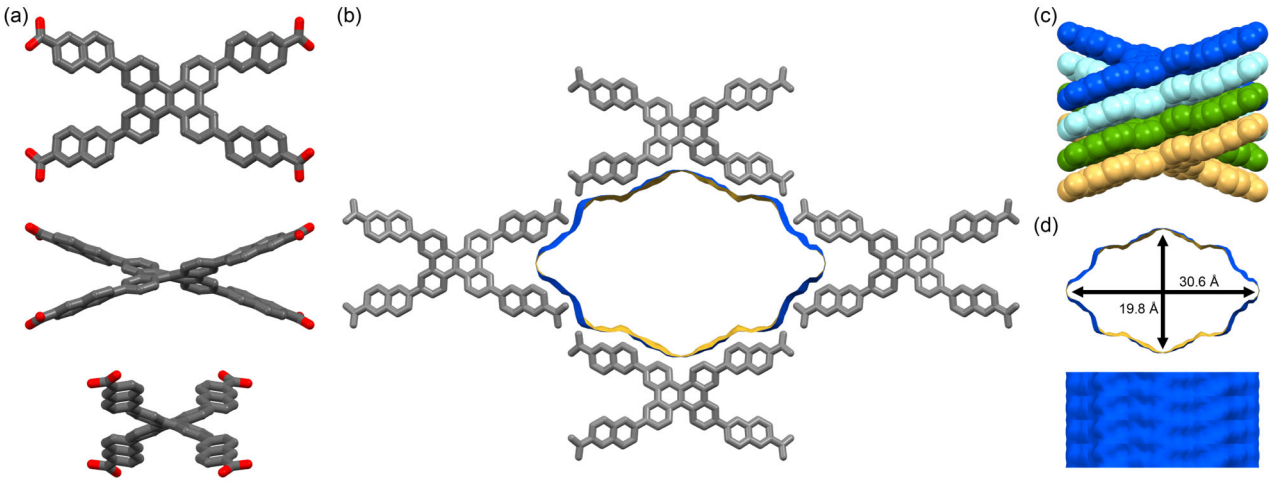

Fig. S4 Crystal structure of **C2N6DBC-1** with major site. (a) molecular conformations viewed down the *c* axis (top), *b* axis (middle), and *a* axis (bottom). (b) packing diagrams and visualized void surface with blue (outside) and yellow (inside). (c) 1D π-stacked columnar structure. (d) visualized void surface viewed down along the *c* axis (top) and the *ab* planes (bottom). The structure in minor site is not shown for clarity.

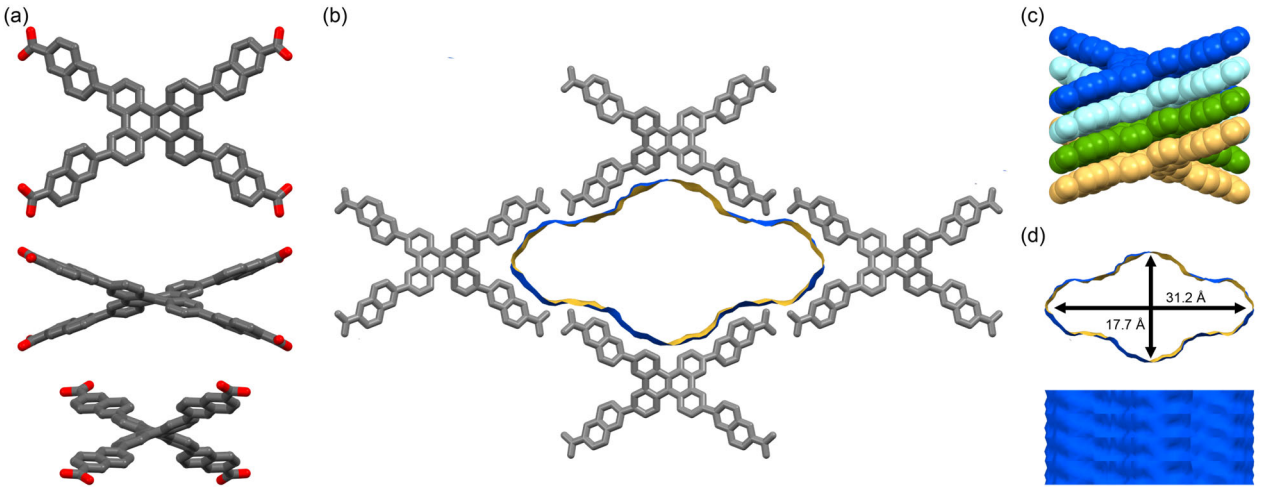

Fig. S5 Crystal structure of **C2N6DBC-2** with major site. (a) molecular conformations viewed down the *c* axis (top), *a* axis (middle), and *b* axis (bottom). (b) packing diagrams and visualized void surface with blue (outside) and yellow (inside). (c) 1D π-stacked columnar structure. (d) visualized void surface viewed down along the *c* axis (top) and the *ab* planes (bottom). The structure in minor site is not shown for clarity.

C2N6DBC-2 was yielded from crystallization by slow evapouration from a mixture of DMF and MeBz at 70 °C(Table S1). The structure is shown in Fig. S5. **C2N6DBC-2** had similar and isostructural HOF to **C2N6DBC-**

1 (Figs. S4,5), but there were some differences (Figs. 4b,d, S6, S11e,f, and Table S3). These peripheral groups were disordered in two positions with a site occupancy of 0.58 and 0.42 (Figs. 4b,d and S6). The bond angle of the peripheral groups Ar-B (Fig. 1) was 125°, suggesting that the strain was larger than that of **C2N6DBC-1** (119°). This disorder and strain made the hydrogen-bond network complex (Fig. S6). A complementary H-bonding with a length of 2.73 Å existed between major–minor, and two truncated H-bond with a length of 2.77 Å and 2.89 Å existed between major–major and minor–minor, respectively, which can exist randomly in the crystals.

The major formed a conformation with naphthyl groups located far apart, and the minor formed the one with naphthyl groups close together. (Scheme S2c) This combination was opposite to that of **C2N6DBC-1**. Planarity was different with RMSD of 0.737 (**C2N6DBC-2**) and 0.716 (**C2N6DBC-1**), which resulted in a different number of interpenetrations with **C2N6DBC-2** of 9-fold and **C2N6DBC-1** of 8-fold (Fig. S11). The rhombic apertures were a the dimensions of 31.6 Å ×10.8 Å for major site, and of 28.1 Å ×17.7 Å for minor site. Void ratio of major and minor were calculated to be 56.4% and 55.2%, respectively. The void ratio was smaller than that of **C2N6DBC-1** despite the void dimension were smaller. This mismatch is due to the difference in the assembling of peripheral groups. In other words, **C2N6DBC-1** formed ideal transected hydrogen bonds, while **C2N6DBC-2** did not form because the pore surface in **C2N6DBC-1** was more undulated.

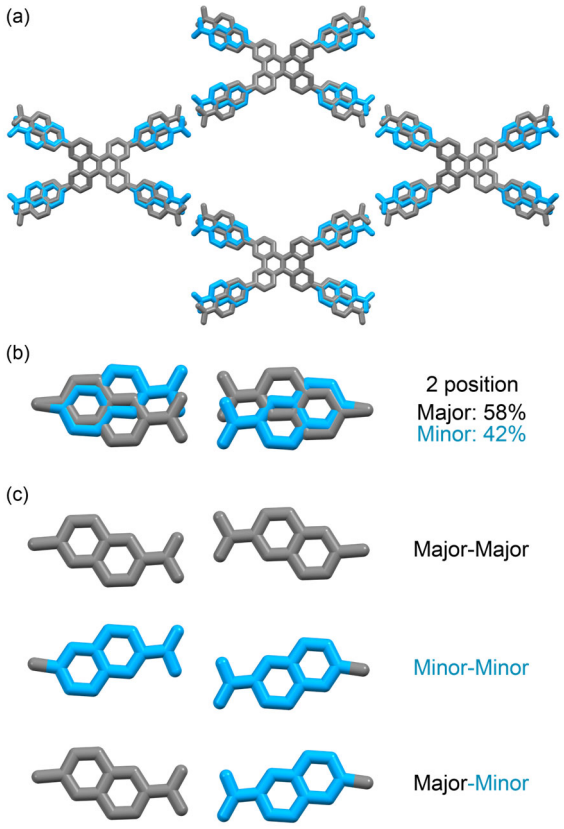

Fig. S6 Disordered peripheral structure in **C2N6DBC-2**. (a) Rhombic network, (b) 2-carboxynaphthyl groups of major (ratio: 58% and conformation: far) and minor (ratio: 42%, conformation: close) sites, and (c) H-bonding

networks between major–major, minor–minor, major–minor. Major and minor showed grey and cyan, respectively. “Conformation” denotes the molecular conformation with naphthyl groups (far) far apart shown in right of Scheme S2c, and (close) close together shown in left of Scheme S2c

3-3. Crystallography of **C1N4DBC-1**

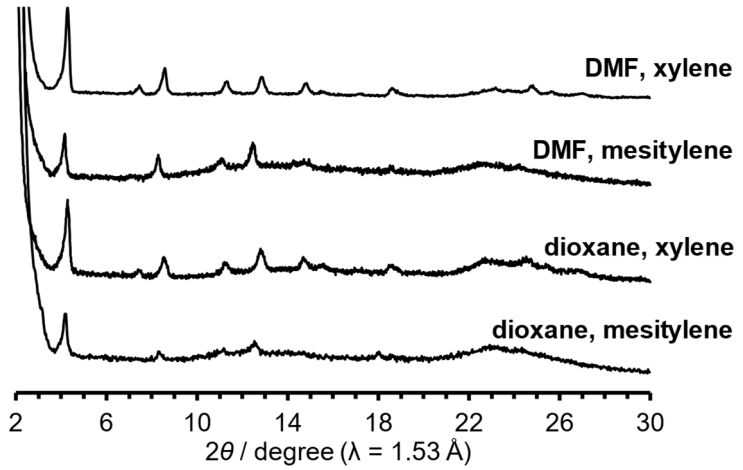

Fig. S7 PXRD patterns of as-formed crystalline balks of **C1N4DBC-1** crystalized from each mixed solution.

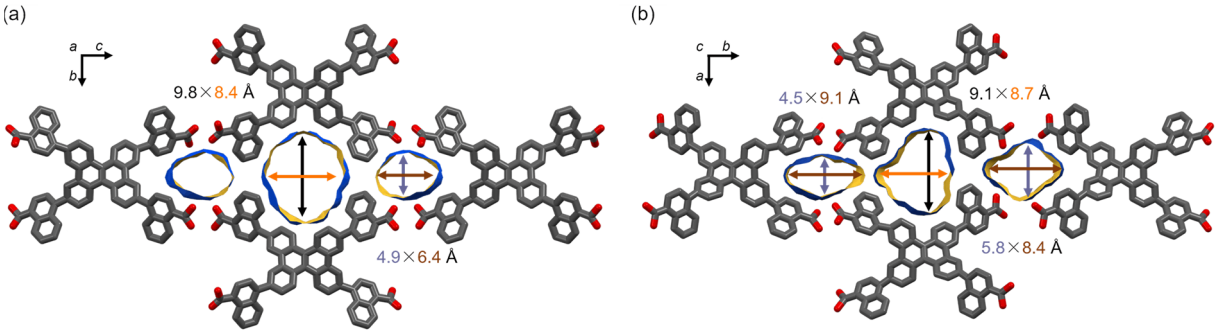

Fig. S8 (a) Preliminary single crystal structure of **C1N4DBC-1x** from electron diffraction measurement. (b) Crystal structure of **C1N4DBC-1a** from PXRD analysis. Void surfaces are visualized with blue (outside) and yellow (inside).

C1N4DBC-1x was an isostructural HOFs via shape-fitted docking of DBC core. (Figs. 7a,b,c and S8a) The constituent molecule exhibited a conformation with the naphthyl groups far apart (Scheme S2a). The stacking axis of the DBC molecule was slightly tilted at 2.6°, with a period of about 4.0 Å (Fig. 7b). The bond angle of the peripheral groups Ar-B (Fig. 1) was about 130°. The carboxylic acid formed two complementary dimers (Fig. 7c). One was a distorted dimer with an O•••O bond length of 2.7 Å and with a tilt of 10°, and the other was a dimer with an O•••O bond length of 2.7 Å. Compared to other naphthyl DBC structures, the pores were shrunk along the b axis, which was the height of rhomboid. The facing 1-naphthyl groups were close to each other until they were in contact,

resulting in the pore divided into three channels. One channel was a larger central part (9.8 Å × 8.4 Å) and the others were smaller parts on the side (4.9 Å × 6.4 Å). **C1N4DBC-1a** had asymmetrical pores on both sides, whereas **C1N4DBC-1x** had symmetrical pores on both sides (Fig. S8a). but There was a good agreement between the simulation pattern of this structure with the experimental one (Fig. S22c), suggesting that the initial structure was transferred to this structure upon activation.

3-4. Crystallography of **CPDBC-1**

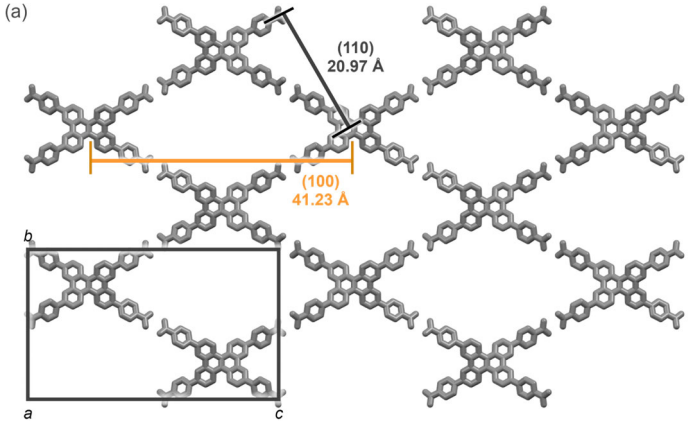

Fig. S9 Crystal structure of **CPDBC-1** as a reference.[S19]

3-5. Crystal data

Table S2. Structural data of single crystals (**CPDBC-1**, **C1N4DBC-1x**[a], **C1N5DBC-1, C2N6DBC-1**, and **C2N6DBC-2)**.[b]

	CPDBC-1	**C1N4DBC-1x**[a]	**C1N5DBC-1**	**C2N6DBC-1**	**C2N6DBC-2**
RMSD of DBC core	0.680	0.73	0.6689	0.7164	0.7369
Bond angle of peripheral group ω (Ar-B, major) / °	121.48	122	123.72	122.92	125.88
Bond angle of peripheral group ω (Ar-B, minor) / °	—	—	123.72	119.40	114.11
Dihedral angle of B-B' / °	13.10	15	9.04	15.11	16.87
Dihedral angle of C-C' / °	20.74	22	20.46	38.65	39.73
Dihedral angle of Ar-B (major) / °	36.65	36.7	41.48	31.35	29.28
Dihedral angle of Ar-B (minor) / °	—	—	41.48	31.92	28.27
π-π stacking distance between DBC core / Å	3.762	4.0	3.861	3.838	3.797
π-π stacking distance between naphthyl groups / Å	3.422	—	3.345	3.535	3.486
void size (major) / Å×Å	29.1×15.3	9.8×8.4, 4.9×6.4	26.8×23.3	22.7×17.9	31.6×18.0
void size (minor) / Å×Å	—	—	26.8×23.3	30.8×19.8	28.1×17.7
void ratio (major) / %	56.4	32	58.3	58.4	56.4
void ratio (minor) / %	—	—	58.3	59.7	55.2
chemical occupancy (major) / %	—	—	55.0	60.7	57.5
chemical occupancy (minor) / %	—	—	45.0	39.3	42.5
reference	Ref. S19	this work	this work	this work	This work

[a] Single crystal structure after activation form the electron diffraction experiment. [b] RMSD denotes “root mean square derivation”. “Ar” and “B” means aromatic moieties shown in Fig.1. “Major” or “minor” denote the framework constructed by only molecules with disordered major site or minor site at peripheral groups.

Table S3. Crystal data of **C1N5DBC-1** and **C2N6DBC-1** and **C2N6DBC-2**.

	C1N5DBC-1	**C2N6DBC-1**	**C2N6DBC-2**	**C1N4DBC-1x**
Chemical formula	$C_{70}H_{40}O_8$	$C_{70}H_{40}O_8$	$C_{70}H_{40}O_8$	$C_{70}H_{40}O_8$
M_r	1009.02	1009.02	1009.02	1009.02
Crystal system	*Orthorhombic*	*Orthorhombic*	*Orthorhombic*	*Monoclinic*
space group	*Pban*	*Pban*	*Fddd*	*C2/c*
Temperature (K)	293	293	293	293
a (Å)	38.629 (1)	48.3296 (8)	52.040 (4)	4.0 (5)
b (Å)	32.6902 (13)	28.3016 (10)	97.015 (2)	35.6 (15)
c (Å)	3.8606 (1)	3.8380 (1)	3.7969 (1)	43.4 (8)
V (Å^3)	4875.1 (3)	5249.6 (2)	19169.3 (16)	6249 (869)
Z	2	2	8	4
Radiation type	Synchrotron, λ = 0.81059 Å	Synchrotron, λ = 0.81081 Å	Synchrotron, λ = 0.81063 Å	Transmission electron micro-scope, λ = 0.0251 Å
Crystal size (mm)	0.15 × 0.03 × 0.03	0.20 × 0.02 × 0.01	0.20 × 0.05 × 0.002	0.001 × 0.001 × 0.001
No. of measured, Independent, and observed [$I > 2\sigma(I)$] reflections	54995, 5966, 4288	43209, 6244, 3155	40772, 5693, 1901	5507, 2631, 1013
R_{int}	0.074	0.088	0.091	0.130
$(\sin\theta/\lambda)_{max}$ (Å^{-1})	0.677	0.676	0.679	0.500
$R1[F^2 > 2\sigma(F^2)]$, $wR2(F^2)$, S	0.087, 0.292, 1.12	0.104, 0.358, 1.14	0.098, 0.363, 0.94	0.277, 0.664, 1.03
No. of reflections	5966	6244	5693	2631
No. of parameters	205	247	235	306
No. of restraints	199	431	264	546
$\Delta\rho_{max}$, $\Delta\rho_{min}$ (e Å^{-3})	0.45, −0.18	0.28, −0.14	0.28, −0.16	0.34, −0.24
CCDC Nos.	2210180	2210179	2210181	-

Table S4. Lattice parameters estimated from PXRD patterns of **C1N4DBC-1**, **-1(benzene)**, and **-1a**.

Name	**C1N4DBC-1**	**C1N4DBC-1(benzene)**	**C1N4DBC-1a**
System	*Orthorhombic*	*Monoclinic*	*Monoclinic*
Space group	*Pnnn*	*Pn*	*Pn*
a / Å	23.2816(5)	22.3800(8)	17.8138(43)
b / Å	41.7595(10)	42.1796(14)	43.313(11)
c / Å	4.09925(8)	4.6813(2)	3.9778(10)
α / degree	90	90	90
β / degree	90	95.9104(8)	90.798(49)
γ / degree	90	90	90
V / Å^3	3985.50	4395.59	3080.09
R_{wp} / %	3.50	2.88	7.59
R_p / %	1.87	2.09	5.01
Temperature / K	298	298	298

3-6. Table of PXRD patterns and *d* spacing

Table S5. Peak parameter of **CBPDBC-1** and lattice spacing of predicted frameworks.

$2\theta_{obs.}$ / °	$d_{obs.}$ / Å	*h*	*k*	*l*	$2\theta_{calc.}$ / °	$d_{calc.}$ / Å
1.54	57.37	0	0	1	1.583	55.8
3.08	28.68	0	0	2	3.167	27.9
4.74	18.64	0	0	3	4.751	18.6
6.28	14.07	0	0	4	6.336	13.95

Table S6. Lattice parameters of simulation of **CPDBC-1** and observed **C1N4DBC-1**.

h	*k*	*l*	$2\theta_{CPDBC\text{-}1\ obs.}$ / °	$d_{CPDBC\text{-}1\ obs.}$ / Å	$2\theta_{C1N4DBC\text{-}1\ calc.}$ / °	$d_{C1N4DBC\text{-}1\ calc.}$ / Å
0	1	1	4.21	20.988	4.30	20.559
0	2	0	7.27	12.164	7.45	12.164
0	2	2	8.43	10.493	8.55	10.339
0	3	1	11.11	7.9615	11.34	7.8056
0	3	3	12.67	6.9892	12.89	6.8703
0	4	0	14.55	6.0885	14.78	5.9951

Table S7. Peak parameter of **C2N6DBC-1** and lattice spacing of predicted frameworks.

C2N6DBC-1		Predicted lattice spacing of (110), (220), (330), and (440), respectively		
$2\theta_{obs.}$ / °	$d_{obs.}$ / Å	close d_{calc} / Å	far d_{calc} / Å	heteromeric d_{calc} / Å
3.964	23.69	21.52	26.65	24.57
7.344	12.04	10.76	13.33	12.28
11.13	7.953	7.175	8.884	8.190
14.93	5.932	5.381	6.663	6.142

Table S8. Peak parameter of **C1N5DBC-1** and lattice spacing of predicted frameworks.

C1N5DBC-1		Predicted lattice spacing of (110), (220), (330), and (440), respectively	
$2\theta_{obs.}$ / °	$d_{obs.}$ / Å	close d_{calc} / Å	far d_{calc} / Å
3.568	24.76	24.36	15.21
7.061	12.52	12.18	7.606
10.63	8.32	8.12	5.07
14.2	6.235	6.09	3.803

There are two possible high-symmetrical conformations in naphthyl substituted DBC derivatives. One is a conformation with naphthyl groups close together, which denoted “close”, and the other is a conformation with naphthyl group far apart, which is denoted “far”. (Scheme S2) Possible frameworks based on these conformations are shown in scheme S3. Comparing the obtained diffraction patterns, **C1N5DBC-1** is in good agreement with the “far” framework, which is constructed by “far” molecules. (Table S7c) **C2N6DBC-1** is relatively consistent with the “heteromeric” framework, which is constructed by both of “close" and “far” molecules. (Table S8)

3-7. Plausible molecular conformations and predicted frameworks.

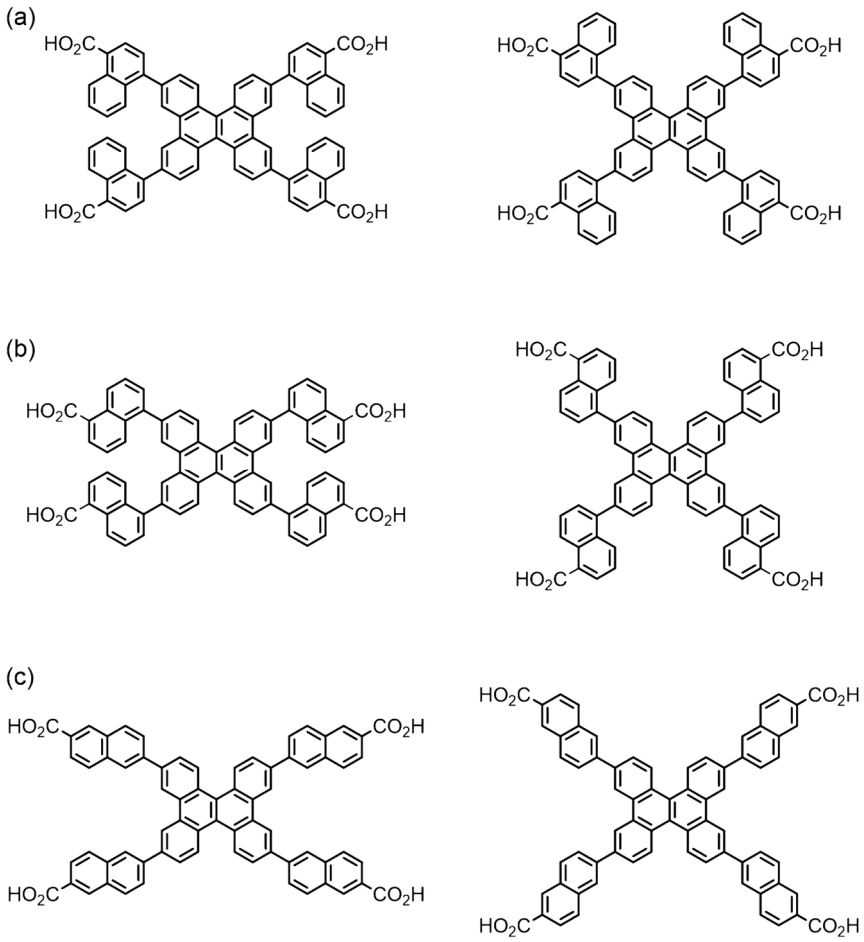

Scheme S2. Tow plausible conformations of (a) **C1N4DBC**, (b) **C1N5DBC** and (c) **C2N6DBC** with naphthyl groups close together (left) and far apart (right).

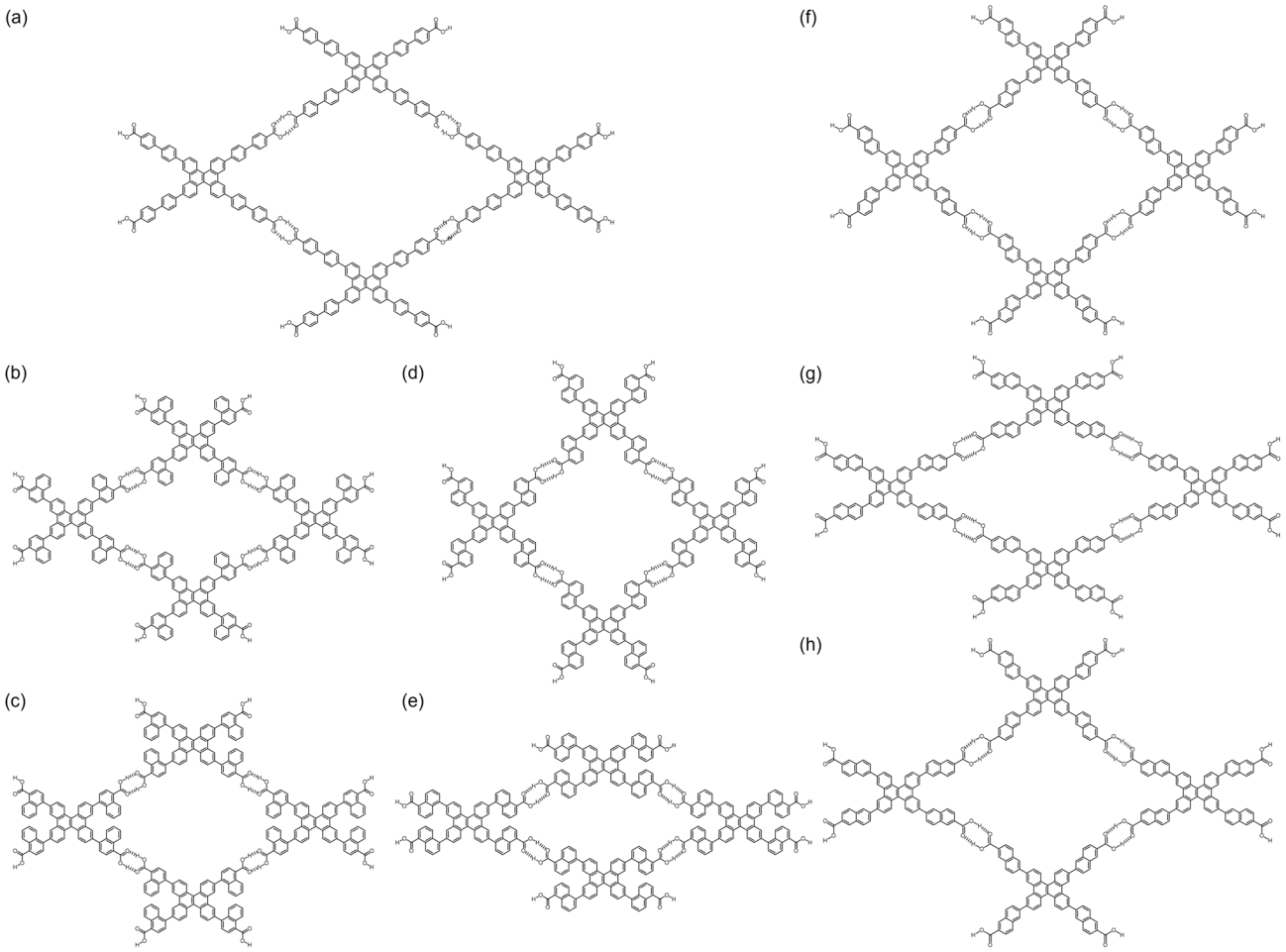

Scheme S3. Predicted rhombic 3D frameworks of (a) **CBPDBC**, (b,c) **C1N4DBC**, (d,e) **C1N5DBC** and (f–h) **C2N6DBC**, which are constructed by molecular conformation shown in scheme S2.

3-8. POM images of **C1N4DBC-1**

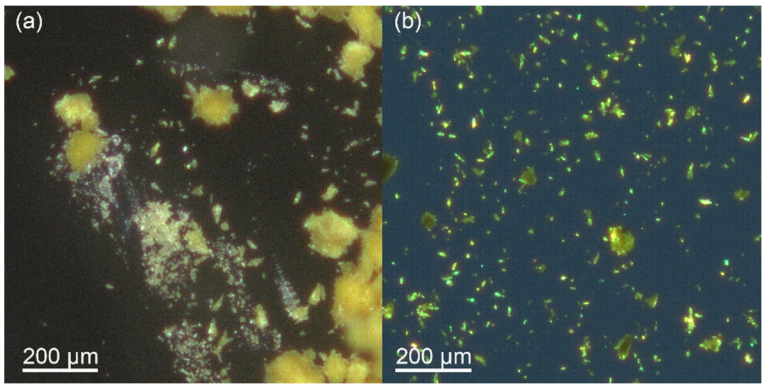

Fig. S10 Polarized optical microscopy (POM) images of (a) **C1N4DBC-1a** and (b) **C1N4DBC-1x** under ambient light. Scale bar: 200 μm.

3-9. Interpenetration of DBC HOFs

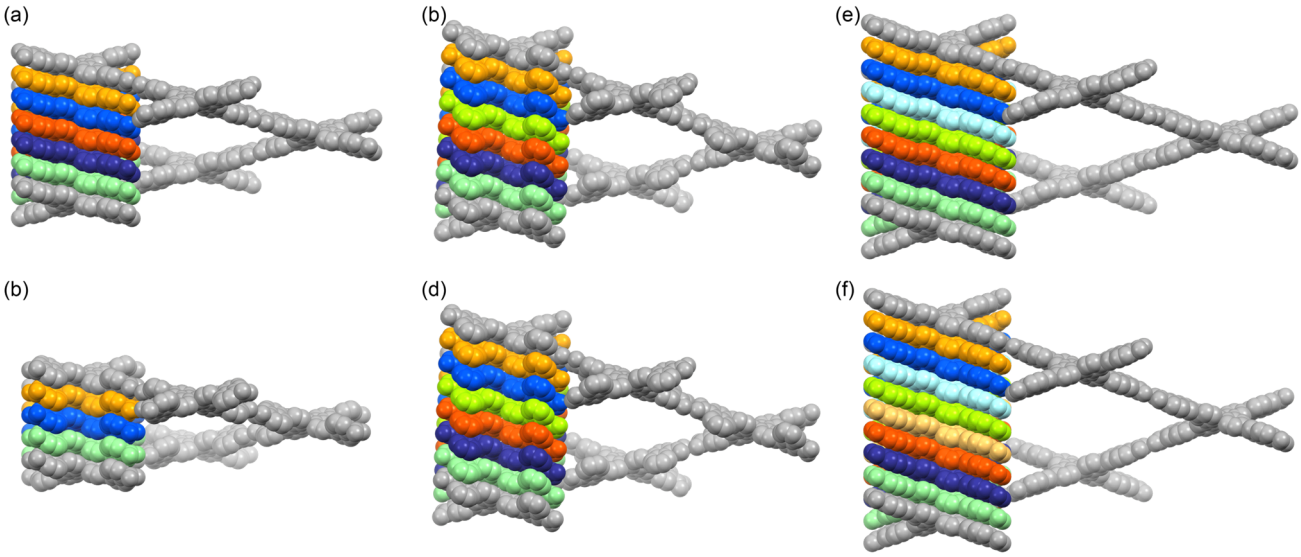

Fig. S11 Single ***dia***-network (coloured grey) and 1D stacked columnar structures, for which the number of colours in the stacked molecules correspond to the number of the frameworks interpenetrated. (a) **CPDBC-1** as a reference[S19], (b) **C1N5DBC-1**, (c) **C1N4DBC-1x**, (d) **C1N4DBC-1a**, (e) **C2N6DBC-1** and (f) **C2N6DBC-2**.

Single ***dia***-networks and 1D stacked columnar structures are shown in Fig. S11. **C1N4DBC-1** had nearly the same arrangement of carboxylic acid moieties as that of **CPDBC-1**, but due to increasing distortion of the DBC core, the helical pitch increased, and the number of interpenetrations increased to 7-fold from 6-fold. The location of carboxylic acid dimers in **C1N5DBC-1** differed from those in **C1N4DBC-1** and was closer in height to the DBC plane. Therefore, the helical pitch became smaller, resulting in a 4-fold interpenetration. In the HOFs of **C2N6DBC**, the number of interpenetrations increased because the helical pitch was elongated with the longer length of peripheral groups. The number of interpenetrations was 8-fold of **C2N6DBC-1** and 9-fold of **C2N6DBC-2**, which were different due to the distortion of the DBC cores (Table S2).

4. Measurement

4-1. Thermogravimetric analysis

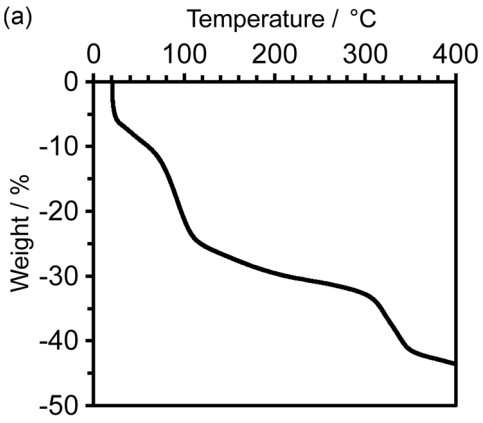

Fig. S12 TG profile of **C1N4DBC-1(Mes)**.

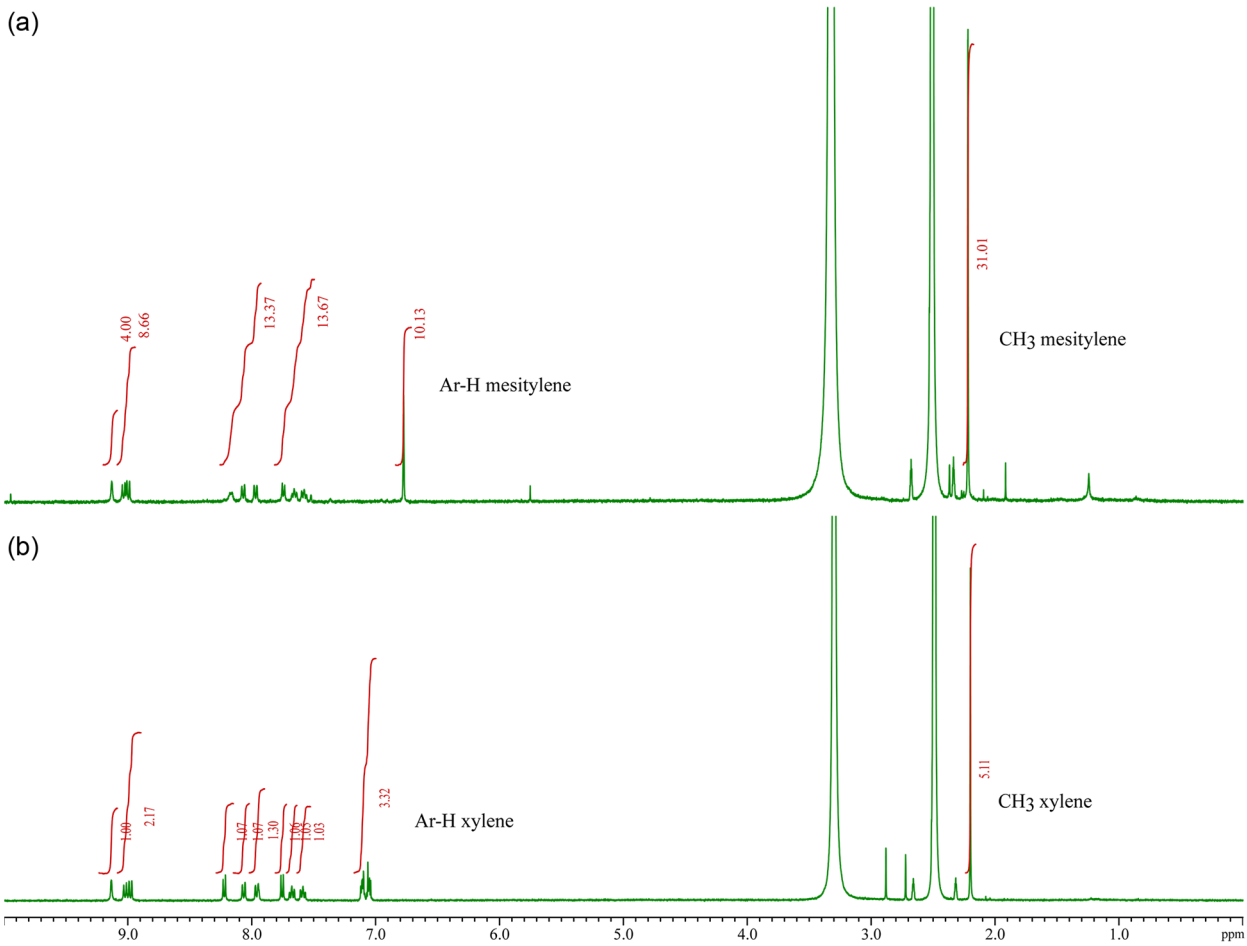

Fig. S13 ^{1}H-NMR (DMSO-d_6, 400 MHz) of (a) **C1N4DBC-1(Mes)** crystalized with Mes and (b) **C1N4DBC-1(Xy)** crystalized with Xy.

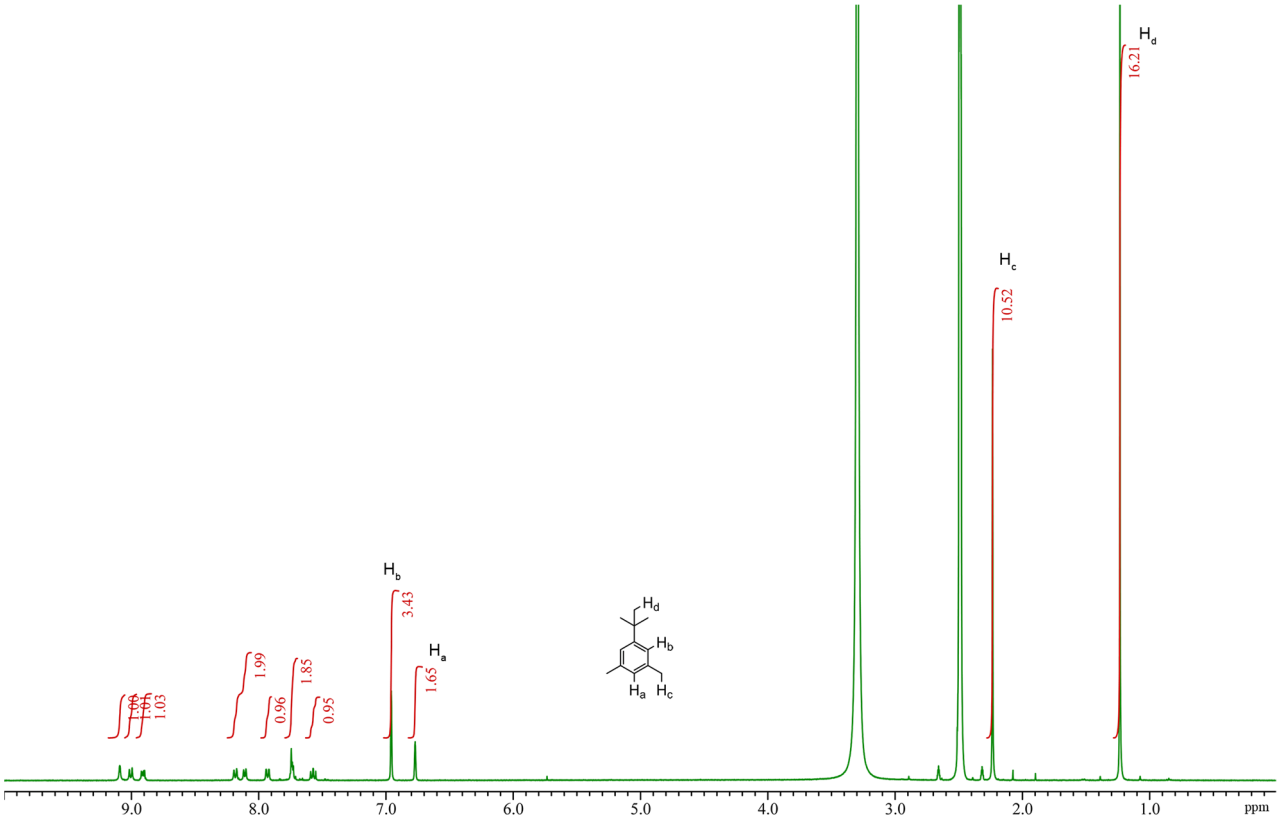

Fig. S14 ^{1}H-NMR (DMSO-d_6, 400 MHz) of **C1N5DBC-1**.

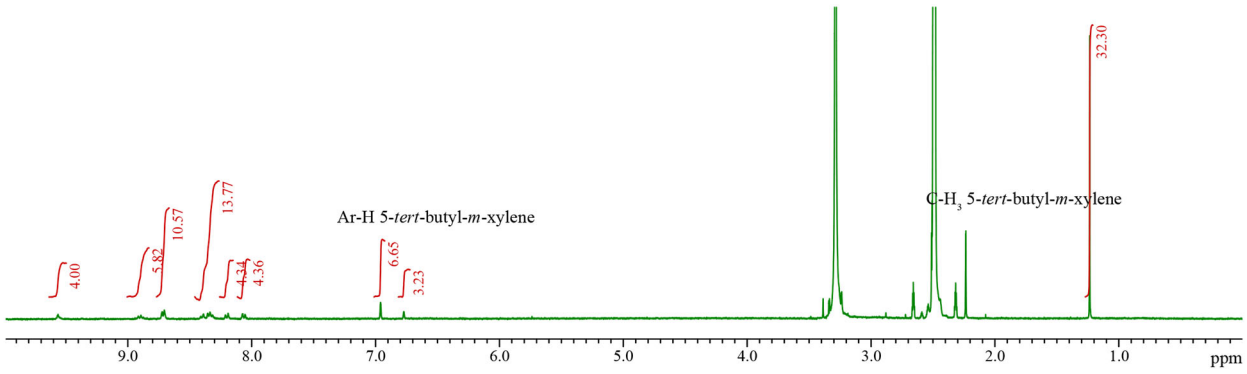

Fig. S15 ^{1}H-NMR (DMSO-d_6, 400 MHz) of **C2N6DBC-1**.

4-2. Activation of the HOFs

To remove guests at the pores, activation was performed by freeze-drying (FD) in addition to thermal vacuum (TV) and displacement vacuum (RV). Freeze-dry (FD) method was that the as-formed crystalline powder was immersed in benzene to replace the included solvent with benzene, followed by freeze-drying to remove benzene by sublimation. The TV method was that the powder was heated at 90–150 °C under vacuum. The RV method was that as-formed crystalline powder was immersed in benzene to replace the included solvent with benzene, followed by heating at 60–100 °C under vacuum to remove benzene. The complete removal of the solvent was confirmed by ^{1}H-NMR (Figs. S17–S19)

The activations of **C1N4DBC-1(Xy)**, **C1N4DBC-1(Mes)**, **C1N5DBC-1**, **C2N6DBC-1**, and **C2N6DBC-2** by TV method were performed at 90, 90, 120, 180, and 180 °C, respectively. Those of RV method were performed at 60, 60, 60, 100, and 100 °C, respectively. The activation of **C2N6DBC-1** by FD method was failed as it could not completely remove the benzene, so the RV method was subsequently used to remove the remaining benzene to give activated HOFs, which was denoted FD-RV (^{1}H-NMR in Fig. S19).

For **C1N4DBC-1(Xy)** (Fig. S16a), TV is the best method, by which activated HOF remained high crystallinity. The activated HOFs by RV and FD showed less crystallinity. This trend was also shown in **C1N4DBC-1(Mes)** (Fig. S16b). For **C2N6DBC-2** (Fig. S16c), the activated HOF by TV and RV was transformed to amorphous with no crystallinity. The HOF could not be activated by the FD method and was amorphized after complete removal of residual benzene by the RV method. These results indicate that **C2N6DBC-2** cannot be activated without maintaining crystallinity. This trend also was shown in **C2N6DBC-1** (Fig. S16d)

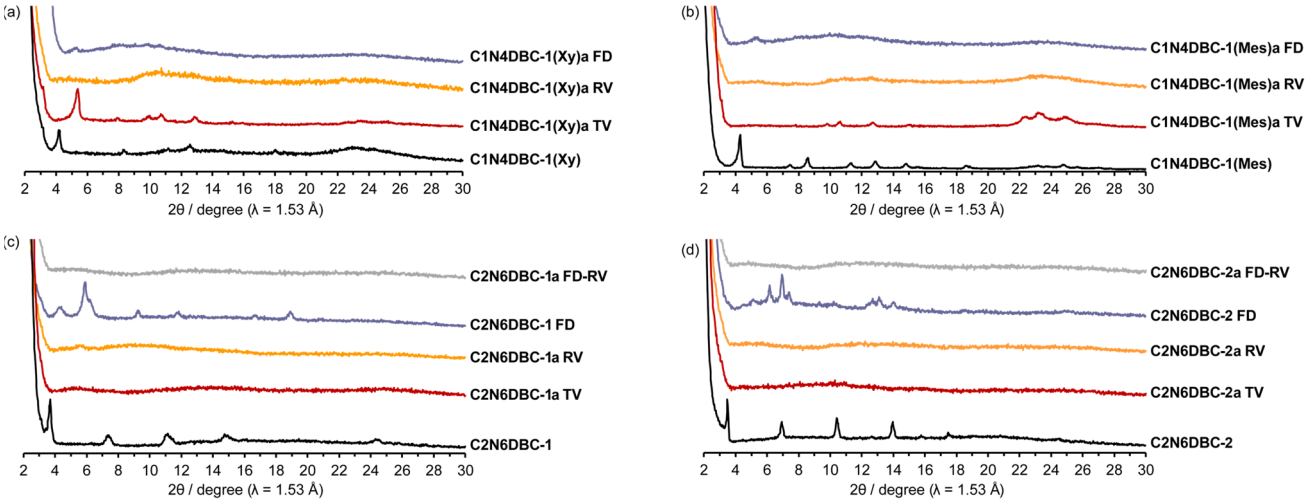

Fig. S16 PXRD patterns of as-formed and activated crystals. Activation of (a) **C1N4DBC-1(Xy)**, (b) **C1N4DBC-1(Mes)**, (c) **C2N6DBC-1** and (d) **C2N6DBC-2**. TV: thermal vacuum, RV: replace vacuum, FD: freeze-dry and FD-RV: FD following RV.

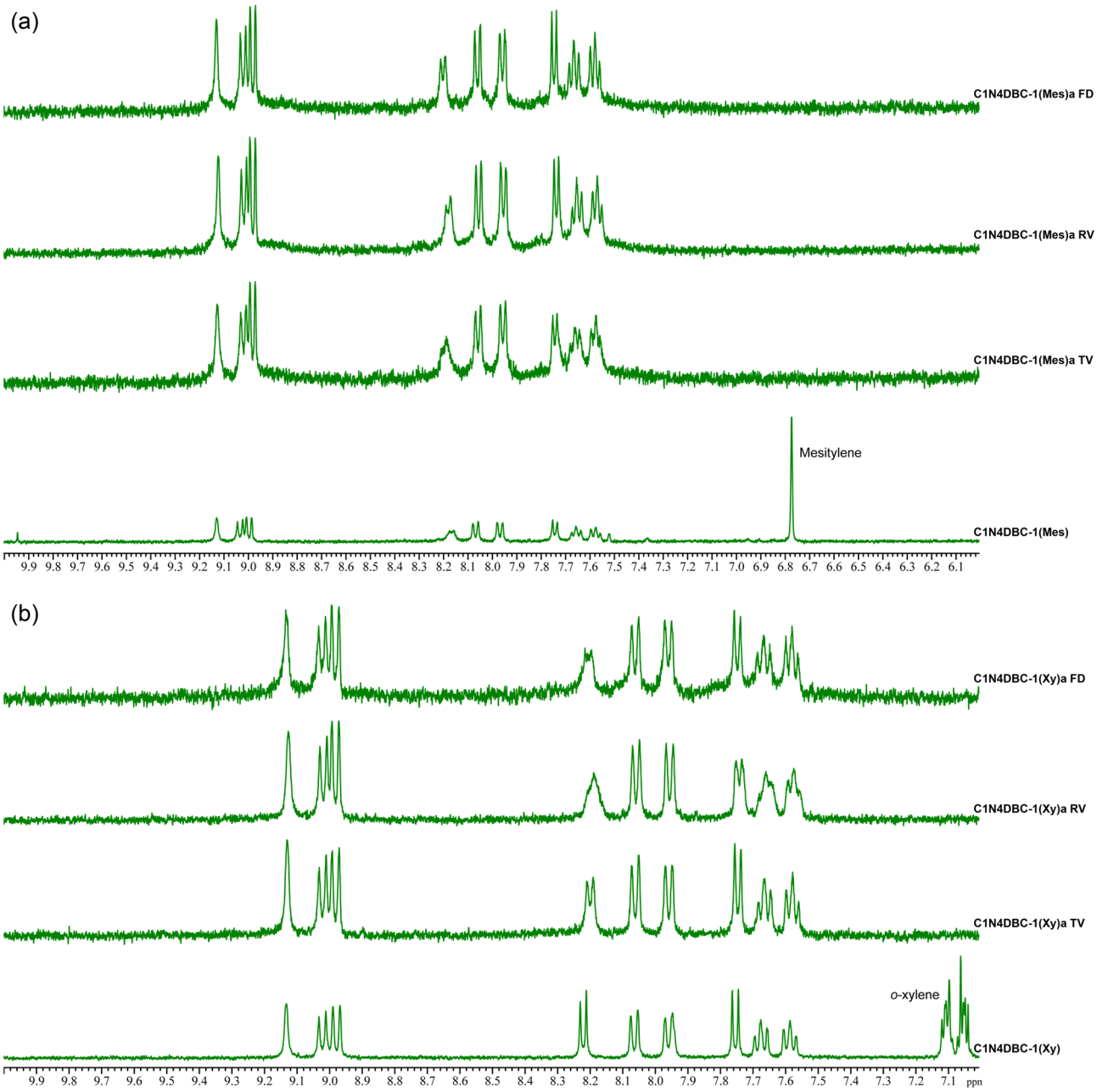

Fig. S17 ^{1}H-NMR of as-formed and activated HOFs. (a) **C1N4DBC-1(Mes)** and (b) **C1N4DBC-1(Xy)**.

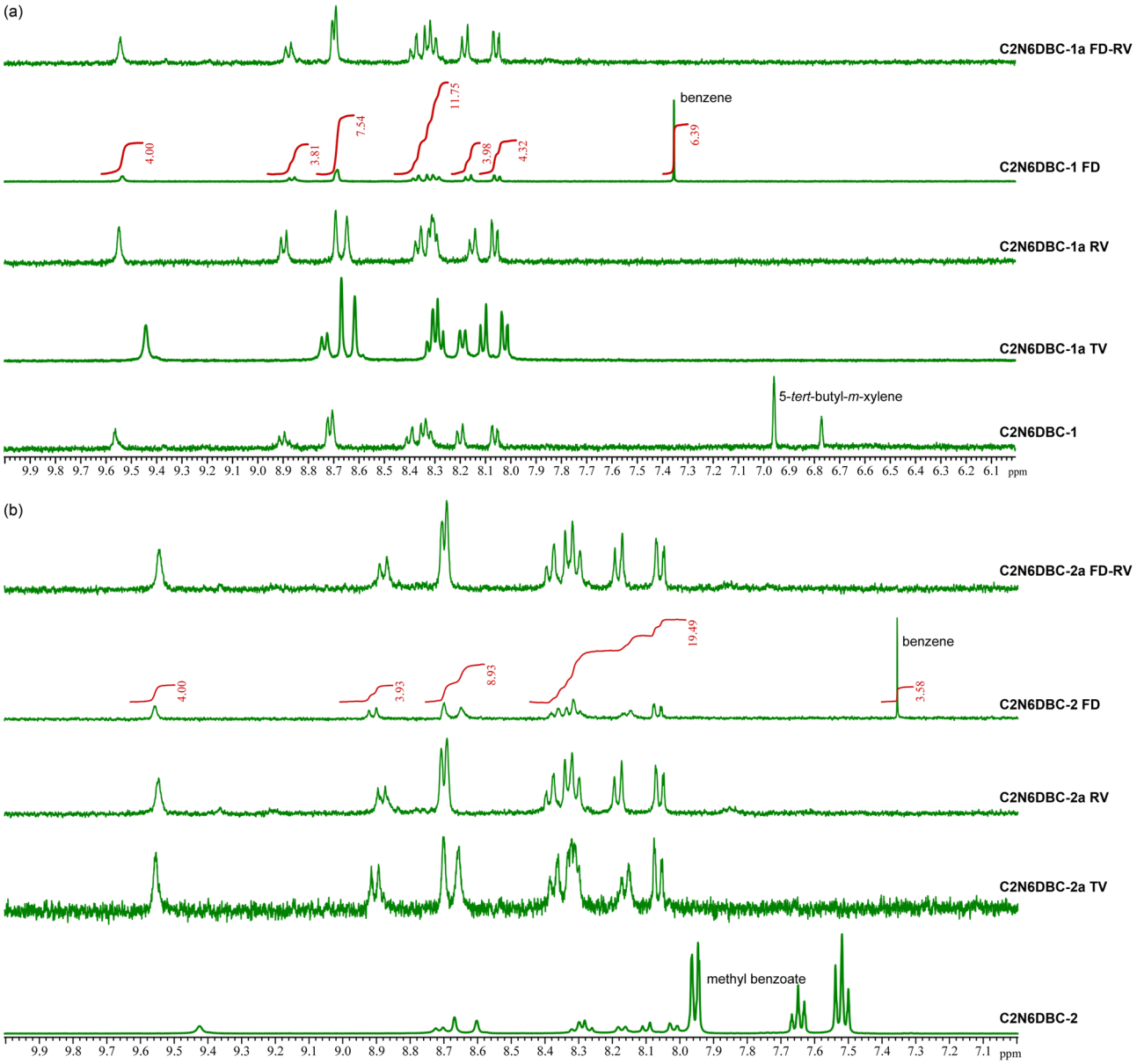

Fig. S18 ^{1}H-NMR of as-formed and activated HOFs. (a) **C2N6DBC-1** and (b) **C2N6DBC-2**.

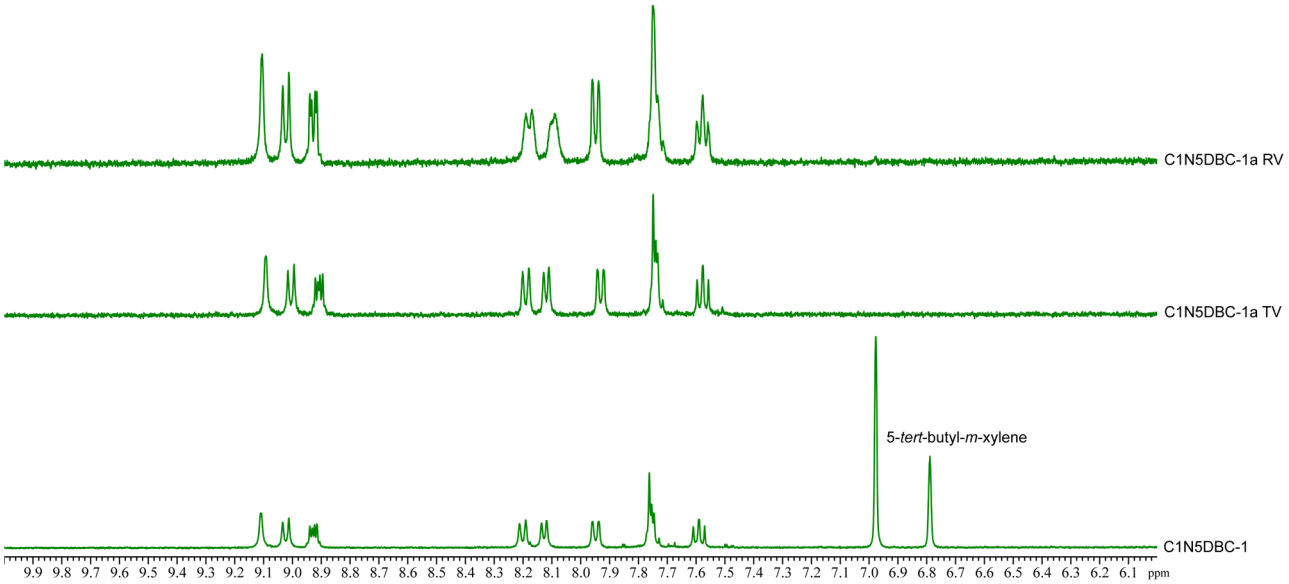

Fig. S18 ^{1}H-NMR of as-formed and activated **C1N5DBC-1**.

4-3. *In situ* PXRD measurement

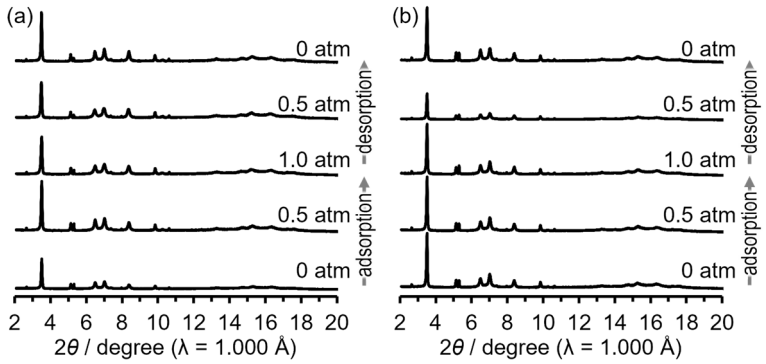

Fig. S20 *In situ* PXRD patterns of **C1N4DBC-1a** upon introduction of (a) N_2 and (b) CO_2.

4-4. BET plot

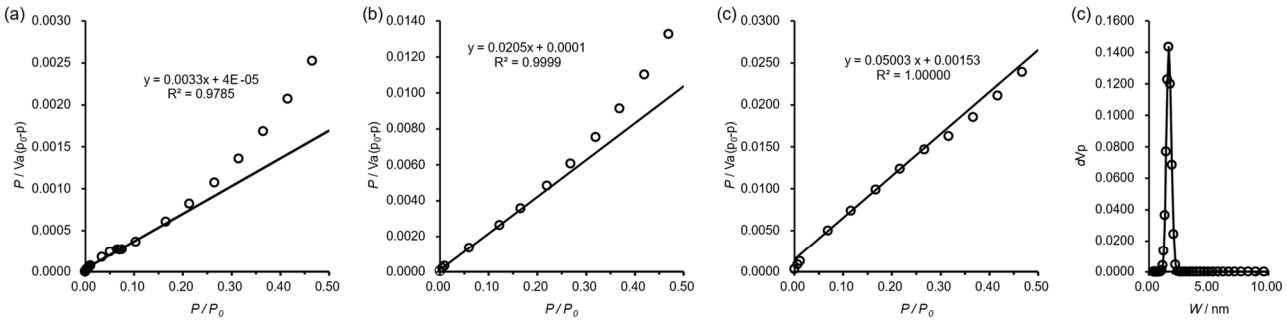

BET range limit	(p/p0=0.1224)
Maxumum Va(p_0-p)	4720.7
Vm [cm^3(STP) g^{-1}]	48.458
as(BET) [m^2g^{-1}]	2.81E+02
C	175.62
Total pore volume (p/p0=0.990) [cm^3g^{-1}]	0.2236
Average pore size [nm]	3.1806

BET range limit	(p/p0=0.3670)
Maxumum Va(p_0-p)	2.88E+04
Vm [cm^3(STP) g^{-1}]	298.74
as(BET) [m^2g^{-1}]	1.30E+03
C	89.592
Total pore volume (p/p0=0.990) [cm^3g^{-1}]	0.5798
Average pore size [nm]	1.7837

BET range limit	(p/p0=0.3670)
Maxumum Va(p_0-p)	2008.9
Vm [cm^3(STP) g^{-1}]	19.399
as(BET) [m^2g^{-1}]	1.13E+02
C	33.661
Total pore volume (p/p0=0.990) [cm^3g^{-1}]	0.1979
Average pore size [nm]	7.0316

N_2 / 77K	C
Gauss	slit
Def. pore size	Solid
*d*s [nm]	0.34
Vp [cm^3g^{-1}]	0.6166
$W_{peak(area)}$ [nm]	1.6705
$W_{peak(vol)}$ [nm]	1.6705

Fig. S21 Brunauer–Emmett–Teller (BET) plots of (a) **C1N4DBC-1a**, (b) **C1N5DBC-1a** and (c) **C2N6DBC-1a**. (d) NLDFT plot of **C1N5DBC-1a**. The calculations of **C1N4DBC-1a** and **C2N6DBC-1a** were conducted from the CO_2 isotherms. The calculations of **C1N5DBC-1a** were conducted from the N_2 isotherm.

4-5. PXRD patterns of naphthyl DBC HOFs with introducing benzene or guest molecules.

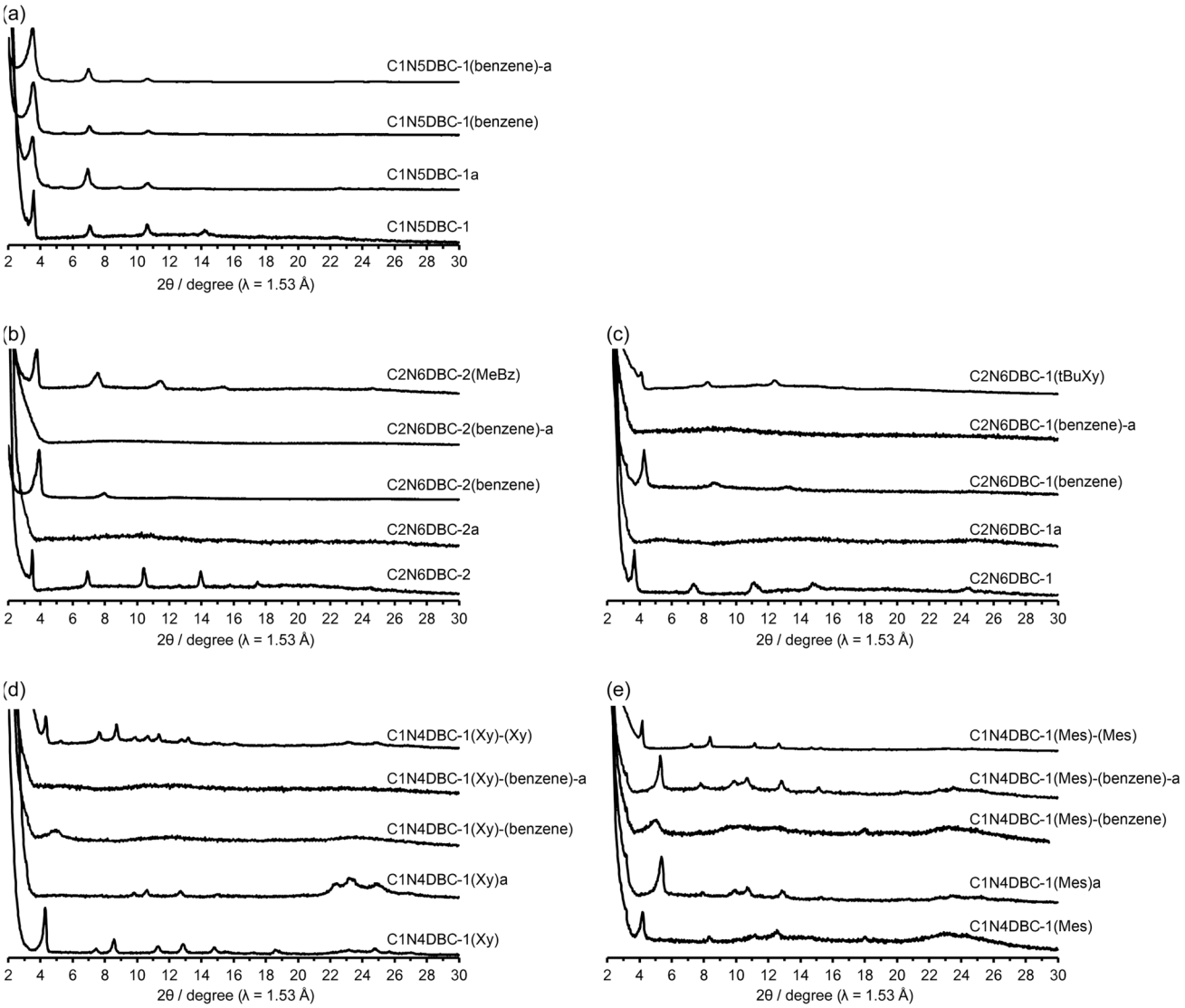

Fig. S22. PXRD patterns of activated, benzene-loaded, and benzene-removed HOFs. (a) **C1N5DBC-1**, (b) **C2N6DBC-2**, (c) **C2N6DBC-1**, (d) **C1N4DBC-1(Xy)**, and (e) **C1N4DBC-1(Mes)**.

To obtain benzene-loaded HOFs denoted as *crystal name***(benzene)** such as **C2N6DBC-1(benzene)**, activated samples were placed in saturated benzene vapour for 24 hours. Activation of benzene-loaded HOFs was performed in heating under vacuum at 70 °C (for **C1N4DBC** and **C1N5DBC**) or 100 °C (for **C2N6DBC**) to yield re-activated HOFs, denoted as *crystal name* **(benzene)-a** such as **C2N6DBC-1(benzene)-a**. The respective guest solvents used in crystallization were introduced by immersing the activated HOF for 24 hours to yield the immersed HOFs, denoted as *crystal name* **(*guest name*)** such as **C2N6DBC-1(tBuXy).**

No changes were observed in **C1N5DBC-1**, which always showed the original structure. (Fig. S22a)

Immersion in the guest solvent restored a similar pattern to that as-formed in **C1N4DBC-1** and **C2N6DBC-1** (The patterns at the top of each Figs. S22b–e). Benzene vapour introduction into **C1N4DBC-1** showed a broad peak

between the lowest pattern of as-formed and activated. (Figs. S22d,e) In simple terms, partial restoration occurred. It was also confirmed that removal of the introduced benzene caused a return to the activated HOF. (see the PXRD pattern of 0 kPa-desorption in Fig. 9)

C2N6DBC-1(benzene) also exhibited a low-angle shift (Figs. S22b,c), indicating the restoration of the crystalline structure from amorphous but not completely as-formed structure. This behavior exhibited a pattern with a wider-angle shift than **C2N6DBC-1** (minimum angle $2\theta = 4.27°$, $d = 20.69$ Å.) In addition to the disorderly structural collapse due to weak hydrogen bonds during the activation of **C2N6DBC**. The **C2N6DBC-1** is not completely identical to the **C1N4DBC**. It is suggested that the pores are restored but not as open as those in the as-formed structure.

Although the peak positions (d spacing) of the *in situ* measurements do not match those of the as-formed structure, the reason is thought to be that benzene vapourized, resulting in the amount of benzene in the pore decreasing. The *in situ* measurement is performed in closed system, in a capillary, whereas the standard measurement is performed in open system, under air.

4-6. PXRD patterns of **C1N4DBC**

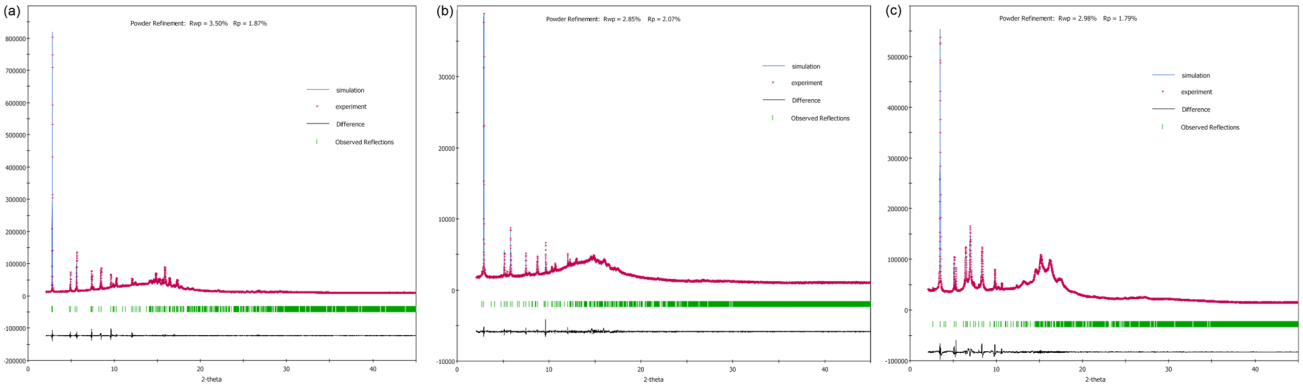

Fig. S23 Pawley refinements of (a) **C1N4DBC-1**, (b) **C1N4DBC-1a** and (c) **C1N4DBC-1(benzene)**: experimental (red), simulation (blue), difference (black, experimental minus refined profiles), and observed reflections (green).

4-7. chemical stability of **C1N5DBC-1a**.

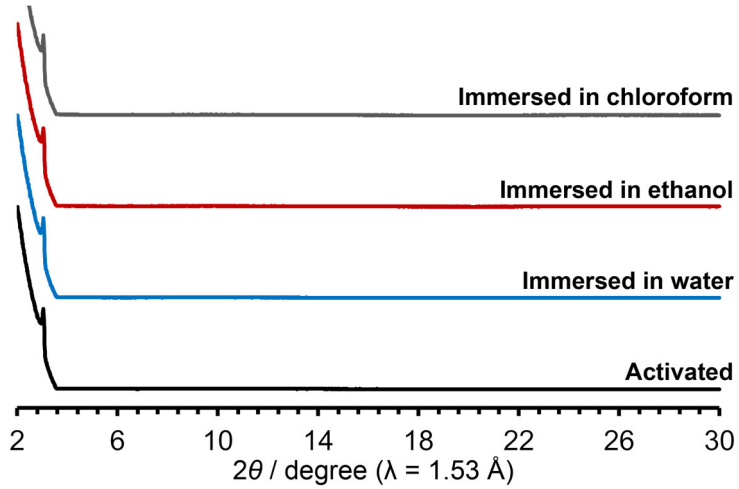

Fig. S24 PXRD patterns of **C1N5DBC-1a**. (black) activated balk crystal and balk ones immersed in (blue) water, (red) ethanol, and (gray) chloroform.

4-8. Solid state fluorescence of the activated naphthyl DBC HOFs

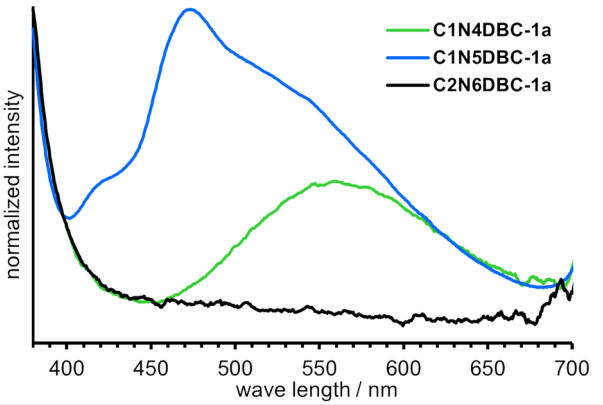

Fig. S25. Solid state fluorescence of (green) **C1N4DBC-1a**, (blue) **C1N5DBC-1**a, and (black) **C2N6DBC-1a**.

C2N6DBC-1a did not show fluorescence and **C1N4DBC-1a** and **C1N5DBC-1a** showed slight fluorescence.

5. Theoretical calculation.

5-1. Geometrical calculations of single molecule

The molecular conformation with naphthyl groups close together denotes “close” (left of Scheme S2), and that with naphthyl groups far apart denotes “far” (right of Scheme S2). Optimized close and far structures of **C1N4DBC**, **C1N5DBC**, and **C2N6DBC** were calculated by the DFT method at the B3LYP-D3/6-311G** level. These calculations were carried out using Gaussian09W. [S16]

Table S9. Bond angle, dihedral angle, and RMSD of optimized structure. Atom and plane name are shown below.[a]

	C1N4DBC_far	C1N4DBC_close	C1N5DBC_far	C1N5DBC_close	C2N6DBC_far	C2N6DBC_close
Bond angle of Ar-B / °	120.29	120.58	120.25	121.04	120.93	120.98
dihedral angle of Ar-B / °	55.88	55.52	36.94	37.34	57.39	40.97
dihedral angle of B-B' / °	13.65	12.5	14.2	14.3	13.75	4.43
dihedral angle of C-C' / °	41.01	36.3	41	41	41.45	36.82
RMSD of DBC core	0.7500	0.6801	0.7605	0.6596	0.7639	0.6496

[a] chemical structure of DBC derivatives.

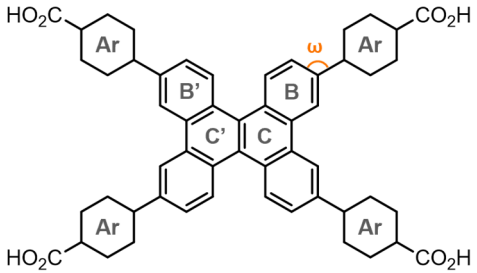

Table S11. Atomic coordinates of **C1N4DBC-close** obtained from the DFT calculation

O	9.7238	2.4373	5.1729
O	8.687	1.1665	6.695
H	9.5658	1.2996	7.0856
C	0	0	0.7066
C	1.2586	0.2753	1.3996
C	2.4912	0.214	0.6901
C	3.6823	0.5857	1.3608
H	4.6206	0.5506	0.8204
C	3.7092	1.0017	2.6757
C	2.4841	1.0912	3.3525
H	2.4645	1.4774	4.3672
C	1.3071	0.7606	2.7296
H	0.3818	0.9408	3.2601
C	4.9833	1.319	3.3727
C	5.9383	2.2578	2.8551
C	7.1959	2.4504	3.534
C	7.4424	1.7182	4.7502
C	6.4657	0.8664	5.2429
H	6.6495	0.3234	6.1613
C	5.2553	0.6665	4.5623
H	4.5343	-0.0427	4.9565
C	8.7195	1.8358	5.5087
O	-9.7238	2.4373	-5.1729
O	-8.687	1.1665	-6.695
H	-9.5658	1.2996	-7.0856
C	0	0	-0.7066
C	-1.2586	0.2753	-1.3996
C	-2.4912	0.214	-0.6901
C	-3.6823	0.5857	-1.3608
H	-4.6206	0.5506	-0.8204
C	-3.7092	1.0017	-2.6757
C	-2.4841	1.0912	-3.3525
H	-2.4645	1.4774	-4.3672
C	-1.3071	0.7606	-2.7296
H	-0.3818	0.9408	-3.2601
C	-4.9833	1.319	-3.3727
C	-5.9383	2.2578	-2.8551
C	-7.1959	2.4504	-3.534
C	-7.4424	1.7182	-4.7502
C	-6.4657	0.8664	-5.2429
H	-6.6495	0.3234	-6.1613
C	-5.2553	0.6665	-4.5623
H	-4.5343	-0.0427	-4.9565
C	-8.7195	1.8358	-5.5087
O	-9.7238	-2.4373	5.1729
O	-8.687	-1.1665	6.695
H	-9.5658	-1.2996	7.0856
C	-1.2586	-0.2753	1.3996
C	-2.4912	-0.214	0.6901
C	-3.6823	-0.5857	1.3608
H	-4.6206	-0.5506	0.8204
C	-3.7092	-1.0017	2.6757
C	-2.4841	-1.0912	3.3525
H	-2.4645	-1.4774	4.3672
C	-1.3071	-0.7606	2.7296
H	-0.3818	-0.9408	3.2601
C	-4.9833	-1.319	3.3727
C	-5.9383	-2.2578	2.8551
C	-7.1959	-2.4504	3.534
C	-7.4424	-1.7182	4.7502
C	-6.4657	-0.8664	5.2429
H	-6.6495	-0.3234	6.1613
C	-5.2553	-0.6665	4.5623
H	-4.5343	0.0427	4.9565
C	-8.7195	-1.8358	5.5087
O	9.7238	-2.4373	-5.1729
O	8.687	-1.1665	-6.695
H	9.5658	-1.2996	-7.0856
C	1.2586	-0.2753	-1.3996
C	2.4912	-0.214	-0.6901
C	3.6823	-0.5857	-1.3608
H	4.6206	-0.5506	-0.8204
C	3.7092	-1.0017	-2.6757
C	2.4841	-1.0912	-3.3525
H	2.4645	-1.4774	-4.3672
C	1.3071	-0.7606	-2.7296
H	0.3818	-0.9408	-3.2601
C	4.9833	-1.319	-3.3727
C	5.9383	-2.2578	-2.8551
C	7.1959	-2.4504	-3.534
C	7.4424	-1.7182	-4.7502
C	6.4657	-0.8664	-5.2429
H	6.6495	-0.3234	-6.1613
C	5.2553	-0.6665	-4.5623
H	4.5343	0.0427	-4.9565
C	8.7195	-1.8358	-5.5087
C	8.122	-3.3767	-2.9767
C	7.8211	-4.0892	-1.8373
C	6.5739	-3.9317	-1.1976
C	5.6566	-3.0385	-1.699
H	9.0731	-3.5156	-3.4689
H	8.5483	-4.79	-1.4379
H	6.3341	-4.52	-0.317
H	4.6906	-2.9362	-1.22
C	-8.122	3.3767	-2.9767
C	-7.8211	4.0892	-1.8373
C	-6.5739	3.9317	-1.1976
C	-5.6566	3.0385	-1.699
H	-9.0731	3.5156	-3.4689
H	-8.5483	4.79	-1.4379
H	-6.3341	4.52	-0.317
H	-4.6906	2.9362	-1.22
C	-8.122	-3.3767	2.9767
C	-7.8211	-4.0892	1.8373
C	-6.5739	-3.9317	1.1976
C	-5.6566	-3.0385	1.699
H	-9.0731	-3.5156	3.4689
H	-8.5483	-4.79	1.4379
H	-6.3341	-4.52	0.317
H	-4.6906	-2.9362	1.22
C	8.122	3.3767	2.9767
C	7.8211	4.0892	1.8373
C	6.5739	3.9317	1.1976
C	5.6566	3.0385	1.699
H	9.0731	3.5156	3.4689
H	8.5483	4.79	1.4379
H	6.3341	4.52	0.317
H	4.6906	2.9362	1.22

Table S12. Atomic coordinates of **C1N5DBC-far** obtained from the DFT calculation

C	2.4803	-0.7011	0.2241
C	2.4236	-3.3242	1.2261
C	1.2408	-1.3962	0.2971
C	3.6607	-1.3556	0.627
C	3.662	-2.6578	1.1144
C	1.2513	-2.7058	0.8367
H	4.6043	-0.8229	0.6045
H	0.3145	-3.2246	0.994
H	2.3929	-4.3302	1.6325
C	-0.0033	-0.6993	-0.0123
C	0.0033	0.6992	-0.0123
C	1.254	1.3841	-0.3218
C	2.4868	0.6774	-0.2485
C	-1.2408	1.396	0.2971
C	-2.4803	0.701	0.2242
C	-2.4868	-0.6775	-0.2484
C	-1.254	-1.3842	-0.3218
C	-1.2767	-2.6934	-0.8622
C	-2.4547	-3.3007	-1.2518
C	-3.6869	-2.6228	-1.1388
C	-3.6734	-1.3208	-0.6511
H	-0.3448	-3.2206	-1.0205
H	-2.4335	-4.3062	-1.6599
H	-4.6118	-0.779	-0.6289
C	3.6734	1.3207	-0.6512
C	3.6868	2.6228	-1.1389
C	2.4546	3.3006	-1.2518
C	1.2767	2.6933	-0.8622
H	4.6118	0.7789	-0.6291
H	2.4334	4.3061	-1.6598
H	0.3447	3.2205	-1.0204
C	-3.6607	1.3555	0.6271
C	-3.662	2.6578	1.1144
C	-2.4235	3.3242	1.2261
C	-1.2513	2.7057	0.8367
H	-4.6043	0.8228	0.6047
H	-2.3928	4.3302	1.6324
H	-0.3144	3.2245	0.9938
C	-4.9432	3.3207	1.4781
C	-7.3843	4.6439	2.0203
C	-5.1729	3.8825	2.7808
C	-5.9389	3.4019	0.5219
C	-7.1546	4.0583	0.7963
C	-6.4088	4.5732	3.0533
H	-5.762	2.9783	-0.4622
H	-7.9149	4.1173	0.023
H	-8.3125	5.1601	2.2139
C	4.9735	3.2748	-1.5028
C	7.4268	4.5677	-2.0478
C	5.974	3.3372	-0.5505
C	5.2042	3.8398	-2.8043
C	6.4411	4.5314	-3.0732
C	7.2003	3.9723	-0.8286
H	5.7966	2.9093	0.4315
H	7.9702	4.0052	-0.0634
H	8.3666	5.0653	-2.2339
C	4.9433	-3.3208	1.478
C	7.3844	-4.6439	2.0202
C	5.173	-3.8825	2.7807
C	5.9389	-3.402	0.5217
C	7.1547	-4.0583	0.7961
C	6.4089	-4.5732	3.0532
H	5.762	-2.9784	-0.4623
H	7.915	-4.1174	0.0228
H	8.3126	-5.1601	2.2138
C	-4.9736	-3.2748	-1.5027
C	-7.4269	-4.5677	-2.0477
C	-5.9741	-3.3372	-0.5503
C	-5.2044	-3.8398	-2.8042
C	-6.4413	-4.5314	-3.0731
C	-7.2004	-3.9723	-0.8285
H	-5.7966	-2.9094	0.4317
H	-7.9702	-4.0053	-0.0632
H	-8.3667	-5.0653	-2.2337
C	6.6278	5.097	-4.3845
C	5.6662	4.9133	-5.3655
C	4.4833	4.201	-5.1052
C	4.2566	3.6823	-3.8517
H	5.85	5.3325	-6.3482
H	3.7534	4.0605	-5.8962
H	3.349	3.1225	-3.6588
C	6.5961	-5.1415	4.366
C	5.6139	-4.988	5.334
C	4.4333	-4.2723	5.0698
C	4.2203	-3.731	3.8238
H	5.7671	-5.4177	6.3157
H	3.6955	-4.1442	5.8555
H	3.3165	-3.1647	3.6323
C	-6.628	-5.0969	-4.3844
C	-5.6664	-4.9132	-5.3655
C	-4.4835	-4.2009	-5.1052
C	-4.2568	-3.6822	-3.8516
H	-5.8502	-5.3324	-6.3482
H	-3.7537	-4.0604	-5.8961
H	-3.3492	-3.1225	-3.6587
C	-6.5959	5.1415	4.366
C	-5.6136	4.9881	5.3341
C	-4.4331	4.2724	5.0699
C	-4.2202	3.7311	3.8238
H	-5.7668	5.4179	6.3157
H	-3.6952	4.1443	5.8555
H	-3.3164	3.1647	3.6323
C	-7.8279	5.8968	4.7353
O	-8.7993	6.1133	4.0332
O	-7.7908	6.3683	6.0127
H	-8.6334	6.8347	6.1355
C	7.8049	5.9011	-4.836
O	8.0989	6.0795	-6.0026
O	8.5211	6.4877	-3.8415
H	9.2262	6.9823	-4.2923
C	7.8281	-5.8967	4.7352
O	8.7995	-6.1132	4.033
O	7.7911	-6.3681	6.0127
H	8.6337	-6.8345	6.1354
C	-7.8051	-5.901	-4.8359
O	-8.0992	-6.0794	-6.0025
O	-8.5213	-6.4877	-3.8414
H	-9.2264	-6.9822	-4.2922

Table S13. Atomic coordinates of **C1N5DBC-close** obtained from the DFT calculation

C	-2.33924	2.221966	4.864673
C	-4.40718	3.843142	3.79641
C	-3.55228	1.60913	4.467754
C	-2.24519	3.642561	4.781337
C	-3.25953	4.460084	4.264024
C	-4.53497	2.455968	3.88669
H	-1.34465	4.156651	5.108518
H	-5.42777	2.028993	3.432275
H	-5.20577	4.428248	3.345714
C	-3.734	0.177627	4.574691
C	-2.57764	-0.6143	4.679058
C	-1.40428	-0.00371	5.265781
C	-1.27715	1.404225	5.34512
C	-2.65697	-1.97437	4.191606
C	-3.90775	-2.61332	4.012921
C	-5.10052	-1.88662	4.290184
C	-5.0101	-0.50444	4.583553
C	-6.21401	0.146711	4.96686
C	-7.46591	-0.47089	4.958111
C	-7.57479	-1.8003	4.587532
C	-6.39454	-2.48586	4.268172
H	-6.1896	1.168857	5.341738
H	-8.34561	0.094073	5.258324
H	-6.51215	-3.53667	4.014435
C	-0.07363	1.940836	5.89043
C	0.960777	1.154028	6.415504
C	0.788922	-0.21955	6.413047
C	-0.36968	-0.77267	5.864795
H	0.079118	3.016306	5.939133
H	1.542002	-0.8725	6.848582
H	-0.47585	-1.85188	5.964499
C	-3.9126	-3.97152	3.577948
C	-2.75284	-4.68763	3.250467
C	-1.54053	-4.02575	3.344312
C	-1.50475	-2.70307	3.789384
H	-4.8497	-4.51075	3.461785
H	-0.61533	-4.52219	3.060303
H	-0.52966	-2.21875	3.766938
C	-2.82595	-6.09232	2.811777
C	-2.83945	-8.7907	2.084251
C	-3.95623	-6.63072	2.124134
C	-1.73113	-6.92122	3.107745
C	-1.73495	-8.2584	2.744604
C	-3.97587	-8.00945	1.762576
H	-0.86776	-6.51855	3.634699
H	-0.88347	-8.89224	2.978525
H	-2.79099	-9.84554	1.821139
C	2.181733	1.770946	6.961575
C	4.582513	2.888436	7.85957
C	3.415618	1.324895	6.458115
C	2.151293	2.80079	7.950223
C	3.372346	3.365435	8.417079
C	4.606676	1.880231	6.899877
H	3.445116	0.542795	5.70124
H	5.554567	1.534183	6.496161
H	5.539681	3.30333	8.168417
C	-3.10247	5.923922	4.211191
C	-2.95438	8.714514	4.187532
C	-1.83882	6.560224	4.015508
C	-4.25732	6.705543	4.380345
C	-4.18529	8.089227	4.369704
C	-1.75634	7.983195	3.99996
H	-5.22333	6.227146	4.532665
H	-5.08346	8.685836	4.507059
H	-2.95207	9.802725	4.196279
C	-8.88246	-2.47707	4.541411
C	-11.4162	-3.64511	4.351248
C	-9.96399	-1.7651	3.995089
C	-9.07943	-3.81023	5.013489
C	-10.3632	-4.41562	4.899073
C	-11.2221	-2.34073	3.905314
H	-9.82016	-0.74885	3.631846
H	-12.052	-1.77915	3.484356
H	-12.4201	-4.05566	4.265159
C	3.31225	4.392436	9.400208
C	2.087865	4.87348	9.883187
C	0.901399	4.318986	9.432076
C	0.936969	3.293699	8.488434
H	2.063019	5.674911	10.61898
H	-0.05197	4.67868	9.810684
H	-0.01766	2.87998	8.165756
C	-0.48017	8.591824	3.813952
C	0.675227	7.81153	3.647589
C	0.59082	6.42868	3.656377
C	-0.64768	5.817386	3.833467
H	1.645283	8.281264	3.500169
H	1.483576	5.82322	3.522449
H	-0.6712	4.728411	3.826357
C	-10.5266	-5.7515	5.361114
C	-9.47219	-6.45324	5.960666
C	-8.22744	-5.85798	6.083179
C	-8.03664	-4.56044	5.611046
H	-9.62345	-7.46692	6.326584
H	-7.40365	-6.3973	6.543712
H	-7.04425	-4.12749	5.730537
C	-5.12198	-8.52295	1.0867
C	-6.20724	-7.69005	0.770389
C	-6.17967	-6.34751	1.111493
C	-5.07141	-5.83077	1.777502
H	-7.08213	-8.08798	0.260893
H	-7.0178	-5.70089	0.864529
H	-5.08818	-4.76973	2.023275
C	-5.23923	-9.96071	0.717075
O	-4.79954	-10.9216	1.317793
O	-5.91629	-10.1243	-0.43685
H	-5.91028	-11.0947	-0.57506
C	4.508528	5.046337	9.973334
O	4.6636	6.244404	10.11859
O	5.400528	4.157654	10.44367
H	6.09151	4.71261	10.86176
C	-0.31418	10.07015	3.755494
O	-1.08985	10.88861	3.301481
O	0.854102	10.46053	4.302652
H	0.834865	11.4372	4.222769
C	-11.8002	-6.49789	5.270209
O	-12.3053	-7.15468	6.161295
O	-12.3155	-6.47913	4.028812
H	-13.096	-7.06881	4.084974

Table S14. Atomic coordinates of **C2N6DBC-far** obtained from the DFT calculation

H	1.6356	4.3209	2.3621
C	1.2359	3.3122	2.3944
C	0.2343	0.6902	2.4369
C	0.85	2.699	1.2187
C	1.1147	2.6453	3.6317
C	0.6364	1.3374	3.6193
C	0.3079	1.3908	1.2003
H	1.0118	3.221	0.2844
H	0.6335	0.7862	4.5521
C	0	0.6997	-0.0467
C	0	-0.6997	-0.0467
C	-0.3079	-1.3908	1.2003
C	-0.2343	-0.6902	2.4369
C	0.3079	-1.3902	-1.2935
C	0.2391	-0.6889	-2.5303
C	-0.2391	0.6889	-2.5303
C	-0.3079	1.3902	-1.2935
C	-0.8416	2.7022	-1.3108
C	-1.2241	3.3183	-2.4855
C	-1.1145	2.6477	-3.7225
C	-0.6351	1.3408	-3.7127
H	-1.0153	3.2174	-0.3748
H	-1.6655	4.3093	-2.4488
H	-0.5742	0.8119	-4.6562
C	-0.6364	-1.3374	3.6193
C	-1.1147	-2.6453	3.6317
C	-1.2359	-3.3122	2.3944
C	-0.85	-2.699	1.2187
H	-0.6335	-0.7862	4.5521
H	-1.6356	-4.3209	2.3621
H	-1.0118	-3.221	0.2844
C	0.6351	-1.3408	-3.7127
C	1.1145	-2.6477	-3.7225
C	1.2241	-3.3183	-2.4855
C	0.8416	-2.7022	-1.3108
H	0.5742	-0.8119	-4.6562
H	1.6655	-4.3093	-2.4488
H	1.0153	-3.2174	-0.3748
C	-1.5304	3.3027	-4.9846
C	-2.296	4.6045	-7.3907
C	-2.1824	2.5958	-5.9825
C	-1.2624	4.6886	-5.192
C	-1.6315	5.3168	-6.3557
C	-2.5758	3.2124	-7.1952
H	-2.4279	1.5485	-5.8307
H	-0.7332	5.2428	-4.4233
H	-1.4104	6.3701	-6.5043
C	1.5304	-3.3027	-4.9846
C	2.296	-4.6045	-7.3907
C	1.2624	-4.6886	-5.192
C	2.1824	-2.5958	-5.9825
C	2.5758	-3.2124	-7.1952
C	1.6315	-5.3168	-6.3557
H	0.7332	-5.2428	-4.4233
H	2.4279	-1.5485	-5.8307
H	1.4104	-6.3701	-6.5043
C	1.5164	3.2955	4.9005
C	2.3197	4.5469	7.3212
C	2.6574	4.1509	4.9461
C	0.7962	3.0867	6.0662
C	1.1695	3.6923	7.2907
C	3.0453	4.7543	6.1168
H	3.2416	4.2997	4.0437
H	-0.0948	2.4654	6.045
H	3.9237	5.3934	6.139
C	-1.5164	-3.2955	4.9005
C	-2.3197	-4.5469	7.3212
C	-0.7962	-3.0867	6.0662
C	-2.6574	-4.1509	4.9461
C	-3.0453	-4.7543	6.1168
C	-1.1695	-3.6923	7.2907
H	0.0948	-2.4654	6.045
H	-3.2416	-4.2997	4.0437
H	-3.9237	-5.3934	6.139
C	0.4366	3.4874	8.4926
C	0.82	4.0879	9.667
C	1.9644	4.9322	9.6965
C	2.6938	5.1525	8.5427
H	-0.4377	2.8427	8.4684
H	0.2585	3.9266	10.5795
H	3.5631	5.8013	8.5873
C	-0.4366	-3.4874	8.4926
C	-0.82	-4.0879	9.667
C	-1.9644	-4.9322	9.6965
C	-2.6938	-5.1525	8.5427
H	0.4377	-2.8427	8.4684
H	-0.2585	-3.9266	10.5795
H	-3.5631	-5.8013	8.5873
C	3.2478	-2.498	-8.2257
C	3.6196	-3.1203	-9.3924
C	3.3371	-4.5008	-9.5867
C	2.6885	-5.2213	-8.6008
H	3.4628	-1.4435	-8.0762
H	4.1295	-2.5701	-10.1742
H	2.4836	-6.274	-8.7691
C	-3.2478	2.498	-8.2257
C	-3.6196	3.1203	-9.3924
C	-3.3371	4.5008	-9.5867
C	-2.6885	5.2213	-8.6008
H	-3.4628	1.4435	-8.0762
H	-4.1295	2.5701	-10.1742
H	-2.4836	6.274	-8.7691
C	-3.7186	5.2173	-10.8313
O	-3.504	6.3932	-11.0536
O	-4.3493	4.4174	-11.73
H	-4.5496	4.9829	-12.4937
C	3.7186	-5.2173	-10.8313
O	3.504	-6.3932	-11.0536
O	4.3493	-4.4174	-11.73
H	4.5496	-4.9829	-12.4937
C	2.4186	5.603	10.9423
O	3.3859	6.3344	11.0284
O	1.6327	5.3182	12.0131
H	2.0175	5.8037	12.7611
C	-2.4186	-5.603	10.9423
O	-3.3859	-6.3344	11.0284
O	-1.6327	-5.3182	12.0131
H	-2.0175	-5.8037	12.7611

Table S15. Atomic coordinates of **C2N6DBC-close** obtained from the DFT calculation

H	-1.4041	2.5494	4.4475	C	2.1686	-5.2147	4.2525	H	-1.2683	9.6746	5.0803
C	-1.0053	2.5432	3.4382	C	0.2294	-6.1911	3.1871	C	2.0112	6.4305	-6.5446
C	0	2.4949	0.8172	C	0.4897	-7.405	3.7729	C	2.4963	7.5661	-7.1461
C	-0.7304	1.3375	2.8244	C	2.4658	-6.4524	4.8734	C	3.2482	8.5082	-6.391
C	-0.773	3.7645	2.7711	H	2.8411	-4.3782	4.4197	C	3.4917	8.2847	-5.0483
C	-0.2893	3.7095	1.4662	H	-0.647	-6.0718	2.558	H	1.4367	5.71	-7.1204
C	-0.1913	1.2701	1.5165	H	-0.1677	-8.2518	3.5957	H	2.3133	7.7566	-8.1969
H	-0.9769	0.4218	3.3462	C	-1.9887	-4.773	-3.1747	H	4.0671	9.0169	-4.4905
H	-0.1942	4.6382	0.9159	C	-3.0019	-7.1247	-4.4056	C	-2.0112	-6.4305	-6.5446
C	0	0	0.8262	C	-2.7434	-5.7293	-2.4317	C	-2.4963	-7.5661	-7.1461
C	0	0	-0.5731	C	-1.7583	-5.0104	-4.5204	C	-3.2482	-8.5082	-6.391
C	0.4234	1.2125	-1.2635	C	-2.2482	-6.172	-5.166	C	-3.4917	-8.2847	-5.0483
C	0.4743	2.4493	-0.561	C	-3.2325	-6.8654	-3.0273	H	-1.4367	-5.71	-7.1204
C	-0.4234	-1.2125	-1.2635	H	-2.9568	-5.5343	-1.3855	H	-2.3133	-7.7566	-8.1969
C	-0.4743	-2.4493	-0.561	H	-1.1645	-4.3077	-5.0982	H	-4.0671	-9.0169	-4.4905
C	0	-2.4949	0.8172	H	-3.8157	-7.5787	-2.4514	C	3.5917	-6.6216	5.7264
C	0.1913	-1.2701	1.5165	C	-1.0724	5.0631	3.4182	C	3.8586	-7.8334	6.3153
C	0.7304	-1.3375	2.8244	C	-1.6101	7.5762	4.6303	C	3.0055	-8.9463	6.0768
C	1.0053	-2.5432	3.4382	C	-0.2294	6.1911	3.1871	C	1.9056	-8.8123	5.2496
C	0.773	-3.7645	2.7711	C	-2.1686	5.2147	4.2525	H	4.2425	-5.7706	5.9078
C	0.2893	-3.7095	1.4662	C	-2.4658	6.4524	4.8734	H	4.717	-7.9553	6.965
H	0.9769	-0.4218	3.3462	C	-0.4897	7.405	3.7729	H	1.2683	-9.6746	5.0803
H	1.4041	-2.5494	4.4475	H	0.647	6.0718	2.558	C	3.2523	-10.2765	6.6916
H	0.1942	-4.6382	0.9159	H	-2.8411	4.3782	4.4197	O	2.5594	-11.2615	6.5258
C	0.9876	3.588	-1.2091	H	0.1677	8.2518	3.5957	O	4.3567	-10.2969	7.4824
C	1.4622	3.5543	-2.5175	C	1.9887	4.773	-3.1747	H	4.4197	-11.203	7.8264
C	1.4538	2.3127	-3.1884	C	3.0019	7.1247	-4.4056	C	-3.7943	-9.7503	-6.9969
C	0.9579	1.1799	-2.575	C	1.7583	5.0104	-4.5204	O	-4.4427	-10.59	-6.4032
H	1.0228	4.529	-0.6731	C	2.7434	5.7293	-2.4317	O	-3.4963	-9.8702	-8.3169
H	1.8943	2.236	-4.1775	C	3.2325	6.8654	-3.0273	H	-3.8973	-10.7067	-8.6043
H	1.0427	0.2318	-3.0906	C	2.2482	6.172	-5.166	C	-3.2523	10.2765	6.6916
C	-0.9876	-3.588	-1.2091	H	1.1645	4.3077	-5.0982	O	-2.5594	11.2615	6.5258
C	-1.4622	-3.5543	-2.5175	H	2.9568	5.5343	-1.3855	O	-4.3567	10.2969	7.4824
C	-1.4538	-2.3127	-3.1884	H	3.8157	7.5787	-2.4514	H	-4.4197	11.203	7.8264
C	-0.9579	-1.1799	-2.575	C	-3.5917	6.6216	5.7264	C	3.7943	9.7503	-6.9969
H	-1.0228	-4.529	-0.6731	C	-3.8586	7.8334	6.3153	O	4.4427	10.59	-6.4032
H	-1.8943	-2.236	-4.1775	C	-3.0055	8.9463	6.0768	O	3.4963	9.8702	-8.3169
H	-1.0427	-0.2318	-3.0906	C	-1.9056	8.8123	5.2496	H	3.8973	10.7067	-8.6043
C	1.0724	-5.0631	3.4182	H	-4.2425	5.7706	5.9078				
C	1.6101	-7.5762	4.6303	H	-4.717	7.9553	6.965				

5-2. Energy estimation for stacking and H-bonding of carboxynaphthyl groups.

Atomic coordinates in the crystal structures were adopted except for DBC moieties. Only hydrogen atoms were optimized at B3LYP-D3/6-311G+(d,p) level of theory. The complexation energy of stacking (Fig. S26) and H-bonding (Figs. 4cd and S6c) were evaluated by B3LYP-D3/6-311G+(d,p) (Table S16). The corrections of basis set superposition error (BSSE) are evaluated by means of counterpoise method. These calculations were carried out using Gaussian09W[S16], or Gaussian16.[S17]

Table S16. Complexation energy (kcal mol^{-1}) of stacked dimer (stacking) and H-bonded dimer (H-bonding) of naphthoic acid groups in **C1N5DBC-1**, **C2N6DBC-1**, and **C2N6DBC-2**.

Framework	**C1N5DBC-1**		**C2N6DBC-1**		**C2N6DBC-2**	
interactions	Stacking	H-bonding	Stacking	H-bonding	Stacking	H-bonding
Major-Major	−7.24	−25.29[b]	−7.42	−9.42[a]	−7.27	−1.75[a]
Minor-minor	−6.35	−19.88[b]	−7.48	−21.88[b]	−7.28	−32.81[b]
Major-minor	-8.31	-22.57[b]	-7.10	-3.14[a]	−7.28	−6.60[a]

[a] truncated H-bonding monomer. [b] self-complementary H-bonding dimer.

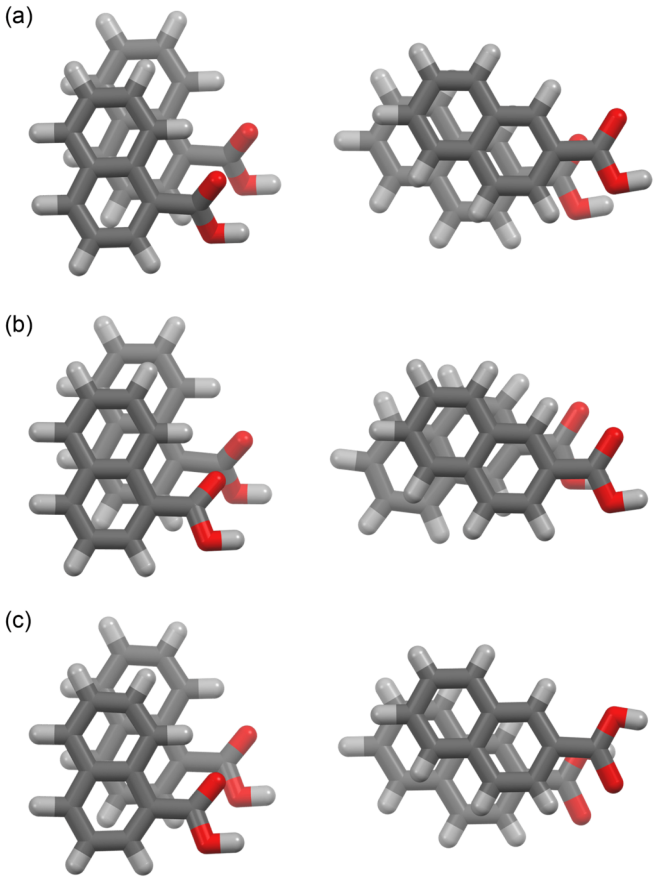

Fig. S26 Optimized structures of stacking carboxynaphthyl groups between (a) major–major, (b) major–minor, and (c) minor–minor of (left) **C1N5DBC-1** and (right) **C2N6DBC-1**.

6. NMR spectra

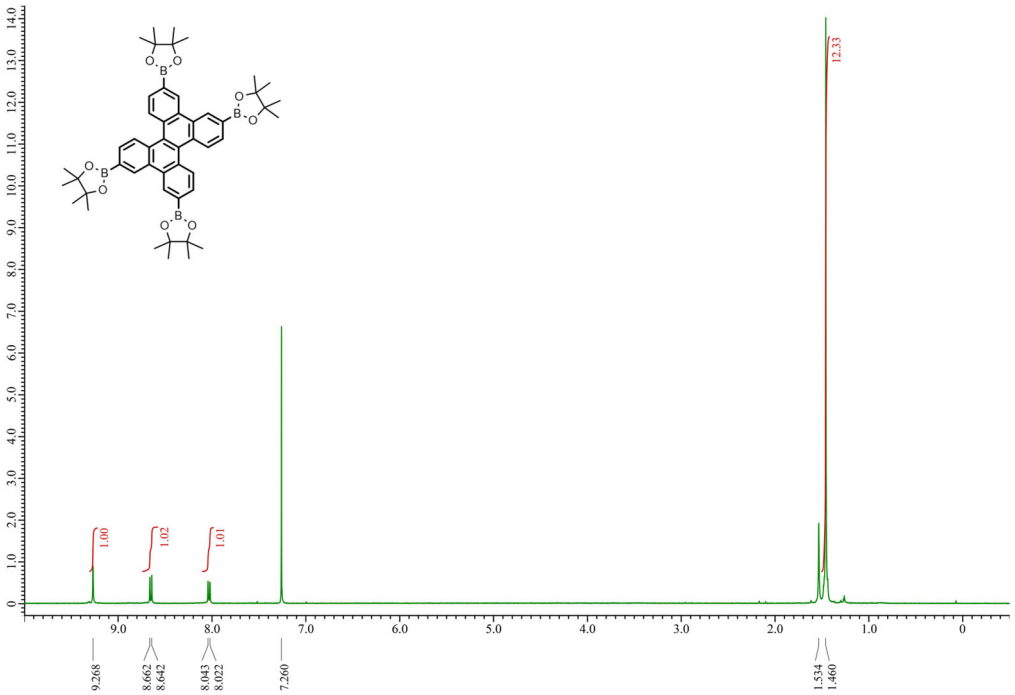

Fig. S27 ^{1}H-NMR (400 MHz, $CDCl_3$) spectrum of 2,7,10,15-tetrakis(4,4,5,5-tetramethyl-1,3,2-dioxaborolan-2-yl)dibenzo[*g,p*]chrysene (**2**).

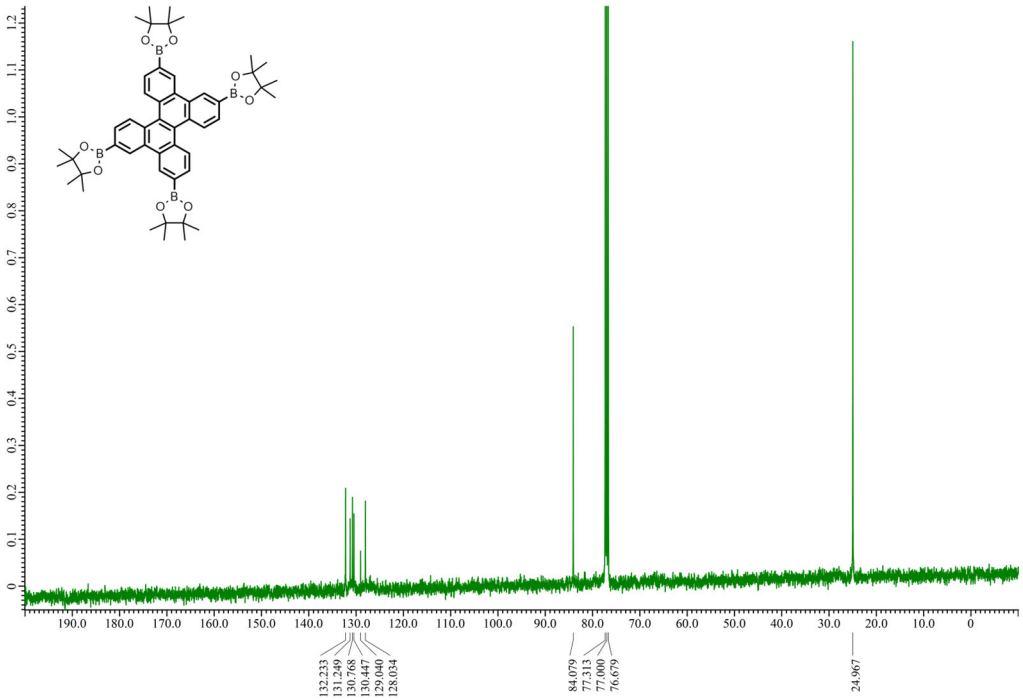

Fig. S28 ^{13}C-NMR (100 MHz, $CDCl_3$) spectrum of 2,7,10,15-tetrakis(4,4,5,5-tetramethyl-1,3,2-dioxaborolan-2-yl)dibenzo[*g,p*]chrysene (**2**).

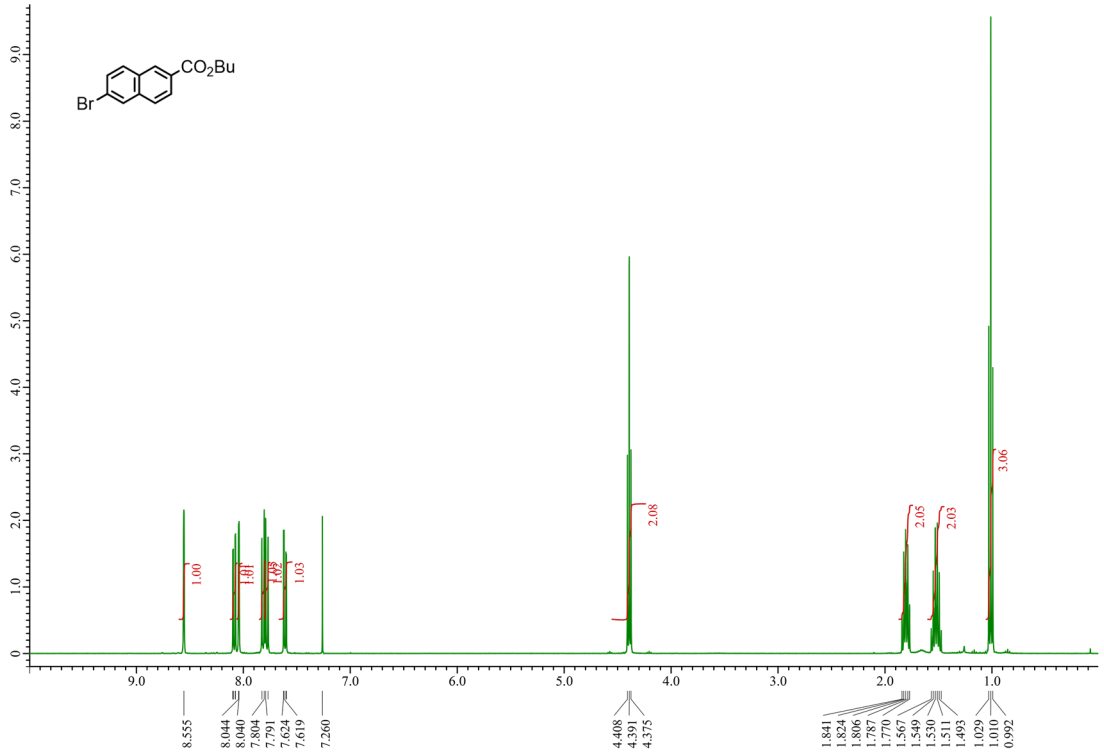

Fig. S29. ^{1}H-NMR (400 MHz, $CDCl_3$) spectrum of butyl 6-bromo-2-naphthoate (**8**).

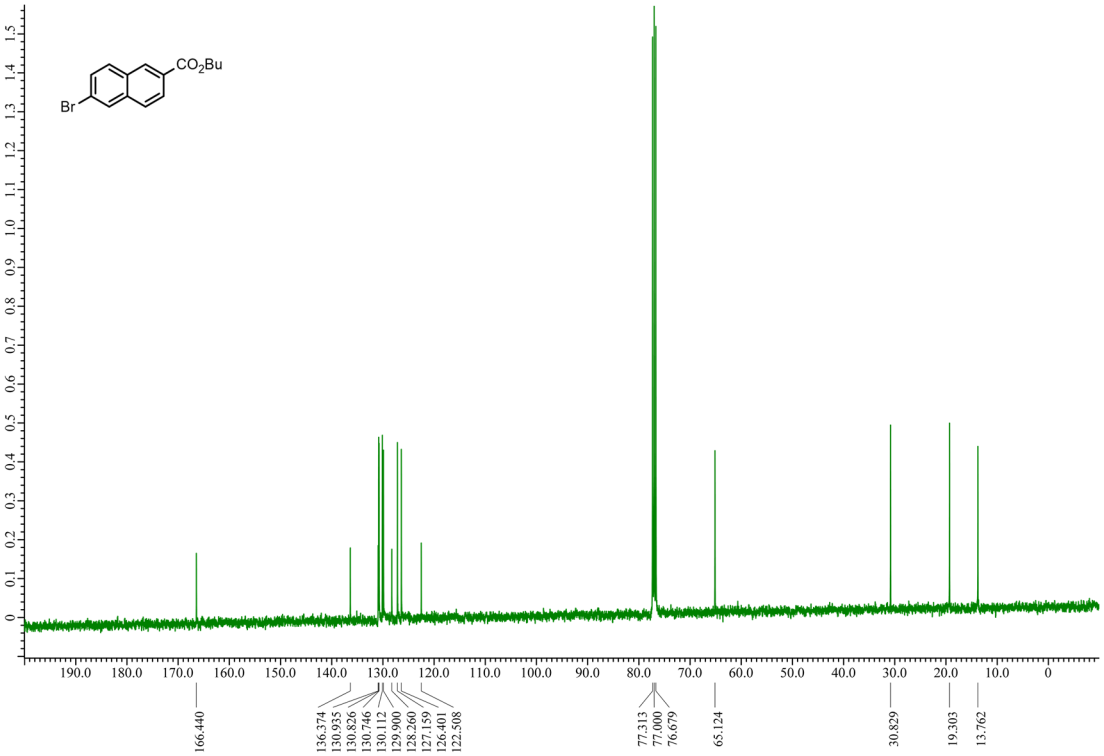

Fig. S30 ^{13}C-NMR (100 MHz, $CDCl_3$) spectrum of butyl 6-bromo-2-naphthoate (**8**).

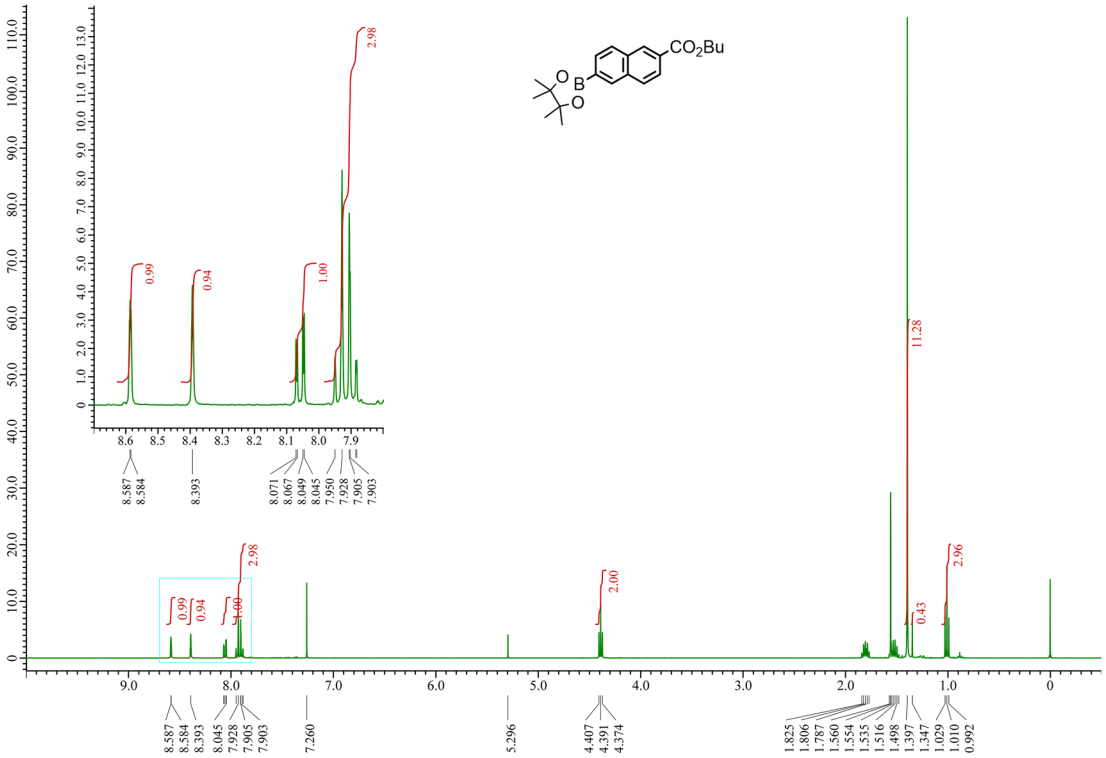

Fig. S31 ^{1}H-NMR (400 MHz, $CDCl_3$) spectrum of butyl 6-(4,4,5,5-tetramethyl-1,3,2-dioxaborolan-2-yl)-2-naphthoate (**9**).

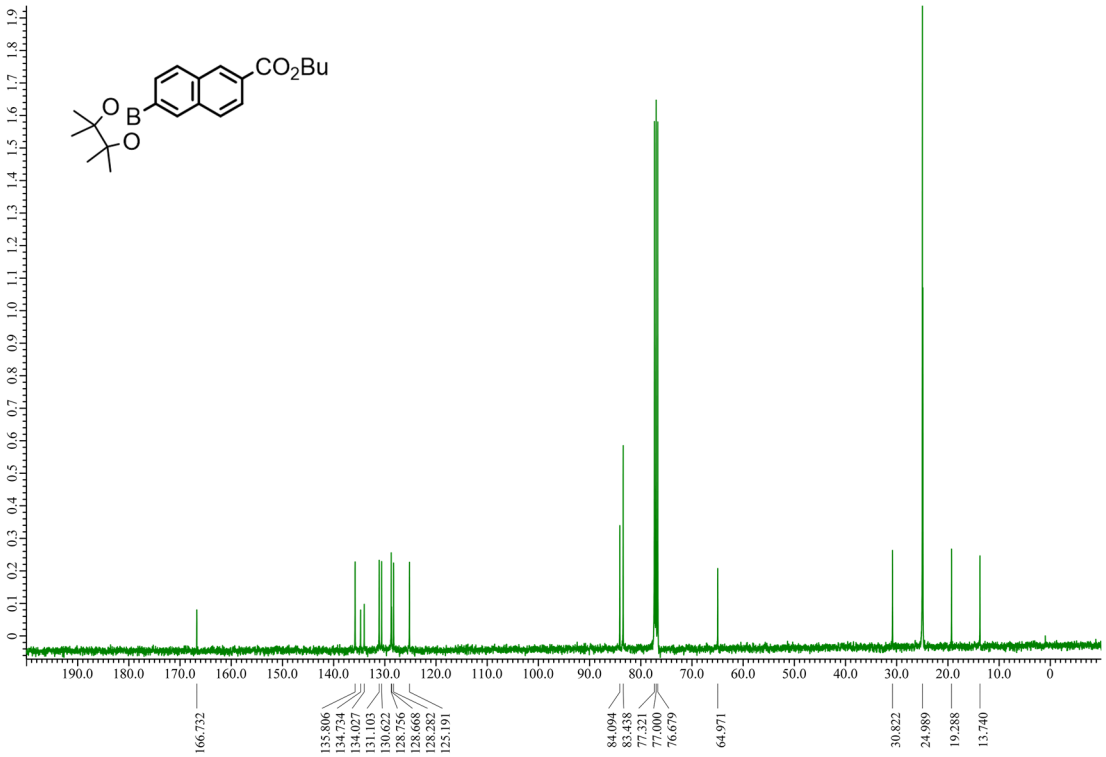

Fig. S32 ^{13}C-NMR (100 MHz, $CDCl_3$) spectrum of butyl 6-(4,4,5,5-tetramethyl-1,3,2-dioxaborolan-2-yl)-2-naphthoate (**9**).

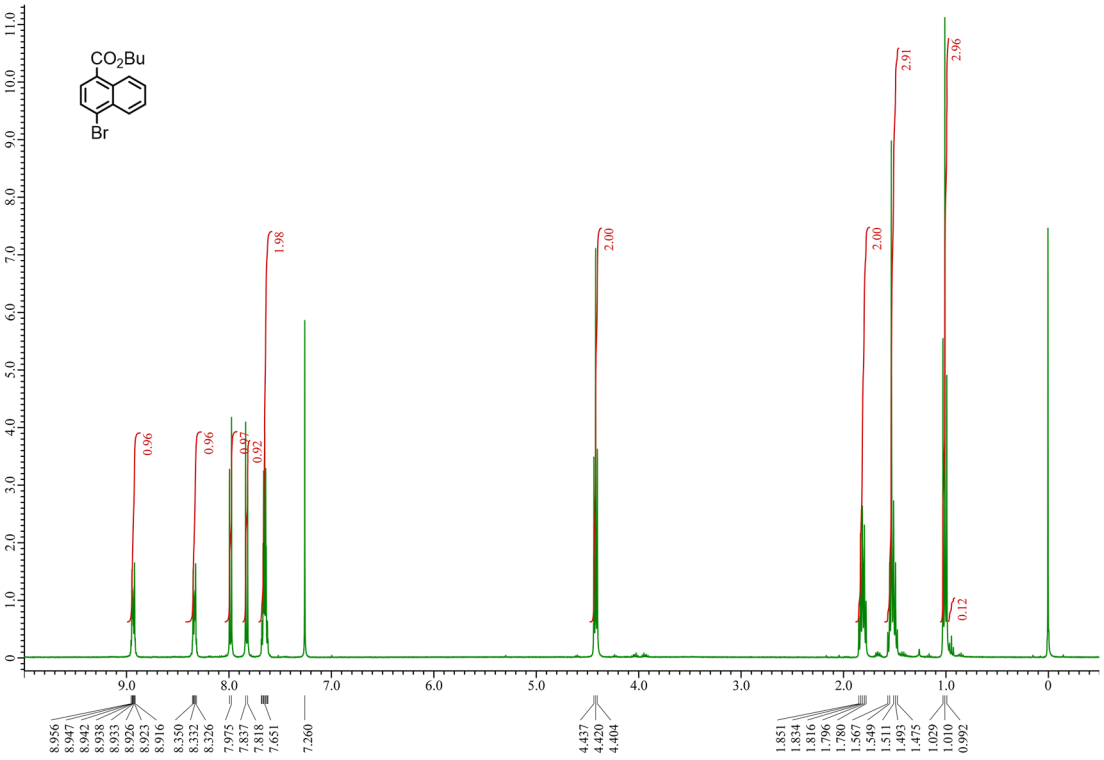

Fig. S33 ^{1}H-NMR (400 MHz, $CDCl_3$) spectrum of butyl 4-bromo-1-naphthoate (**11**).

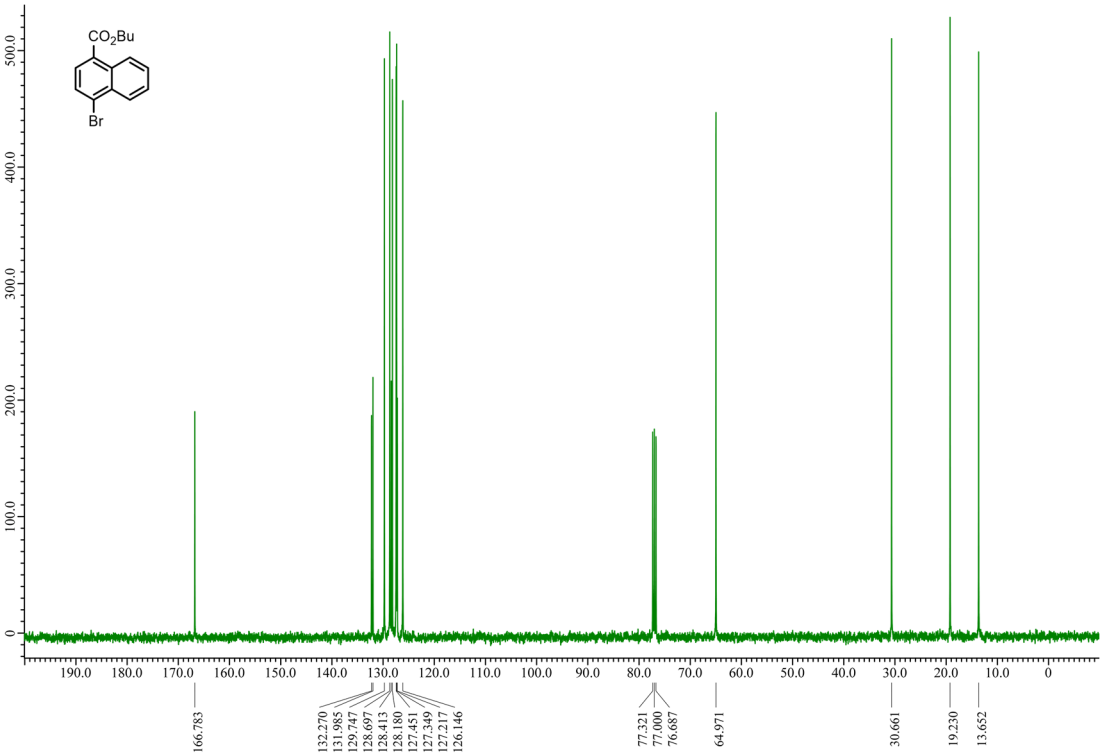

Fig. S34 ^{13}C-NMR (100 MHz, $CDCl_3$) spectrum of butyl 4-bromo-1-naphthoate (**11**).

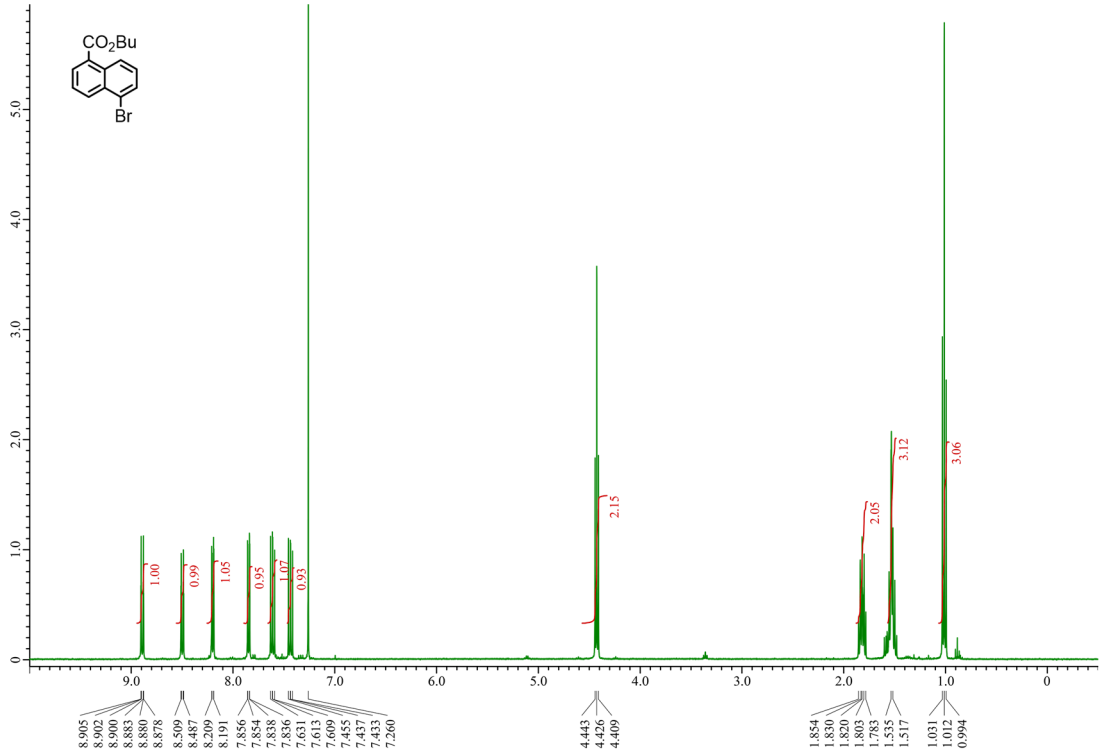

Fig. S35 ^{1}H-NMR (400 MHz, $CDCl_3$) spectrum of butyl 5-bromo-1-naphthoate (**13**).

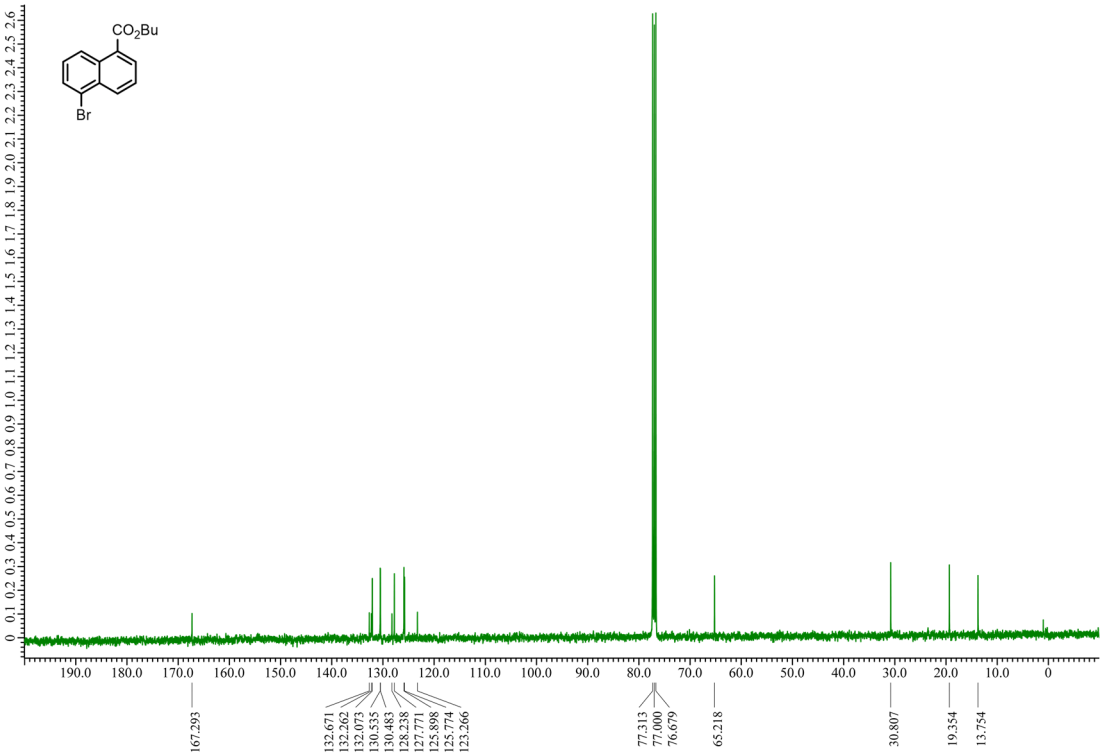

Fig. S36 ^{13}C-NMR (100 MHz, $CDCl_3$) spectrum of butyl 5-bromo-1-naphthoate (**13**).

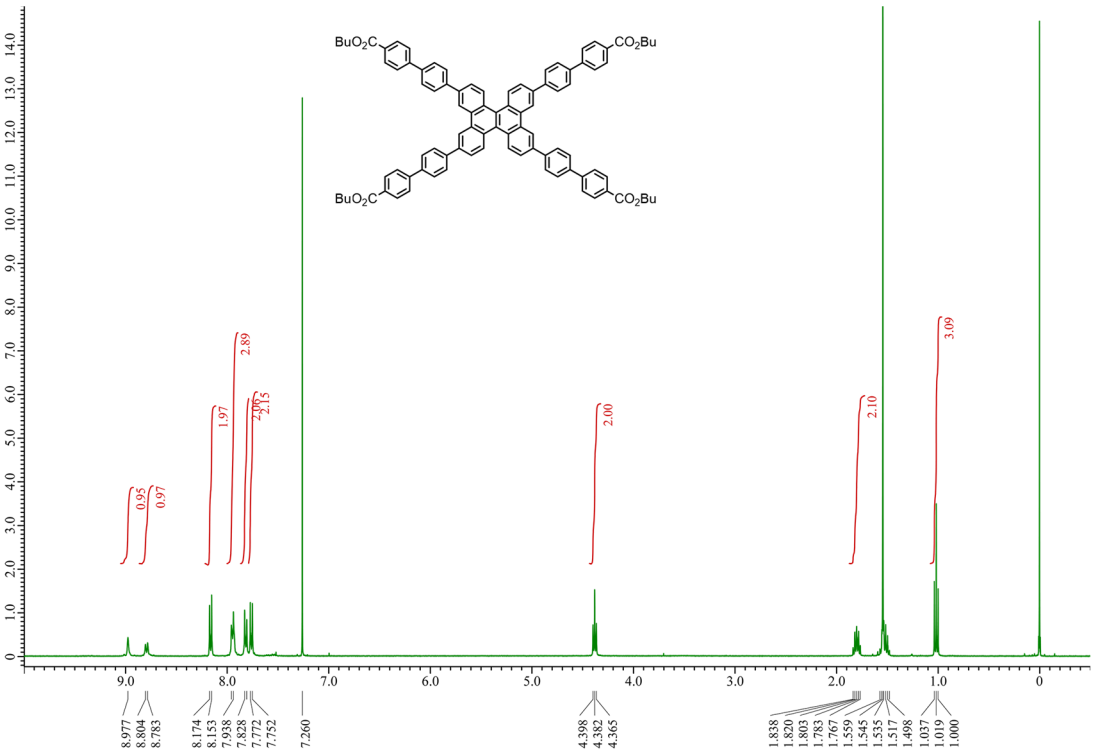

Fig. S37 ^{1}H-NMR (400 MHz, $CDCl_3$) spectrum of tetrabutyl 4',4''',4''''',4''''''-(dibenzo[*g,p*]chrysene-2,7,10,15-tetrayl)tetrakis([1,1'-biphenyl]-4-carboxylate) (**3a**).

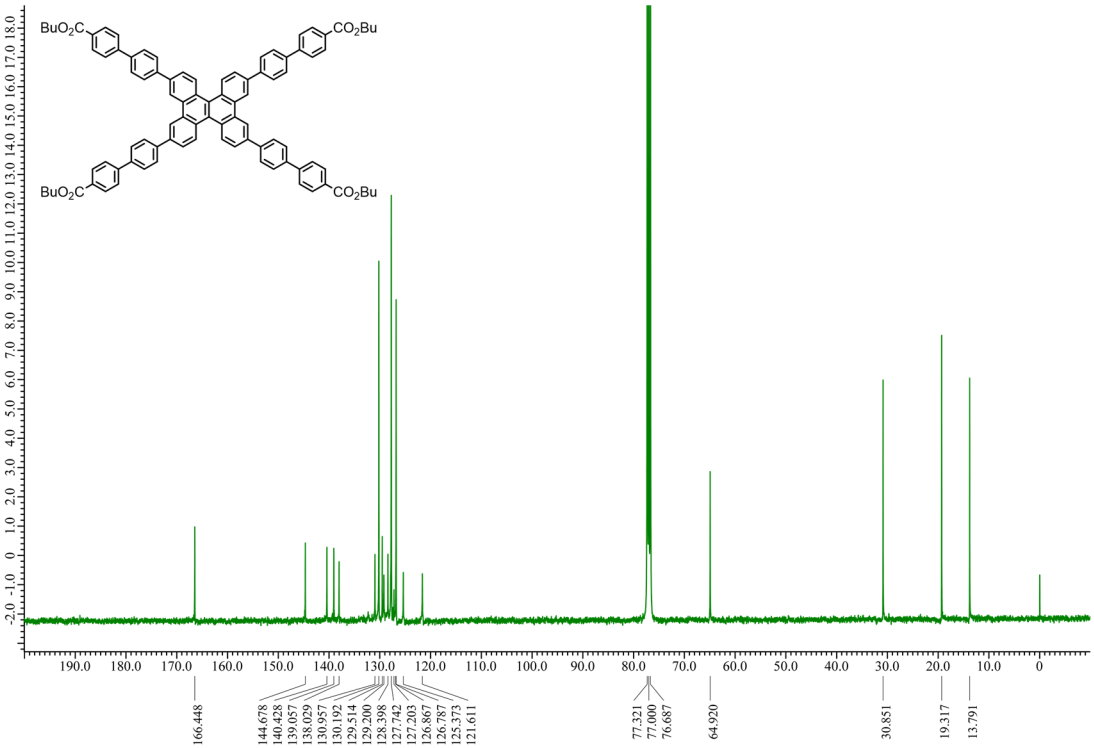

Fig. S38 ^{13}C-NMR (100 MHz, $CDCl_3$) spectrum of tetrabutyl 4',4''',4''''',4''''''-(dibenzo[*g,p*]chrysene-2,7,10,15-tetrayl)tetrakis([1,1'-biphenyl]-4-carboxylate) (**3a**).

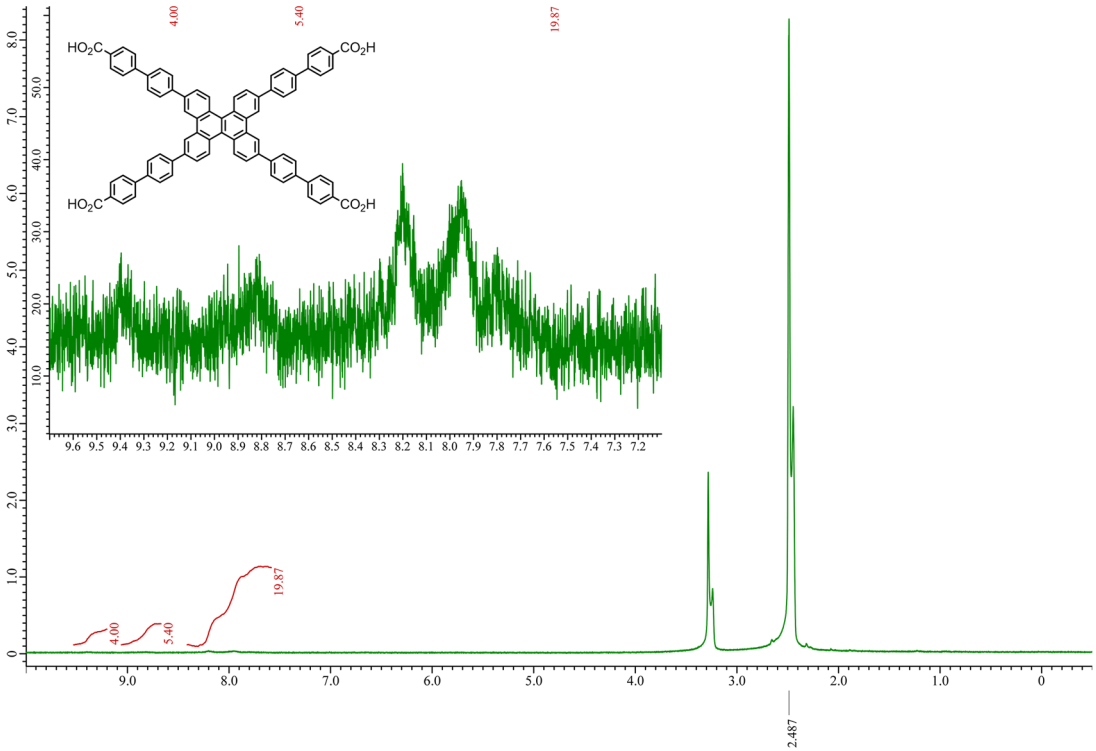

Fig. S39 ^{1}H-NMR (400 MHz, DMSO-d_6) spectrum of 4',4''',4''''',4''''''-(dibenzo[*g,p*]chrysene-2,7,10,15-tetrayl)tetrakis(([1,1'-biphenyl]-4-carboxylic acid)) (**CBPDBC**).

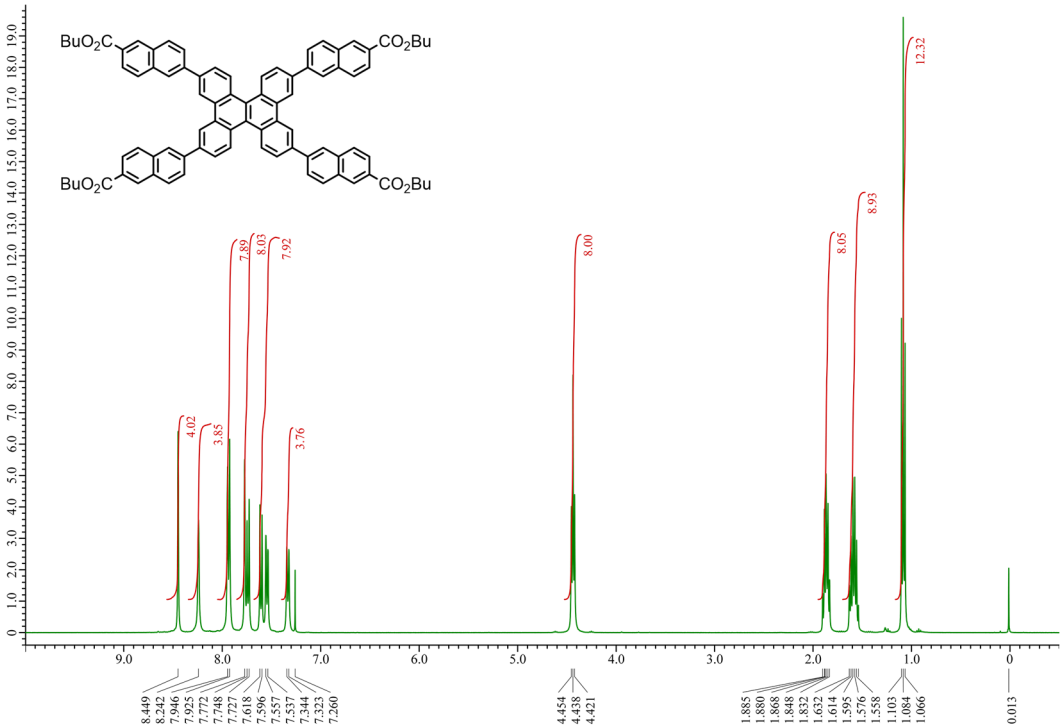

Fig. S40 ^{1}H-NMR (400 MHz, $CDCl_3$) spectrum of tetrabutyl 6,6',6'',6'''-(dibenzo[*g,p*]chrysene-2,7,10,15-tetrayl)tetrakis(2-naphthoate) (**3b**).

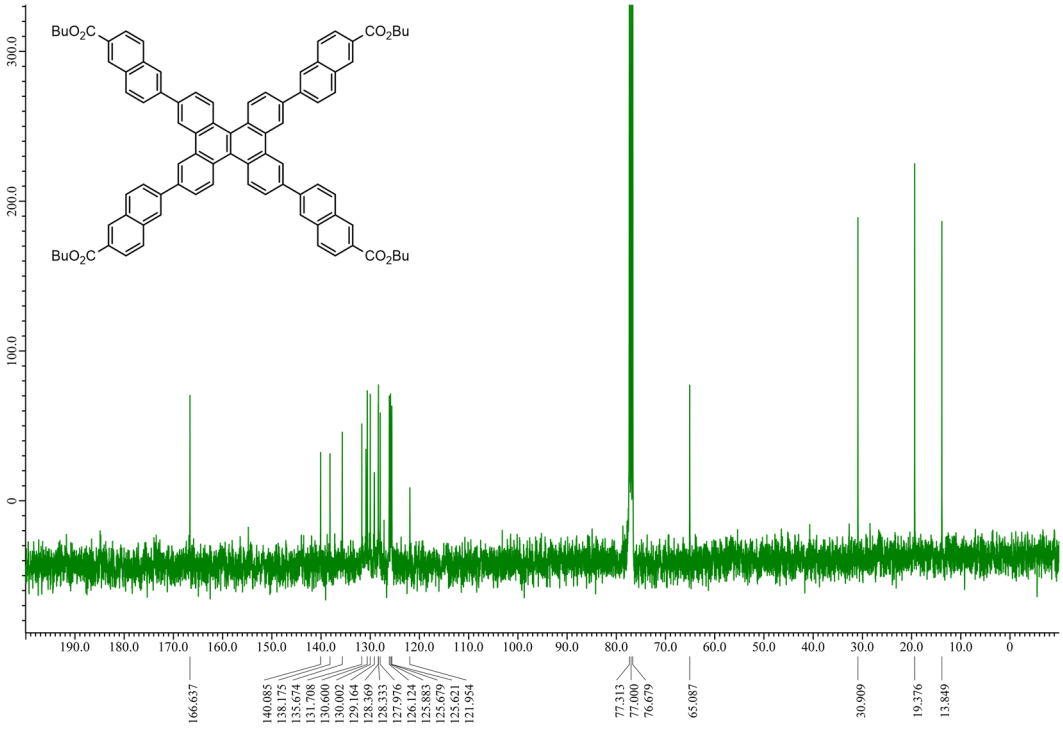

Fig. S41 ^{13}C-NMR (100 MHz, $CDCl_3$) spectrum of tetrabutyl 6,6',6",6'"-(dibenzo[*g,p*]chrysene-2,7,10,15-tetrayl)tetrakis(2-naphthoate) (**3b**).

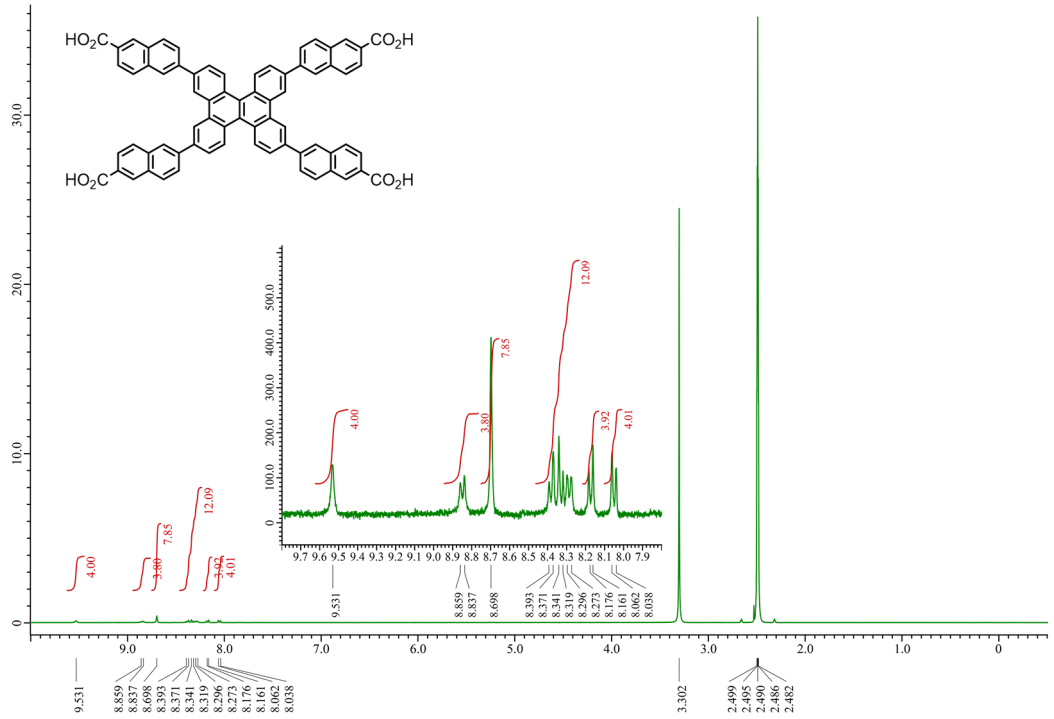

Fig. S42 ^{1}H-NMR (400 MHz, DMSO-d_6) spectrum of 6,6',6",6'"-(dibenzo[*g,p*]chrysene-2,7,10,15-tetrayl)tetrakis(2-naphthoic acid) (**C2N6DBC**).

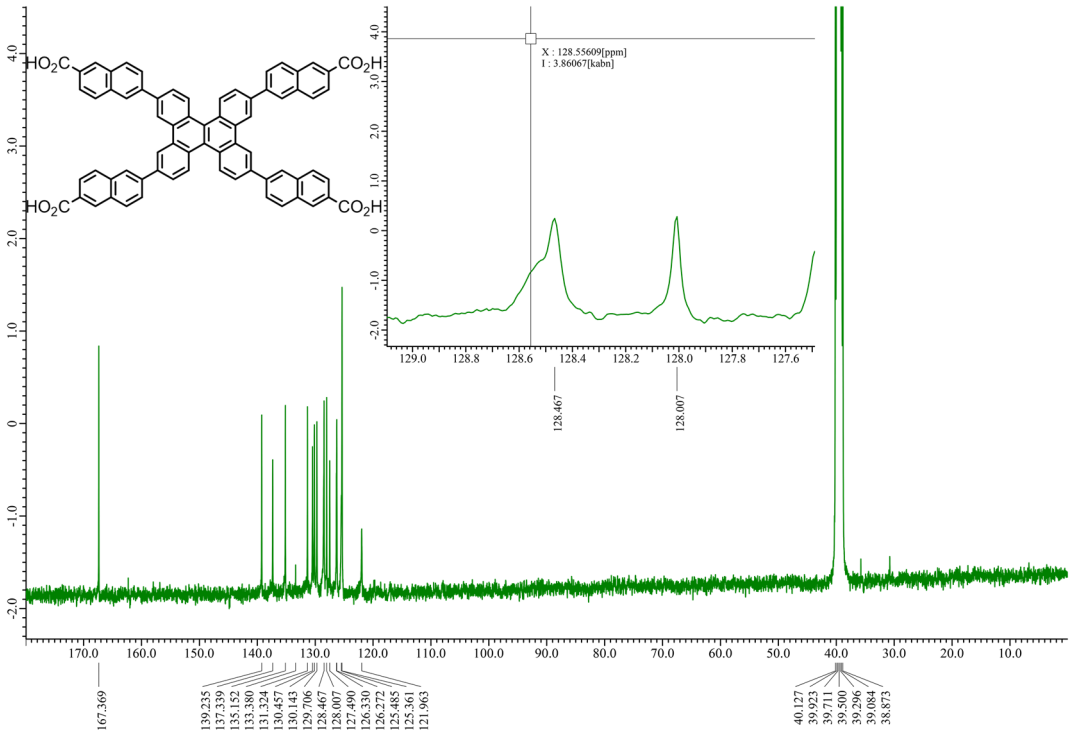

Fig. S43 ^{13}C-NMR (100 MHz, DMSO-d_6) spectrum of 6,6',6",6"'-(dibenzo[*g,p*]chrysene-2,7,10,15-tetrayl)tetrakis(2-naphthoic acid) (**C2N6DBC**).

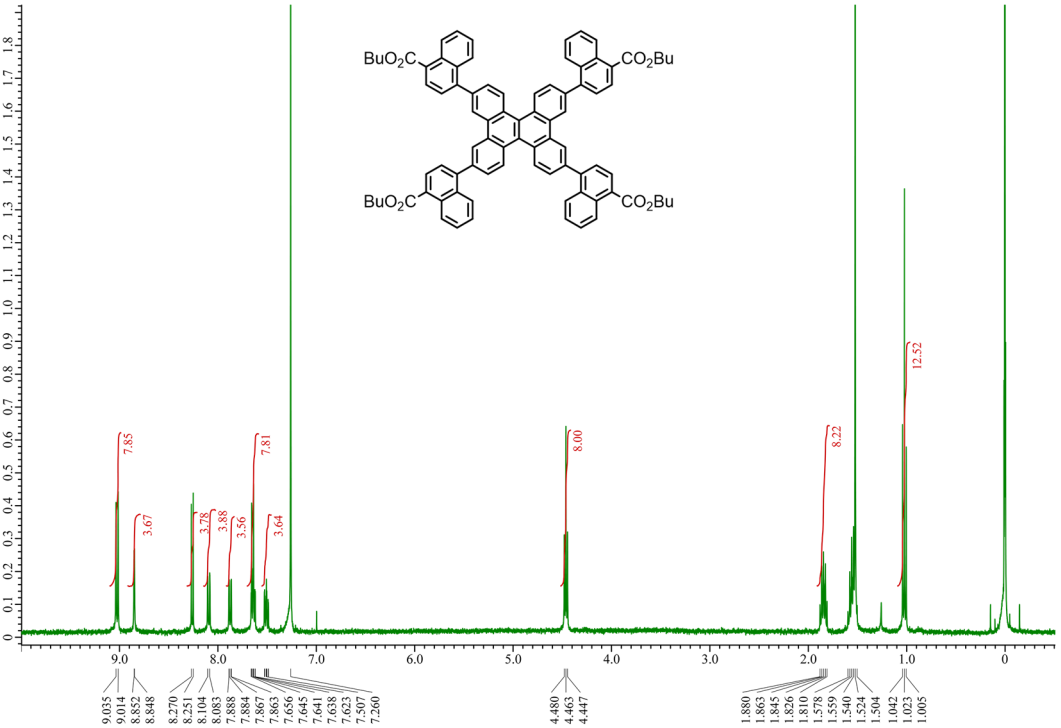

Fig. S44 ^{1}H-NMR (400 MHz, $CDCl_3$) spectrum of tetrabutyl 4,4',4",4"'-(dibenzo[*g,p*]chrysene-2,7,10,15-tetrayl)tetrakis(1-naphthoate) (**3c**).

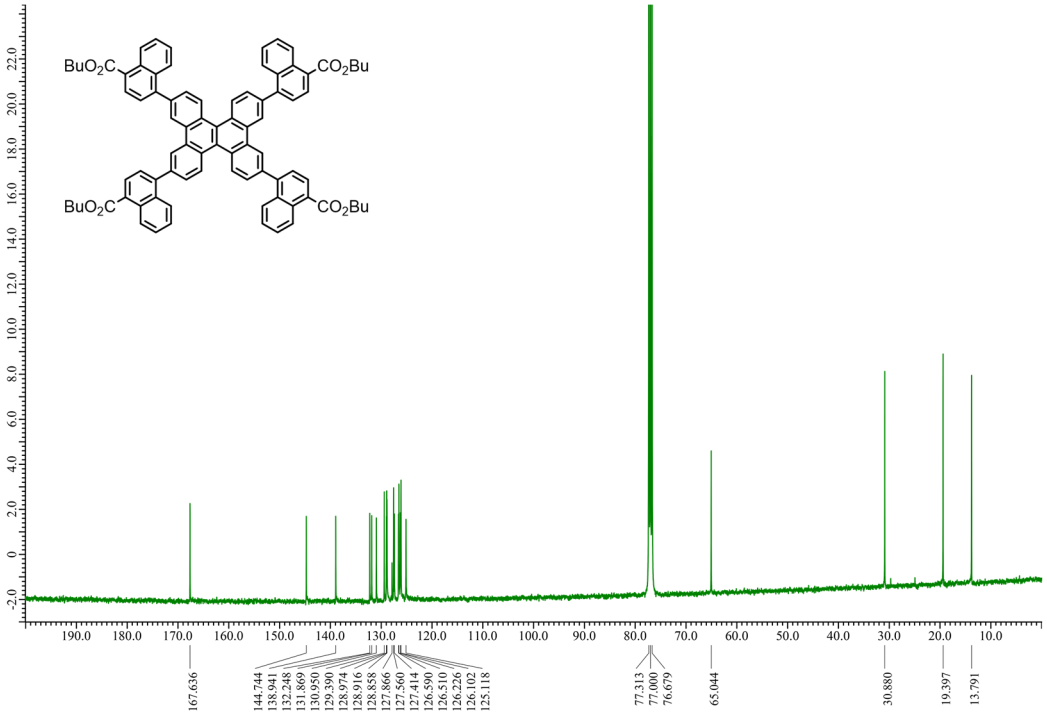

Fig. S45 ^{13}C-NMR (100 MHz, $CDCl_3$) spectrum of tetrabutyl 4,4',4",4"'-(dibenzo[*g,p*]chrysene-2,7,10,15-tetrayl)tetrakis(1-naphthoate) (**3c**).

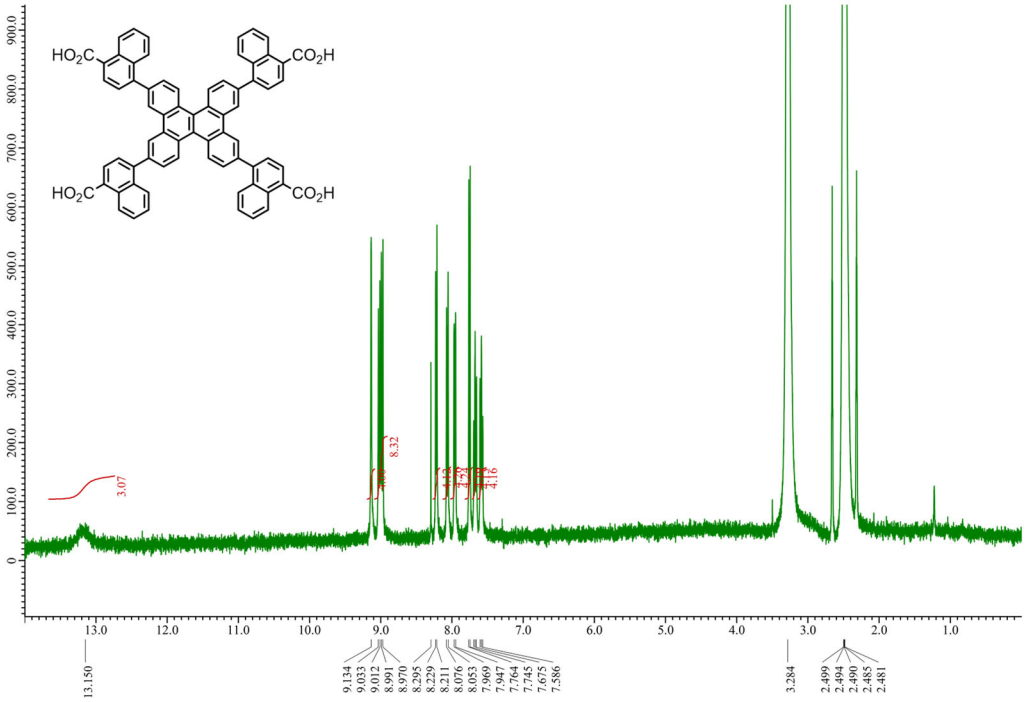

Fig. S46 ^{1}H-NMR (400 MHz, DMSO-d_6) spectrum of 4,4',4",4"'-(dibenzo[*g,p*]chrysene-2,7,10,15-tetrayl)tetrakis(1-naphthoic acid) (**C1N4DBC**).

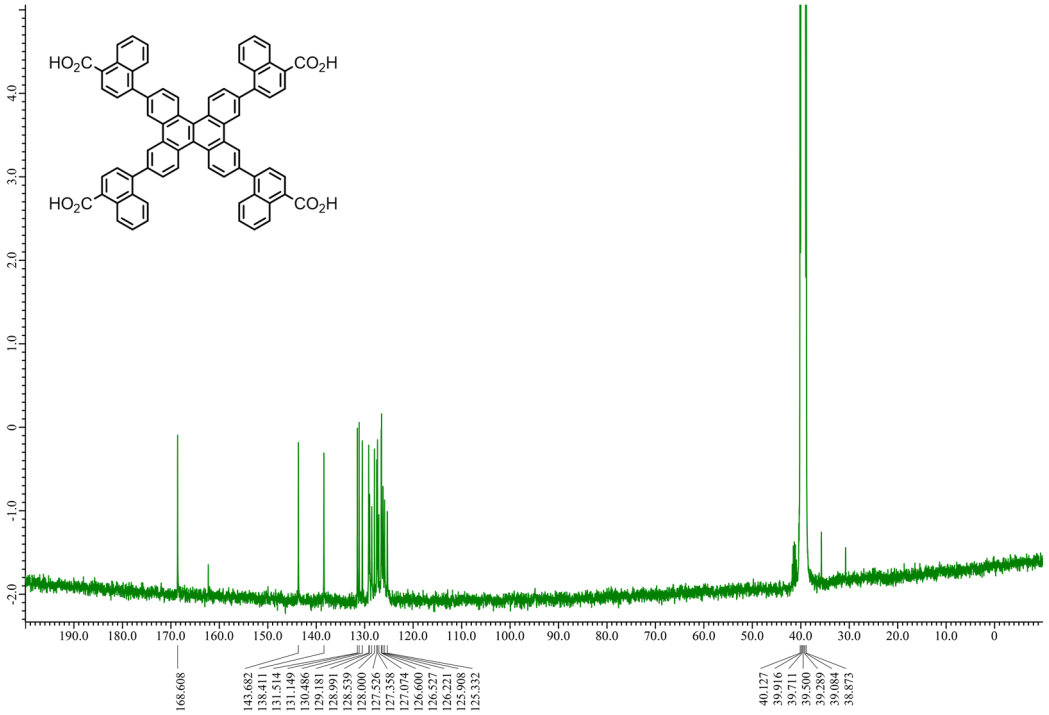

Fig. S47 ^{13}C-NMR (100 MHz, DMSO-d_6) spectrum of 4,4',4'',4'''-(dibenzo[*g,p*]chrysene-2,7,10,15-tetrayl)tetrakis(1-naphthoic acid) (**C1N4DBC**).

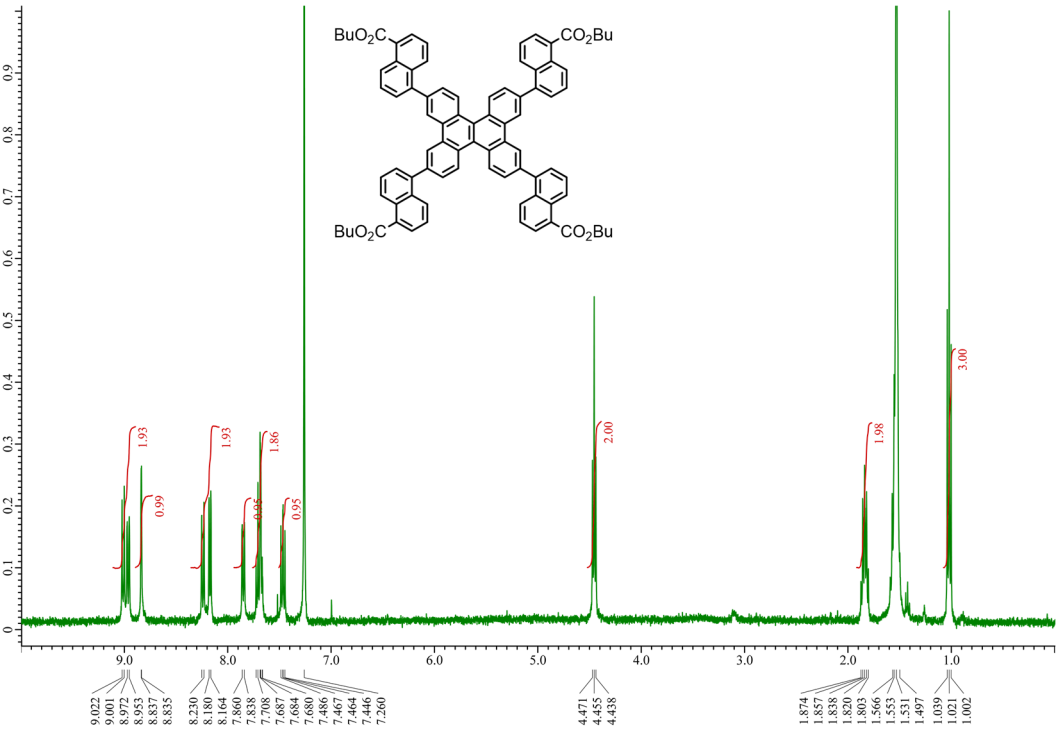

Fig. S48 ^{1}H-NMR (400 MHz, $CDCl_3$) spectrum of tetrabutyl 5,5',5'',5'''-(dibenzo[*g,p*]chrysene-2,7,10,15-tetrayl)tetrakis(1-naphthoate) (**3d**).

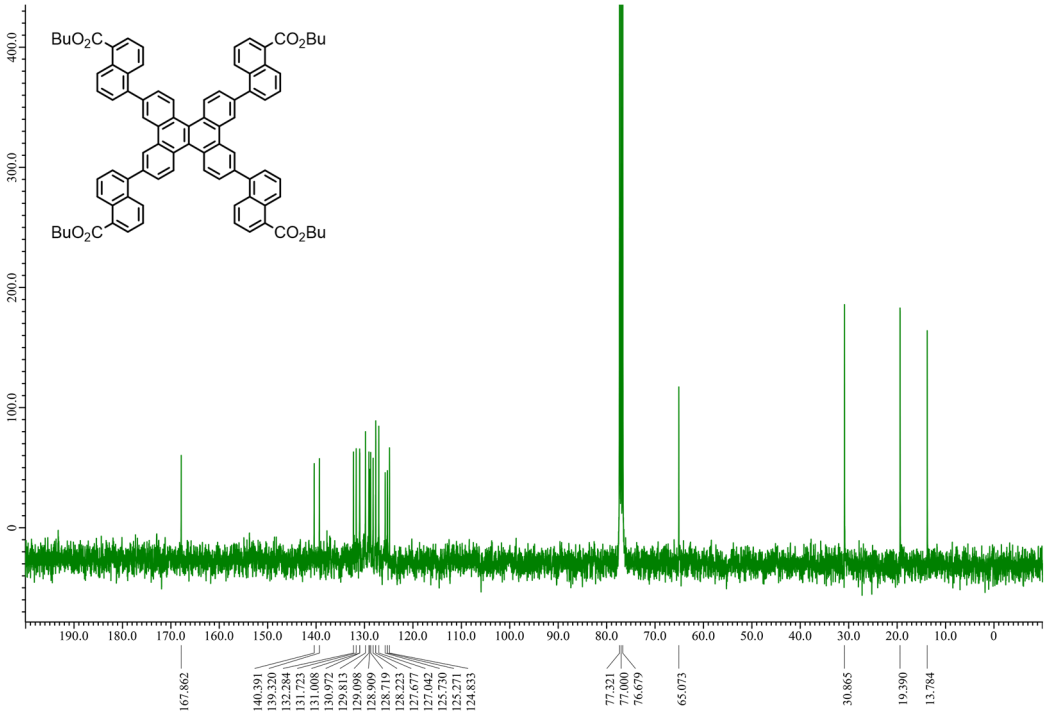

Fig. S49 ^{13}C-NMR (100 MHz, $CDCl_3$) spectrum of tetrabutyl 5,5',5",5'"-(dibenzo[*g,p*]chrysene-2,7,10,15-tetrayl)tetrakis(1-naphthoate) (**3d**).

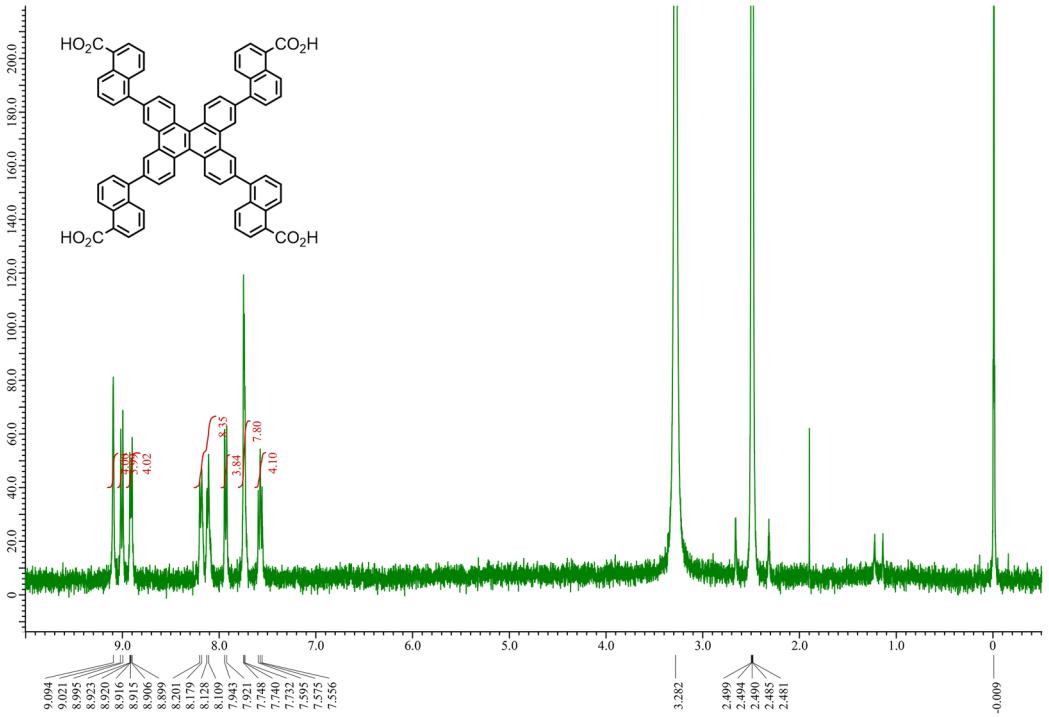

Fig. S50 ^{1}H-NMR (400 MHz, DMSO-d_6) spectrum of 5,5',5",5'"-(dibenzo[*g,p*]chrysene-2,7,10,15-tetrayl)tetrakis(1-naphthoic acid) (**C1N5DBC**).

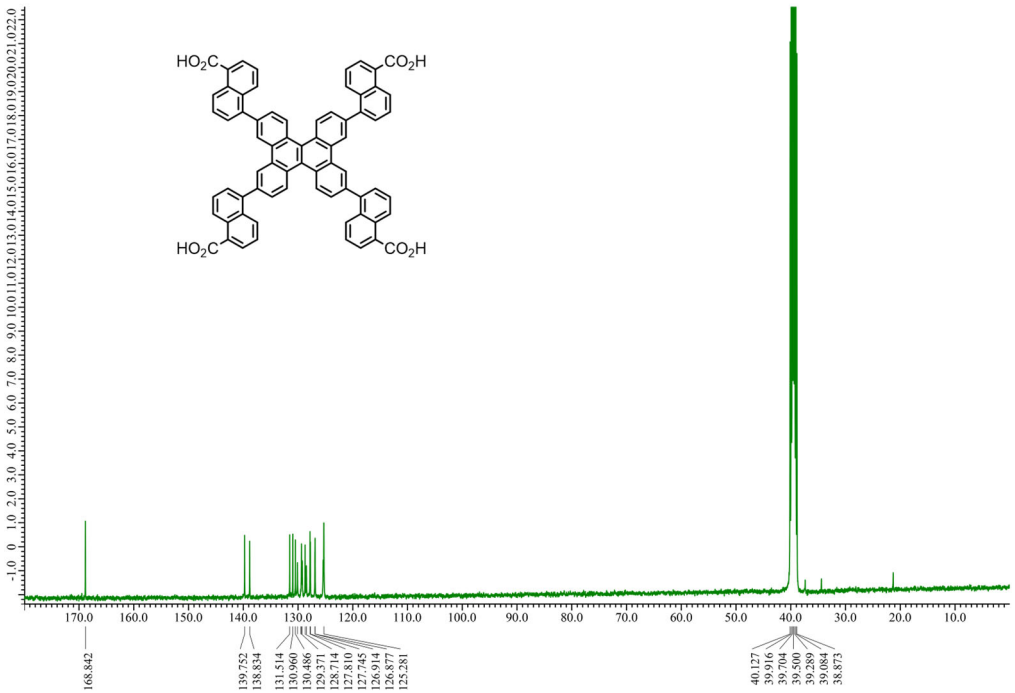

Fig. S51 ^{13}C-NMR (100 MHz, DMSO-d_6) spectrum of 5,5',5'',5'''-(dibenzo[*g,p*]chrysene-2,7,10,15-tetrayl)tetrakis(1-naphthoic acid) (**C1N5DBC**).

7. Reference

S1. C. F. MacRae, I. Sovago, S. J. Cottrell, P. T. A. Galek, P. McCabe, E. Pidcock, M. Platings, G. P. Shields, J. S. Stevens, M. Towler and P. A. Wood, *J. Appl. Crystallogr.*, 2020, **53**, 226–235.

S2. K. Momma and F. Izumi, "VESTA 3 for three-dimensional visualization of crystal, volumetric and morphology data," *J. Appl. Crystallogr.*, 2011, **44**, 1272–1276.

S3. Rigaku Oxford Diffraction (2015), Software CrysAlisPro 1.171.38.41o. Rigaku Corporation, Tokyo, Japan.

S4. G. M. Sheldrick, *Acta Crystallogr. Sect. A*, 2015, **71**, 3–8.

S5. (a) Rigaku (2018). CrystalStructure. Version 4.3. Rigaku Corporation, Tokyo, Japan. (b) O. V. Dolomanov, L. J. Bourhis, R. J. Gildea, J. A. K. Howard and H. Puschmann, H. J. Appl. Cryst., 2009, **42**, 339–341. (c) L. J. Bourhis, O. V. Dolomanov, R. J. Gildea, J. A. K. Howard and H. Puschmann, Acta Crystallogr. Sect. A, 2015, **71**, 59–75.

S6. G. M. Sheldrick, *Acta Crystallogr. Sect. C*, 2015, **71**, 3–8.

S7. (a) P. v. d. Sluis and A. L. Spek, *Acta Crystallogr. Sect. A,* 1990, **46**, 194. (b) A. L. Spek, *Acta Crystallogr. Sect. D*, 2009, **65**, 148–155.

S8. (a) M. Yamakata, S. Goto, T. Uruga, K. Takeshita, T.Ishikawa,Nucl. Instrum. *Methods Phys. Res. A*, 2001, 467–468, 667. (b) E.Nishibori, M. Takata, K. Kato, M. Sakata, Y.Kubota, S. Aoyagi, Y. Kuroiwa, M. Yamakata, N. Ikeda,Nucl. Instrum. *Methods Phys. Res. A*, 2001, 467–468, 1045. (c) S. Kawaguchi, M. Takemoto, K. Osaka, E. Nishibori,C.Moriyoshi, Y. Kubota, Y. Kuroiwa, K. Sugimoto, *Rev. Sci. Instrum.*, 2017, **88**, 085111.

S9. Material Studio ver 6.0; Accelrys Software Inc.: San Diego, CA, 2011.

S10. Neumann, M. A. *J. Appl. Crystallogr*. 2003, **36**, 356–365.

S11. Pawley, G. S. *J. Appl. Crystallogr*. 1981, **14**, 357–361.

S12. Engel, G. E.; Wilke, S.; König, O.; Harris, K. D. M.; Leusen, F. J. J. *J. Appl.Crystallogr*. 1999, **32**, 1169–1179.

S13. Rietveld, H. M. *J. Appl. Crystallogr*. 1969, **2**, 65–71.

S14. Baldinozzi, G.; Berar, J.-F. *J. Appl. Crystallogr*. 1993, **26**, 128–129.

S15. Dollase, W. A. *J. Appl. Crystallogr*. 1986, **19**, 267–272.

S16. Gaussian 09, Revision D.01, M. J. Frisch, G. W. Trucks, H. B. Schlegel, G. E. Scuseria, M. A. Robb, J. R. Cheeseman, G. Scalmani, V. Barone, B. Mennucci, G. A. Petersson, H. Nakatsuji, M. Caricato, X. Li, H. P. Hratchian, A. F. Izmaylov, J. Bloino, G. Zheng, J. L. Sonnenberg, M. Hada, M. Ehara, K. Toyota, R. Fukuda, J. Hasegawa, M. Ishida, T. Nakajima, Y. Honda, O. Kitao, H. Nakai, T. Vreven, J. A. Montgomery, Jr., J. E. Peralta, F. Ogliaro, M. Bearpark, J. J. Heyd, E. Brothers, K. N. Kudin, V. N. Staroverov, T. Keith, R. Kobayashi, J. Normand, K. Raghavachari, A. Rendell, J. C. Burant, S. S. Iyengar, J. Tomasi, M. Cossi, N. Rega, J. M. Millam, M. Klene, J. E. Knox, J. B. Cross, V. Bakken, C. Adamo, J. Jaramillo, R. Gomperts, R. E. Stratmann, O. Yazyev, A. J. Austin, R. Cammi, C. Pomelli, J. W. Ochterski, R. L. Martin, K. Morokuma, V. G. Zakrzewski, G. A. Voth, P. Salvador, J. J. Dannenberg, S. Dapprich, A. D. Daniels, O. Farkas, J. B. Foresman, J. V. Ortiz, J. Cioslowski, and D. J. Fox, Gaussian, Inc., Wallingford CT, 2013.

S17. Gaussian 16, Revision C.01, M. J. Frisch, G. W. Trucks, H. B. Schlegel, G. E. Scuseria, M. A. Robb, J. R. Cheeseman, G. Scalmani, V. Barone, G. A. Petersson, H. Nakatsuji, X. Li, M. Caricato, A. V. Marenich, J. Bloino, B. G. Janesko, R. Gomperts, B. Mennucci, H. P. Hratchian, J. V. Ortiz, A. F. Izmaylov, J. L. Sonnenberg, D.

Williams-Young, F. Ding, F. Lipparini, F. Egidi, J. Goings, B. Peng, A. Petrone, T. Henderson, D. Ranasinghe, V. G. Zakrzewski, J. Gao, N. Rega, G. Zheng, W. Liang, M. Hada, M. Ehara, K. Toyota, R. Fukuda, J. Hasegawa, M. Ishida, T. Nakajima, Y. Honda, O. Kitao, H. Nakai, T. Vreven, K. Throssell, J. A. Montgomery, Jr., J. E. Peralta, F. Ogliaro, M. J. Bearpark, J. J. Heyd, E. N. Brothers, K. N. Kudin, V. N. Staroverov, T. A. Keith, R. Kobayashi, J. Normand, K. Raghavachari, A. P. Rendell, J. C. Burant, S. S. Iyengar, J. Tomasi, M. Cossi, J. M. Millam, M. Klene, C. Adamo, R. Cammi, J. W. Ochterski, R. L. Martin, K. Morokuma, O. Farkas, J. B. Foresman, and D. J. Fox, Gaussian, Inc., Wallingford CT, 2019.

S18. Yuto Suzuki, Mario Gutiérrez, Senri Tanaka, Eduardo Gomez, Norimitsu Tohnai, Nobuhiro Yasuda, Nobuyuki Matubayasi, Abderrazzak Douhal and Ichiro Hisaki, *Chem. Sci.*, 2021, **12**, 9607–9618.

S19. Y. Suzuki, N. Tohnai, A. Saeki and I. Hisaki, *Chem. Commun.*, 2020, **56**, 13369–13372.

S20. X. S. Ke, Y. Hong, P. Tu, Q. He, V. M. Lynch, D. Kim and J. L. Sessler, *J. Am. Chem. Soc.*, 2017, **139**, 15232–15238.